

LINEAR LIBRARY  
C01 0068 3427



**Transport Coefficients**  
**in**  
**Quantum Chromodynamics**

Detlof Wilhelm von Oertzen

Submitted in partial fulfilment of the  
requirements for the degree of

**Doctor of Philosophy**

in the Department of Physics

**University of Cape Town**

August 1990

The University of Cape Town has been given  
the right to reproduce this thesis in whole  
or in part. Copyright is held by the author.

The copyright of this thesis vests in the author. No quotation from it or information derived from it is to be published without full acknowledgement of the source. The thesis is to be used for private study or non-commercial research purposes only.

Published by the University of Cape Town (UCT) in terms of the non-exclusive license granted to UCT by the author.

## Abstract

Relativistic kinetic theory provides a transport equation for classical, spinless, colored particles in a non-Abelian external field. We review the methods of solution used in the literature to find the transport coefficients for quark and gluon systems. Most authors use the relaxation time approximation of the Boltzmann equation to compute the transport coefficients, but this method has shortcomings in mixtures.

We use the Chapman Enskog (CE) method to solve the classical transport equations for quarks and gluons for the transport coefficients. The differential cross-sections describing the particle interaction are obtained from the lowest order scattering diagrams of quantum chromodynamics. We study a pure quark system, a pure gluon system and a quark antiquark ( $q\bar{q}$ ) mixture. For mixtures of quarks, antiquarks and gluons, we find the shear viscosity, heat conductivity and cross-coefficients. The coefficients pertaining to  $q\bar{q}$  mixtures, namely the thermal diffusion, diffusion and Dufour coefficient, the viscosities and heat conductivity are obtained and the conductivity of a  $q\bar{q}$  mixture in an external field is computed.

We compare our transport coefficients to others in the literature by rewriting them in terms of characteristic relaxation times. Although our results are generally larger than others, they are of the same order of magnitude, with important implications for quark-gluon (QG) plasma signatures. The quark to gluon shear viscosity ratio is found to be  $\sim 5$  times the number of quark flavors, emphasising the importance of quarks in dynamical QG calculations. The coefficients for a field-free  $q\bar{q}$  mixture indicate no  $q\bar{q}$  separation in the presence of a temperature gradient.

In the CE method, the transport coefficients depend naturally on a logarithmic factor due to the divergent scattering cross-sections, reflecting the plasma shielding effects. This logarithm is evaluated by relating it to typical plasma parameters.

We apply our results to the QG phase in the early universe and ultra-relativistic heavy ion collisions. A comparison of the QG to pion transport coefficients at the quark-hadron phase transition shows that the latter are  $\sim 10^3$  smaller. Dissipative effects increase the plasma lifetime, resulting in a longer high energy density and temperature plasma phase.

# Contents

<b>1</b>		<b>1</b>
1.1	Prelude . . . . .	1
1.2	Introduction . . . . .	1
<b>2</b>	<b>The Transport Equation</b>	<b>8</b>
2.1	Derivation . . . . .	9
<b>3</b>	<b>Literature Review</b>	<b>13</b>
3.1	Weinberg . . . . .	16
3.2	Danielewicz and Gyulassy . . . . .	17
3.3	Gavin . . . . .	18
3.4	Hosoya and Kajantie . . . . .	19
3.5	Baym, Monien, Pethick and Ravenhall . . . . .	20
3.6	Further Approaches . . . . .	21
<b>4</b>	<b>The Chapman Enskog Method</b>	<b>24</b>
4.1	Solution . . . . .	25
4.2	One Component System . . . . .	32
4.3	Two Component System . . . . .	36
4.4	System with Weak External Field . . . . .	41
<b>5</b>	<b>Results</b>	<b>44</b>
5.1	One Component Systems . . . . .	46
5.1.1	Simple Quark System . . . . .	46
5.1.2	Simple Gluon System . . . . .	49
5.2	Two Component System . . . . .	51
5.2.1	Quark Antiquark System . . . . .	51
5.2.2	Quark-Gluon System . . . . .	54
5.3	Quark Antiquark System in an External Field . . . . .	58
<b>6</b>	<b>Comparison of the Results</b>	<b>59</b>
6.1	Simple Gluon System Shear Viscosity . . . . .	61
6.2	QGP Shear Viscosity . . . . .	63
6.3	QGP Heat Conductivity . . . . .	64

6.4	Quark Antiquark Conductivity . . . . .	66
6.5	Summary . . . . .	69
<b>7</b>	<b>Applications</b>	<b>71</b>
7.1	Early Universe . . . . .	72
7.2	Heavy Ion Collisions . . . . .	79
7.2.1	Entropy Evolution . . . . .	80
7.2.2	Energy Density Evolution . . . . .	83
7.2.3	Temperature Evolution . . . . .	85
7.3	Summary . . . . .	86
<b>8</b>	<b>Summary</b>	<b>87</b>
	Acknowledgements . . . . .	90
<b>A</b>	<b>The Collision Bracket</b>	<b>91</b>
A.1	Results for Square Collision Brackets . . . . .	103
<b>B</b>	<b>The Collision Integral</b>	<b>107</b>
<b>C</b>	<b>The Matrix Elements</b>	<b>113</b>
C.1	Differential Cross-Sections . . . . .	126
<b>D</b>	<b>The Cut-off Problem</b>	<b>128</b>
<b>E</b>	<b>Useful Relations</b>	<b>137</b>
E.1	Thermodynamic Quantities and Relations . . . . .	137
E.2	Constants . . . . .	141
<b>F</b>	<b>Quark-like Systems</b>	<b>142</b>
F.1	Simple Quark-like System . . . . .	142
F.2	Quark Antiquark-like System . . . . .	144
	<b>Bibliography</b>	<b>148</b>

# List of Figures

6.1	Characteristic Viscous Relaxation Times of a Gluon System. . . .	63
6.2	Characteristic Viscous Relaxation Times of a QGP. . . . .	63
6.3	Characteristic Heat Conduction Relaxation Times of a QGP. . . .	65
6.4	Conductivity of a Quark Antiquark System. . . . .	68
7.1	QGP-HG Phase Diagram. . . . .	72
7.2	Cosmological Phase Transition. . . . .	76
7.3	Pion Volume Viscosity. . . . .	76
7.4	Quark-Gluon and Pion Shear Viscosity. . . . .	78
7.5	Quark-Gluon and Pion Heat Conductivity. . . . .	78
7.6	Bjorken's Picture of Heavy Ion Collisions. . . . .	79
7.7	Entropy Evolution in Viscous Scaling Hydrodynamics. . . . .	83
7.8	Energy Density Evolution in Viscous Scaling Hydrodynamics. . .	84
7.9	Temperature Evolution in Viscous Scaling Hydrodynamics. . . . .	85
C.1	t-Channel Diagram for Quark-Quark Scattering. . . . .	116
C.2	u-Channel Diagram for Quark-Quark Scattering. . . . .	116
C.3	s-Channel Diagram for Quark-Antiquark Scattering. . . . .	119
C.4	t-Channel Diagram for Quark-Antiquark Scattering. . . . .	119
C.5	s-Channel Diagram for Quark-Gluon Scattering. . . . .	120
C.6	t-Channel Diagram for Quark-Gluon Scattering. . . . .	121
C.7	u-Channel Diagram for Quark-Gluon Scattering. . . . .	121
C.8	s-Channel Diagram for Gluon-Gluon Scattering. . . . .	124
C.9	t-Channel Diagram for Gluon-Gluon Scattering. . . . .	124
C.10	u-Channel Diagram for Gluon-Gluon Scattering. . . . .	125
C.11	4-Point Diagram for Gluon-Gluon Scattering. . . . .	125
D.1	Plasma Parameter $\mathcal{P}$ for a QGP. . . . .	134

# List of Tables

1.1	Summary of Symbols used. . . . .	7
4.1	Thermodynamic Forces, Flows and the Transport Coefficients. . .	34
6.1	Shear Viscosities and Viscous Relaxation Times of a Gluon System.	62
6.2	Shear Viscosities and Characteristic Viscous Relaxation Times of a QGP. . . . .	64
6.3	Heat Conductivities and Heat Conduction Relaxation Times of a QGP. . . . .	66
6.4	Conductivity of a Quark Antiquark System. . . . .	67
C.1	Feynman Rules of QCD in the Feynman Gauge. . . . .	114
C.2	Trace Relations and Color Sums. . . . .	118
D.1	Plasma Parameters and Coulomb Logarithms. . . . .	136

# Chapter 1

## 1.1 Prelude

*“Armed with giant machines and grand ambitions, physicists spend billions in the race to discover the building blocks of matter”*<sup>1</sup>. With these words from a recent article in TIME magazine the attention of the general public was focussed on the development of particle accelerators. These machines are built to unlock fundamental secrets of nature in a quest characterized by the Faustian words: *“Daß ich erkenne, was die Welt im Innersten zusammenhält”*<sup>2</sup>.

Discovery of the New is exciting. Furthermore, the pleasure derived from understanding the interactions between the building blocks of matter is coupled to the ultimate hope of understanding All. This short prelude then is intended to motivate the reader when some of the ensuing details make a common purpose doubtful.

## 1.2 Introduction

Current experimental efforts with ultra-relativistic heavy ions offer the unique possibility of studying strongly interacting matter in the laboratory [1] – [3]. Available beam energies range between 14.5 GeV/A at the Brookhaven AGS to 200 GeV/A at CERN’s SPS, making possible the study of matter under extreme conditions. Since the total nucleon-nucleon center of momentum (cm) frame energy of these accelerators lies between 3 and 10 GeV per nucleon, the expected particle densities ( $1 - 7/\text{fm}^3$ ) and energy densities ( $1 - 10 \text{ GeV}/\text{fm}^3$ ) make the creation of a new phase of matter probable: the quark-gluon plasma (QGP), a system of deconfined quarks and gluons. Future accelerators such as RHIC at

---

<sup>1</sup>M.D. Lemonick in TIME magazine 16, April 16, (1990) 42, *The Ultimate Quest*

<sup>2</sup>*“That I may detect the inmost force which binds the world, and guides its course”*.  
from J.W. v. Goethe, *“Faust”*, Random House, New York, 1950

Brookhaven, the LHC at CERN and the SSC in Texas, hopefully will provide beams as heavy as uranium and cm energies orders of magnitude larger than at present. In view of these, the opportunity to verify the theory of strong interactions, quantum chromodynamics (QCD), and thus showing the existence of a phase transition from ordinary nuclear matter to deconfined quarks and gluons, seems better than ever. In order to study such a novel system and facilitate the interpretation of experimental signatures of the expected deconfinement transition, one needs to understand the evolution, and, in particular the properties, such as the transport coefficients, of such an exotic phase of matter. This motivates the present study:

The transport properties of quarks and gluons are calculated in this thesis.

Transport processes arise as a result of collisions between particles, and are responsible for the equilibration of a system. In heavy ion collisions, for example, this process is believed to proceed in two steps:

1. The evolution of the system from a completely violent stage where most of the particle creation takes place, to a system where the local thermodynamic quantities such as the temperature and chemical potentials can be specified.
2. A conversion from a local to a globally equilibrated state in which the spatial non-uniformities disappear.

The late phases of stage 1 in the evolution of the system is the stage we analyse; hereafter the use of local hydrodynamics is justified. The evolution is from a state of non-equilibrium to equilibrium, and a suitable formalism for dealing with non-equilibrium conditions is based on kinetic theory. By using a relativistic kinetic equation which describes the interplay between micro- and macroscopic phenomena, namely the particle collisions versus the hydrodynamical evolution, we find the transport coefficients of the system. The knowledge of these coefficients of the QGP enables one to include dissipative effects in the plasma hydrodynamics which are needed to predict the rate of expansion of the QGP fluid until hadronisation sets in. For example, the kinetic or transport coefficients associated with the entropy production in a one component system are the volume (bulk) and shear viscosities and the heat conductivity, all having a microscopic origin and a macroscopic manifestation. This kinetic description amounts to the formulation of a dynamical QGP where the assumption of thermal and chemical equilibrium has been relaxed. Since many of the proposed signatures of a QGP, such as direct photon emission, lepton pair and strangeness production [3], rely on the notion of an equilibrated system, one needs to carefully reexamine these signals after non-equilibrium effects have been included. But once the question has been raised whether or not the QGP is in equilibrium, a multitude of related questions emerge:

- What is the time-scale of equilibration?

- Is there complete equilibrium before the onset of hadronisation?
- Do pre-equilibrium phenomena influence the QGP signatures?
- Is there a separation of particles and antiparticles?
- Are color fluctuations a dominant pre-equilibrium feature and would these phenomena survive the hadronisation process?
- Is the deconfined phase simply a phase with many degrees of freedom, or do new processes arise? For instance, does the color conduction indicate that the new phase is a color conductor or even a superconductor?

Most of these questions will not be answered here, but by using relativistic transport theory (see for example [4] and [5]), we have determined the transport properties of quarks and gluons in a suitable mathematical framework. Our analysis can be seen as a first step towards understanding the pre-equilibrium plasma phase and a study of non-equilibrium effects.

Several attempts exist in the literature to compute the transport coefficients for a relativistic gas using the Grad method [5] and the relaxation time approach ([6] – [10]). In this thesis we use the **Chapman Enskog (CE)** method, employing the formalism developed by de Groot, van Leeuwen and van Weert [4], to solve for the transport coefficients of a gas composed of quarks, antiquarks and gluons or quarks and antiquarks.

The CE method offers numerous advantages over other methods of solution:

- the approximations involving the CE scheme of solution are well understood and no arbitrariness is introduced due to ambiguous truncation procedures or higher orders of approximation,
- the relativistic Onsager relations can be derived, this is in contrast to the method of Grad and others,
- the difficulty of finding characteristic relaxation times, especially in mixtures, where this is not a well defined concept anymore, is eliminated (in contrast to the relaxation time approximation),
- small angle scattering is taken care of naturally, and no *ad hoc* factors (such as  $1 - \cos \theta$ ) need to be introduced, like for example in the treatment of the characteristic collision cross-section, as used in the relaxation time approximation,
- the method self-consistently provides linear relations between the thermodynamic forces and the corresponding flows, the transport coefficients being the constants of proportionality.

Weak points of the CE method include:

- the weaknesses associated with a Boltzmann-like equation, i.e.
  1. its applicability to dilute gases only, where two-body collisions dominate,
  2. the hypothesis of molecular chaos, i.e. no particle correlations,
  3. the distribution function may only vary slowly in space-time. This restriction, however, defines length- and timescales of the problem, and determines the degree of “maximal non-equilibration” which may be studied.
- it is less general than for example the relativistic moment method [11] since the mean free path of the particles must always be much less than the size of the physical system.

Before proceeding with the main topic of this thesis, the calculation of the transport coefficients for quarks and gluons, we mention some key references of transport theory in general, and work related more specifically to this thesis.

The literature on transport theory is vast and a chronological ordering of historical contributors in the field will not be attempted. Rather, we refer the reader to the classical book of Chapman and Cowling [12] which describes the evaluation of transport coefficients for classical systems and includes an epic historical summary of the early developments of transport theory. The monograph by de Groot, van Leeuwen and van Weert [4] also summarises the most important developments in the field and has an extensive list of references. A review of the early developments of quantum transport theory is given by Carruthers and Zachariasen [13]; and, summarising recent results in quark-gluon transport theory, Elze and Heinz [14] have published a review which provides a valuable source of current references.

We wish to mention a few authors laying the framework of the mathematical methods used in this thesis, they are Eckart [15], Marle [16] and Israel [17]. The work of Heinz ([18] – [22]) provides the starting point for both classical and quantum mechanical quark-gluon transport theory.

Early applications of the relativistic kinetic theory were mainly in cosmology [23], particularly in the physics of the early universe [24] – [25], and neutrino transport in dense stars [26]. In the field of particle physics on laboratory scales, applications have been made in the calculation of the transport coefficients (these references will be discussed in detail in Chapter 3), and in the solution of the transport equations [27] under specific constraints such as boost-invariance ([28] – [30]). However, due to the considerable difficulty and ambiguities in the classical transport theory of quarks and especially gluons, most authors have refrained

from making model independent predictions. A recent review by Mrówczyński [31] summarises the main results and problems.

The structure of this thesis is briefly described below.

In Chapter 2, we derive a covariant transport equation which describes the evolution of the phase space distribution function for classical, spinless, but color carrying particles. The approximations made in the derivation are emphasised.

In Chapter 3, a discussion of previous studies of the transport coefficients for quark-gluon systems is presented. The different methods used and the results are summarised and motivation is provided for the method of solution as used in this thesis.

In Chapter 4, we use the Chapman Enskog method to solve the transport equation for the transport coefficients. The transport coefficients are presented for a simple system, i.e. consisting of one particle species only, a binary mixture, and a collision dominated system in a weak external field. We attempt to keep the main body of the thesis in an easy-to-read form by presenting many technical parts of the calculation in the various Appendices.

Our results are summarised in Chapter 5: the coefficients of heat conductivity and viscosity for both simple quark and gluon systems, a quark-gluon system, and a quark antiquark mixture are presented. An interesting aspect is the unifying feature of the Eucken relation. This is the ratio of heat conductivity to shear viscosity, which is the same for all systems studied. It indicates the similarities between the systems under consideration, such as the cross-sections and the resulting Coulomb logarithms.

Furthermore, the various cross-coefficients of a quark-gluon and quark antiquark mixture are presented: in this instance the vanishing thermal diffusion coefficient (in the first order of approximation) is a most peculiar feature. We also present the various transport coefficients for a system with a weak external field, where the covariant analogue of Ohm's law provides us with the conductivity coefficient. Most of the results show a logarithmic dependence on the cut-off of the divergent scattering cross-sections, known as the Coulomb logarithm from problems in electron plasmas. It is due to the Rutherford-like cross-sections of the quarks and gluons, and a discussion on the evaluation of this most important quantity is presented. The detailed evaluation is carried out in Appendix D.

In Chapter 6 we compare our results with others in the literature, making use of characteristic relaxation times for the shear viscosity and heat conductivity. The relaxation times are a direct measure of the equilibration time-scales in a medium, and therefore provide an intuitive tool for studies in non-equilibrium systems. It is interesting to note that the various other methods used to solve the transport equation for the transport coefficients for one component particle systems produce answers similar to ours. However, their potential for solving multi-component systems is severely limited.

Applications of our results are discussed in Chapter 7, where two possible sce-

narios for QGP formation, namely the early universe and ultra-relativistic heavy ion collisions, are investigated.

In the Summary, possible extensions to our calculations are proposed. The discussion of the main results is followed by an outlook where the remaining problems are summarised.

Throughout this work we use units such that  $c = \hbar = k_B = 1$ , unless otherwise stated. The Einstein summation convention is applied with Greek letters indicating Lorentz indices and Latin letters for color indices. The Minkowski metric  $g^{\mu\nu}$  is given by  $\text{diag} \{ 1, -1, -1, -1 \}$ . The Table 1.1 serves as an easy reference for the various symbols and definitions used in the thesis.

Thermodynamic quantities:

temperature $T$	chemical potential $\mu$
pressure $P$	particle density $n$
energy density $en$	entropy density $sn$
enthalpy density $wn$	
energy per particle $e$	enthalpy per particle $w$
particle density fraction $x_1 \equiv n_1/(n_1 + n_2)$	
energy momentum tensor $T^{\mu\nu}$	hydrodynamic four velocity $U^\mu$

Thermodynamic forces:

$X \equiv -\nabla^\mu U_\mu$	$X_q^\mu \equiv \nabla^\mu \log T - \nabla^\mu P/wn$
$\overset{\circ}{X}^{\mu\nu} \equiv \nabla^\mu U^\nu/2 + \nabla^\nu U^\mu/2 - \Delta^{\mu\nu} \nabla_\alpha U^\alpha/3$	
$X_1^\alpha \equiv (\nabla^\alpha \mu_1)_{P,T} - (\nabla^\alpha \mu_2)_{P,T} - (w_1 - w_2) \nabla^\alpha P/wn$	

Thermodynamic flows:

viscous pressure $\overset{\circ}{\Pi}$	heat flow $I_q^\mu$
traceless viscous pressure $\overset{\circ}{\overset{\circ}{\Pi}}^{\mu\nu}$	

Various other quantities:

time derivative operator $D \equiv U^\nu \partial_\nu$	divergence operator $\nabla^\mu \equiv \Delta^{\mu\nu} \partial_\nu$
projection operator $\Delta^{\mu\nu} \equiv g^{\mu\nu} - U^\mu U^\nu$	
$z \equiv m/T$	$\tau \equiv p^\nu U_\nu/T$
$\frac{\pi^\mu}{\pi^\mu} \equiv \Delta^{\mu\nu} \pi_\nu$	$\frac{\pi^\mu \pi_\mu}{\pi^\mu \pi_\mu} \equiv \Delta^\alpha_\beta \pi_\alpha \pi^\beta$
$\pi^\mu \equiv p^\mu/T$	
$\log(A) \equiv \log_e(A)$	
equilibrium distribution function $f^{(0)}$	
inner product bracket $(A, B) \equiv (T/n) \int \frac{d^3p}{p^0} A(p) B(p) f^{(0)}$	

Transport coefficients:

volume viscosity $\eta_v$	heat conductivity $\lambda$
shear viscosity $\eta$	thermal diffusion coefficient $D_T$
diffusion coefficient $D_d$	Dufour coefficient $D'_T$

Table 1.1: Summary of Symbols used.

# Chapter 2

## The Transport Equation

This Chapter deals with the derivation of the transport equation. This equation describes the evolution of the phase space distribution function of a classical, spinless particle which carries the additional property of “classical” color. The phase space distribution function approach is well known in statistical physics from problems where the number of particles in the system makes an individual particle description impossible. Although the particles in a QGP have a quantum mechanical character, such as spin and color and their interaction, we have treated them as classical particles only. We concentrate on the classical analogue of the quantum mechanical distribution function (Wigner function) for the following reasons:

- It can be shown that the classical equations in the form of color moment equations [20] – [21] are the classical limit of the quantum mechanical equations.
- We have a well developed formalism on hand to compute the transport coefficients from the transport equation, and can expect the results to give a first indication of the magnitude of entropy producing processes, thereby providing a means to measure the degree of non-equilibration of the system.
- Since we will be working exclusively in the perturbative regime of the deconfined phase, one can even argue that the non-Abelian character of QCD will not be a dominant feature [32]. One should thus at first understand a quasi-Abelian mixture of quarks and gluons before considering the quantum effects.

For completeness we present some recent references dealing with the Wigner function approach in the quark-gluon plasma context: the work of Heinz [20] – [21] and Elze, Gyulassy and Vasak [33] – [34] was most recently extended and summarised in the review by Elze and Heinz [14], who also provide an up-to-date list of references.

We now proceed with the derivation of the transport equation.

## 2.1 Derivation

The aim is to find the phase space evolution equation for the quarks and anti-quarks governing the one-particle distribution function  $f$ .

We start off by deriving the equations of motion for quarks and gluons, namely the Dirac and the Yang-Mills equations, from the Lagrange density

$$\mathcal{L}_{\text{QCD}} = -\frac{1}{4}F_a^{\mu\nu}F_{\mu\nu}^a + \bar{\psi}(i\gamma_\mu D^\mu - m)\psi \quad (2.1)$$

of quantum chromodynamics, which is the renormalisable field theory based on the non-Abelian gauge group  $\text{SU}(3)$ <sup>1</sup>. The interactions between the quarks and gluons are determined by the covariant derivative  $D^\mu$  given by

$$D^\mu = \partial^\mu - ig\frac{\lambda^a}{2}A_a^\mu, \quad (2.2)$$

where  $g$  is the strong coupling constant, and  $a = 1, 2, \dots, 8$  the color index of the adjoint representation of  $\text{SU}(3)$ . The field strength tensor,  $F_a^{\mu\nu}$ , is given by

$$F_a^{\mu\nu} = \partial^\mu A_a^\nu - \partial^\nu A_a^\mu + g f_{abc} A_b^\mu A_c^\nu \quad (2.3)$$

in terms of the gluon fields  $A_a^\mu$  and the antisymmetric structure functions,  $f_{abc}$ , defined through the commutation relations of the Gell-Mann color generators

$$\left[ \frac{\lambda^a}{2}, \frac{\lambda^b}{2} \right] = i f_{abc} \frac{\lambda^c}{2}. \quad (2.4)$$

Now, using the Euler-Lagrange equations, the equation of motion of the quark field  $\psi$  (and similarly for the antiquark field  $\bar{\psi}$ ) are derived, giving the Dirac equation

$$(i\gamma_\mu D^\mu - m)\psi = 0. \quad (2.5)$$

Likewise, for the gluons, the Yang-Mills field equations are found to be

$$(D_\alpha F^{\alpha\beta})_a = \partial_\alpha F_a^{\alpha\beta} + g f_{abc} A_\alpha^b F_c^{\alpha\beta} = -g j_a^\beta, \quad (2.6)$$

where  $j_a^\beta$  is the color current.

We now follow the derivation of Wong [36] and Heinz [20]. The expected number of particles in the system is large, calling for a statistical rather than individual particle description. To this end the existence of a phase space distribution

---

<sup>1</sup>Using the Ryder [35] convention.

function  $f = f(x, p, Q)$  is postulated, where  $x$  is the space-time variable,  $p$  the four-momentum and  $Q$  the classical color variable. This distribution function gives the probability of finding a classical, spinless, but color-carrying particle at a specific point in phase space. Note that the inclusion of color as a classical variable implies an extension of phase space. If spin had been included, the phase space could likewise be extended, as was done in the treatment by Heinz [37]. The dynamical evolution equation of the scalar phase space distribution function  $f$  is described by

$$m \frac{df}{d\tau} = C, \quad (2.7)$$

where  $C = C(x, p, Q)$  is a term due to collisions of particles in the system. The derivative  $df/d\tau$  in terms of the dynamical variables  $x, p$  and  $Q$  is given by

$$m \left[ \frac{df}{dx^\mu} \frac{dx^\mu}{d\tau} + \frac{df}{dp^\mu} \frac{dp^\mu}{d\tau} + \frac{df}{dQ^a} \frac{dQ^a}{d\tau} \right] = C(x, p, Q). \quad (2.8)$$

It remains to find the equations of motion for the dynamical variables  $x, p$  and  $Q$ . To this end we obtain the Hamiltonian  $H$  of the system from the Dirac equation (2.5)

$$H = -i \vec{\alpha} \cdot \vec{\nabla} - g \frac{\lambda^a}{2} A_{a0} + g \frac{\lambda^a}{2} \vec{\alpha} \cdot \vec{A}_a + \beta m, \quad (2.9)$$

where the usual [38] symbols for  $\alpha$  and  $\beta$  have been used. This Hamiltonian is now used in the Heisenberg equations of motion for  $x, p$  and the quark color  $Q^a$ . The quantity  $Q^a \equiv -\lambda^a/2$  is viewed as the classical analogue of the Gell-Mann matrices<sup>2</sup>. One finds

$$\frac{d\vec{x}}{d\tau} = i[H, \vec{x}] = \vec{\alpha}, \quad (2.10)$$

$$\frac{dp^\mu}{d\tau} = i[H, p^\mu] = g Q^a F_a^{\mu\nu} \frac{dx_\nu}{d\tau}, \quad (2.11)$$

$$\frac{dQ^a}{d\tau} = i[H, Q^a] = -g f_{abc} \frac{dx^\mu}{d\tau} A_\mu^b Q^c. \quad (2.12)$$

Here,  $dA_a^i/d\tau = dx^\mu/d\tau \partial_\mu A_a^i$  has been used. Inserting (2.10) – (2.12) into (2.8), and noting that  $m dx^\mu/d\tau = p^\mu$ , the explicitly gauge-covariant evolution equation for the quark distribution function is obtained, i.e.

$$[p^\mu \partial_\mu - g Q^a p_\mu F_a^{\mu\nu} \partial_{p,\nu} - g f_{abc} p^\mu A_\mu^b Q^c \partial_Q^a] f = C(x, p, Q). \quad (2.13)$$

<sup>2</sup>I thank Ulrich Heinz for clarifying correspondence.

A similar equation holds for the phase space distribution function  $\bar{f}$  for anti-quarks. Replacing  $Q^a$  with  $-Q^a$ , and noting that (2.12) does not change its sign under this operation, it can be seen that only the second term of the evolution equation (2.13) changes sign. We therefore obtain

$$\boxed{[p^\mu \partial_\mu + g Q^a p_\mu F_a^{\mu\nu} \partial_{p,\nu} - g f_{abc} p^\mu A_\mu^b Q^c \partial_Q^a] \bar{f} = C(x, p, Q)}. \quad (2.14)$$

A similar gauge-covariant equation holds for the gluons, but it should be noted that the task of deriving the proper quantum mechanical equations for gluons still poses a considerable problem [14].

Throughout this work, we will assume, that two-body collisions in the system are the dominant mode of collision. To this end we factorize all two-body and higher order particle correlations into single particle distribution functions and their products, i.e.

$$C(x, p, Q) \rightarrow C[f, f]. \quad (2.15)$$

Hereby, a natural cut-off in the otherwise infinite set of hierarchial equations, the well-known BBGKY hierarchy [39], is achieved. This restriction is known as the Boltzmann approximation. The incorporation of the Yang-Mills equation (2.6) into the transport equation (2.13) (or (2.14)) is known as the Boltzmann-Vlasov set of equations. They describe a system of classical, colored, but spinless particles (antiparticles) interacting with a self-consistently created chromodynamic background field, interpreted as a color plasma. The set of equations is in closed form and can, in principle, be solved.

In this thesis we are interested in the transport coefficients of systems of quarks and gluons. In order to be able to compute them, we will make some simplifications. Two principally different systems will be considered:

- A completely collision dominated system, where all the field effects can be neglected. This assumption simplifies the transport equation (2.13) to

$$p^\mu \partial_\mu f = C[f, f]. \quad (2.16)$$

This equation will be assumed to describe both simple quark and simple gluon systems.

- A system in a weak external field, where non-Abelian effects can be neglected, so that the transport equation (2.13) becomes

$$[p^\mu \partial_\mu - g p^\mu F_{\mu\nu} \partial_p^\nu] f = C[f, f]. \quad (2.17)$$

Both systems will be considered to be locally colorless, i.e. all color currents  $j_a^\mu$  vanish, and the phase space distribution function loses its color dependence.

The QCD character then only enters through the gauge independent interaction cross-sections, as will be discussed later. These assumptions can be justified if the system under consideration is regarded as being well inside the chirally symmetric perturbative regime of the QGP. They are also partially supported by recent calculations in the flux-tube model in ultra-relativistic heavy ion collisions [32], where it is shown that the expected non-linear effects in the plasma are small, and can therefore be neglected in the first approximation.

Now that the transport equation and the corresponding simplifications in form of (2.16) and (2.17) have been derived, we will investigate their solution to find the transport coefficients. In order to provide a motivation for the Chapman Enskog method of solution to be introduced in Chapter 4, we first review some earlier attempts to compute the transport coefficients for a quark-gluon system, this is carried out in Chapter 3.

# Chapter 3

## Literature Review

The aim of this Chapter is to summarise the methods used by other authors to derive expressions for transport coefficients for the QGP, and to present their results. We restrict ourselves to the discussion of some recent papers where explicit numerical results are provided, which can then be compared to ours.

It is interesting to note that the majority of authors prefer the relaxation time approximation. We now show how this method is used (c.f. [6]). The collision term  $C = C[f, f]$  in the transport equation

$$p^\mu \partial_\mu f = C[f, f] \quad (3.1)$$

is approximated by

$$C = -\frac{p^\mu U_\mu}{\tau} (f - f^{(0)}), \quad (3.2)$$

which corresponds to a mapping of all eigenvalues of the collision operator to one value. This value is the relaxation time  $\tau$  and can be viewed as a characteristic time-scale of non-equilibrium processes in the system.

Making an Ansatz for  $f$  in terms of the equilibrium distribution function  $f^{(0)}$  and a deviation  $\delta f$ , i.e.

$$f = f^{(0)} + \delta f, \quad (3.3)$$

one finds a linear expression for  $\delta f$  in terms of the relaxation time and derivatives of the function  $f^{(0)}$ , i.e.

$$\delta f = -\frac{\tau}{p^\mu U_\mu} [p^\mu \partial_\mu f^{(0)}]. \quad (3.4)$$

This explicit expression for the deviation can now be used in the general expression for the energy momentum tensor  $T^{\mu\nu}$ , which is separated into its equilibrium part  $T^{(0)\mu\nu}$  and a deviation  $\Delta T^{\mu\nu}$  due to non-equilibrium processes, i.e.

$$\begin{aligned}
T^{\mu\nu} &\equiv \int \frac{d^3p}{(2\pi)^3 p^0} p^\mu p^\nu f \\
&= \int \frac{d^3p}{(2\pi)^3 p^0} p^\mu p^\nu (f^{(0)} + \delta f) \\
&= T^{(0)\mu\nu} + \Delta T^{\mu\nu}.
\end{aligned} \tag{3.5}$$

The same is done for the particle flow vector, i.e.

$$\begin{aligned}
N^\mu &\equiv \int \frac{d^3p}{(2\pi)^3 p^0} p^\mu f \\
&= \int \frac{d^3p}{(2\pi)^3 p^0} p^\mu (f^{(0)} + \delta f) \\
&= N^{(0)\mu} + \Delta N^\mu.
\end{aligned} \tag{3.6}$$

Because of the ambiguities in the thermodynamic quantities arising from the deviation from equilibrium, a prescription has to be found to define these quantities. This is accomplished by making a special choice of the hydrodynamic four-velocity. In the Eckart choice, one relates the hydrodynamic four-velocity to the particle flow vector, i.e.

$$U^\mu = \frac{N^\mu}{N^\nu U_\nu}, \tag{3.7}$$

which implies that the spatial components of  $N^\mu$  vanish in the local rest frame. Another choice of the four-velocity is the Landau/Lifschitz convention, in which case  $U^\mu$  is related to the flow of energy, i.e.

$$U^\mu = \frac{T^{\mu\nu} U_\nu}{U_\mu T^{\mu\nu} U_\nu}, \tag{3.8}$$

which in turn implies that, in the local rest frame, the flow of energy vanishes. These choices are a matter of convention and still others are possible (c.f. Israel [17]), but they all lead to the same result if applied consistently.

After the decompositions (3.5) and (3.6) have been complemented by a particular choice of the four-velocity, an expression for these non-equilibrium parts in terms of the transport coefficients needs to be obtained. The theory of relativistic imperfect fluids [25] shows that  $\Delta T^{\mu\nu}$  can be written in terms of the transport coefficients and the thermodynamic forces. A particular choice of equilibrium distribution function  $f^{(0)}$  then leaves the transport coefficients uniquely defined

in terms of the relaxation time  $\tau$ , and easy to calculate. The problem remaining, namely to find the correct relaxation time  $\tau$  for the system, makes the latter not only the most important quantity in the evaluation of the transport coefficients, but also the most uncertain.

It turns out that the relaxation time method is reasonably well suited to describe simple systems, i.e. one component systems, but fails when applied to mixtures. The reason is that, in our opinion, the notion of a relaxation time cannot easily be extended to incorporate reaction events that distinguish between different particle species. For example, a scattering event between two quarks and between a quark and a gluon is different. To take this difference into account, some authors, for example Gavin [7], have tried to extend the definition of the relaxation time to include multi-species scattering by setting

$$\tau = \frac{1}{n \sigma} = \sum_{k=1}^N \frac{1}{n_k \sigma_k}. \quad (3.9)$$

Here,  $n$  is the particle density,  $\sigma$  the interaction cross-section and  $N$  is the number of species in the mixture. However, the transport cross-section  $\sigma_k$  is not well defined, and various approaches are suggested in the literature on how to compute it (see for example [40]). But these various methods lead to different estimates of its magnitude, which makes it unsuitable to use. This is a shortcoming of the relaxation time approach. The Chapman Enskog method on the other hand, has a well defined procedure leading to the definition of a transfer cross-section in terms of the differential cross-section, which is a function of the cm differential cross-section for each individual reaction channel. This ensures that, in a mixture, each collision is appropriately weighted in a reaction and it therefore surpasses any ambiguous evaluation procedures. This discussion is substantiated in Appendix B, where it is shown how and why the transfer cross-section arises in the CE method of solution.

In what follows, we briefly describe the methods used by some authors to compute the transport coefficients of quarks and gluons, making use of the terminology established in this section.

### 3.1 Weinberg

Although Weinberg's derivation [24] of the transport coefficients is not specifically aimed at QCD matter, his work provides a good foundation which has been used and extended by many authors. The coefficients Weinberg derived were for massless particles and were intended for the study of cosmological entropy generation. He made use of the Eckart definition of the hydrodynamic four-velocity, and then constructed a general form for the non-equilibrium part of the energy momentum tensor in such a way that the rate of entropy production is positive for all possible fluid configurations. He was led by the principle that all non-equilibrium contributions to the energy momentum tensor must be linear combinations of space-time derivatives of the thermodynamic quantities, such as the temperature, density and four-velocity. This provided the general structure of the non-equilibrium part of the energy momentum tensor as allowed by rotational and space-inversion invariance, leading to a covariant form of the entropy production in terms of the transport coefficients and the thermodynamic forces. He then proved that the volume viscosity  $\eta_v$  is negligible in the extreme relativistic and non-relativistic limits for simple systems, but that it can be finite in mixtures of relativistic and non-relativistic particles. Then, using the results from Thomas [41], who solved the relativistic transport equation for massless particles to first order in the relaxation time  $\tau$ , Weinberg established a link between his approach, based on general macroscopic considerations, and that by Thomas, in order to determine the transport coefficients. They are the volume viscosity  $\eta_v$ , the shear viscosity  $\eta$  and the heat conductivity  $\lambda$ , given by

$$\eta_v|_w = 0, \quad (3.10)$$

$$\eta|_w = \frac{4}{15} b T^4 \tau, \quad (3.11)$$

$$\lambda|_w = \frac{4}{3} b T^3 \tau, \quad (3.12)$$

where  $b = g \frac{\pi^2}{30}$  ( $\frac{7}{8} g \frac{\pi^2}{30}$ ) for bosons (fermions), and  $g$  is the particle multiplicity and  $T$  is the temperature.

The Eucken relation, i.e. the ratio of the heat conductivity to shear viscosity, a quantity often used in non-relativistic kinetic theory [12], is given by

$$\frac{\lambda}{\eta} = \frac{5}{T}, \quad (3.13)$$

a result found by most authors using the relaxation time approximation.

## 3.2 Danielewicz and Gyulassy

These authors [9] provide a wealth of information on estimating the magnitude of transport coefficients in quark-gluon plasmas, and they include some QCD phenomenology to estimate the effects of color shielding. Using the Landau/Lifschitz definition of the four-velocity and the relaxation time approximation to solve the relativistic Boltzmann equation, they arrive at an expression for the heat conductivity in the limit of small baryon number, given by

$$\lambda|_{\text{DG}} = \frac{4}{3T} \tau_q w^2 \frac{N_c N_f T^2}{12}, \quad (3.14)$$

where  $N_c$  ( $N_f$ ) is the number of quark colors (flavors) and  $w$  is the enthalpy per particle. The relaxation time  $\tau_q$  denotes that only quarks are contributing. For a two flavor quark system, i.e. with  $N_c = 3$  and  $N_f = 2$ , one obtains

$$\lambda|_{\text{DG}} = \frac{2}{3} \tau_q \left(\frac{w}{T}\right)^2 T^3. \quad (3.15)$$

They also find a range of validity for the shear viscosity  $\eta$  for scaling hydrodynamical applications. For plasmas well within the perturbative regime, with  $N_f = 2$ , their expression for the shear viscosity is given by

$$\eta|_{\text{DG}} = \frac{17}{10} \frac{T^3}{\pi \alpha_s^2 \log(1/\alpha_s)}, \quad (3.16)$$

which takes the plasma shielding effects into account, as can be seen from the logarithmic factor in the denominator. We postpone the discussion of this feature to section 3.4, where the results of Hosoya and Kajantie [8] are presented.

The authors note that the volume viscosity vanishes in the ultra-relativistic limit, in agreement with previous results,

$$\eta_v|_{\text{DG}} = 0. \quad (3.17)$$

They calculate the volume viscosity for the quark-hadron phase transition, which is finite, as can be expected. Their summary includes an interesting application to the problem of relating final, observed, rapidity densities to initial energy densities. They find that dissipative effects enhance the rapidity density by a factor of 1.3 to 1.6. Furthermore, they find that the energy density and temperature decrease slower with time when dissipative effects are included in calculations of the post-collisional expansion phase in heavy ion collisions. This is in agreement with our results obtained in the discussion of the applications in Chapter 7.

### 3.3 Gavin

Gavin [7] uses the well known non-relativistic form of the Boltzmann equation,

$$\left[ \frac{\partial}{\partial t} + \vec{v} \cdot \vec{\nabla} \right] f = C[f] \quad (3.18)$$

and the corresponding relaxation time (Gavin calls it collision time) approximation for the collision term, i.e.

$$C[f] = -\frac{1}{\tau} (f - f^{(0)}). \quad (3.19)$$

He then proceeds to solve the transport equation in the standard way [40] by finding the non-equilibrium contributions to the energy momentum tensor and the particle flow, using the Eckart convention, and the decomposition of the non-equilibrium contributions in terms of the transport coefficients (following Weinberg). His results, for massless systems, are

$$\eta_{\nu}|_{\text{G}} = 0, \quad (3.20)$$

$$\eta|_{\text{G}} = \frac{4}{15} [\tau_q en_q + \tau_g en_g], \quad (3.21)$$

$$\lambda|_{\text{G}} = \frac{4}{27} \tau_q en_q \frac{c_V}{n_b^2} \left( \frac{\partial n_b}{\partial \mu_b} \right)_T + \frac{4}{3} \tau_g \frac{en_g}{T} \quad (3.22)$$

where  $en_q$  ( $en_g$ ) is the energy density of quarks (gluons),  $n_b$  the baryon number and  $c_V$  the specific heat. The relaxation times are assumed to be different for quarks ( $\tau_q$ ) and gluons ( $\tau_g$ ). The results differ from those presented by Weinberg, since Gavin explicitly incorporates baryon-number conservation.

A comparison with pion transport coefficients is made, and his discussion provides some useful applications. An estimate of the entropy production and energy density evolution in scaling hydrodynamics is given. This will be investigated further in Chapter 6, where we compare our numerical results to others in the literature.

### 3.4 Hosoya and Kajantie

These authors [8] give a description of an approximation scheme for solving the fully covariant kinetic equation, which is very similar to the method employed in this thesis. However, because of the technical difficulty of solving the resultant phase-space integrals (see Appendix B), they elect to use the relaxation time approximation with Eckart's choice of the four-velocity. This method then also allows them to determine the transport coefficients for both fermions and bosons, which remains a forbidding task in our method of solution. The difference with respect to Gavin's analysis is the use of the relativistic Boltzmann equation and its corresponding collision term approximation (i.e. of the type (3.2) as compared to (3.19)). Other aspects of their analysis are similar to Weinberg's and Gavin's treatment.

An interesting feature of their work is the explicit consideration of the infrared divergent transport cross-sections, due to the divergent Rutherford-like cross-sections of the scattering processes at small angles. To avoid this problem they introduce a small angle cut-off  $\theta_{\min}$ , taking care of plasma shielding effects. This will be discussed in greater detail in Appendix D, where Coulomb logarithms are introduced to take this problem into account. Their resulting transport cross-section  $\sigma_t$  then takes the form

$$\begin{aligned}\sigma_t &= \alpha_s^2 \frac{\log(1/\theta_{\min})}{T^2} \\ &= \frac{3}{2} \alpha_s^2 \frac{\log(1/\alpha_s)}{T^2}.\end{aligned}\tag{3.23}$$

A similar logarithmic factor also features in our results, although in our case, it is obtained using a very different method of solution.

Their final results, for a 2-flavor quark-gluon plasma, are

$$\eta_v|_{\text{HK}} = 0,\tag{3.24}$$

$$\eta|_{\text{HK}} = 0.28 \frac{T^3}{\alpha_s^2 \log(1/\alpha_s)},\tag{3.25}$$

$$\lambda|_{\text{HK}} = 0.08 \left(\frac{w}{T}\right)^2 \frac{T^2}{\alpha_s^2 \log(1/\alpha_s)}.\tag{3.26}$$

Because a fully covariant Boltzmann equation is used, this approximation is the most suitable in the framework of the relaxation time approach. In this context, it is interesting to note that the results obtained here display the greatest structural similarity to our results, compared to those of the other authors mentioned in this section.

### 3.5 Baym, Monien, Pethick and Ravenhall

The authors [42] recently published an interesting paper showing how the inclusion of the Landau damping (see also [43] and [44]) of the virtual gluons provides an effective long wavelength cut-off for the diverging scattering cross-sections. They solve the non-relativistic Boltzmann equation with the proper quantum statistics to obtain the shear viscosity of gluons and a quark-gluon plasma, making use of a variational method of solution [45].

They obtain the (corrected) expression

$$\eta|_{\text{BMPR}} \simeq 0.342 \frac{T^3}{\alpha_s^2 \log(1/\alpha_s)} \quad (3.27)$$

for the shear viscosity of a pure gluon system.

Their quark to gluon shear viscosity ratio is given by

$$\frac{\eta_{\text{quark}}}{\eta_{\text{gluon}}}|_{\text{BMPR}} \simeq 1.70 N_f, \quad (3.28)$$

where  $N_f$  is the quark-flavor number. We will discuss this ratio, and the corresponding one from our results, in Chapter 5 .

This paper is one of the few references considering both the effects due to longitudinal and transverse gluon exchange, their different physical manifestations and the corresponding cures to the different divergences.

### 3.6 Further Approaches

Here follows a brief discussion of articles from authors who have considered the transport coefficients of QCD, but have either not presented their results in a form comparable to ours, or have not shown their numerical results.

Horsley and Schoenmaker [46] find the transport coefficients for the scalar  $\lambda\phi^4$  theory, using the Mori approach of linear response theory. The coefficients are then given in terms of auto-correlation functions of certain currents, resulting in the Kubo-type formulae. Their high temperature results are used to find the transport coefficients of quarkless QCD matter. By making an identification of the coupling constant  $\lambda$  in terms of the gluon-gluon cross-section of the type that Hosoya and Kajantie [8] used, they find

$$\eta_v|_{\text{HS}} = 0, \quad (3.29)$$

$$\eta|_{\text{HS}} = c' \frac{T^3}{\alpha_s^2 \log(1/\alpha_s)}, \quad (3.30)$$

$$\lambda|_{\text{HS}} = c' \frac{5 T^2}{\alpha_s^2 \log(1/\alpha_s)}, \quad (3.31)$$

where  $c'$  is in the range

$$0.08 \leq c' \leq 0.25. \quad (3.32)$$

They find, by use of scaling hydrodynamics, that there is a maximum possible increase in entropy of 20% if dissipative effects are included. We will investigate this problem using our results in Chapter 7. Another interesting feature is their investigation of the low temperature, or glueball phase, where they find that the transport coefficients can make an important contribution to the entropy generation.

Ilyin, Panferov and Sinyukov [47] use the Green-Kubo type formulae to obtain the shear viscosity of a QCD plasma at a one-loop perturbation theory level. This method of solution amounts to the evaluation of the correlation function of the spatial components of the energy momentum tensor, in order to obtain  $\eta$ . With the dispersion relations and the damping constant for the collective plasmon mode of the system, they obtain the following estimate for the pure gluon sector

$$\eta|_{\text{IPS}} \geq 2.6 \frac{T^3}{\alpha_s}. \quad (3.33)$$

Their approach is one of the few methods where the color structure of QCD was incorporated in a formal (in contrast to “hand-waving”) manner, and their

analysis warrants further attention, especially in the study of the other kinetic coefficients of the QGP.

Karsch and Wyld [48] obtain, on the basis of lattice Monte Carlo (LMC) computations, an upper bound on the shear viscosity. This was done as follows: using the definition of the energy momentum tensor, they calculated the thermal correlation function of its components. The shear viscosity can then be expressed in terms of diagonal elements of  $T^{\mu\nu}$  (which is advantageous for LMC simulations) as found in the Kubo-type formulae. This gives an estimate of the shear viscosity

$$\eta|_{\text{KW}} \leq 9.5 T^3, \quad (3.34)$$

for  $T$  close to the deconfinement temperature  $T_c$ .

The authors note that further investigations, especially on larger lattices and with particular attention to the space-time components of  $T^{\mu\nu}$  (in order to compute the heat conductivity  $\lambda$ ), should be carried out using their method, to obtain better results.

Chakrabarty [49] solves the relativistic Boltzmann transport equation using the relaxation time approximation. He uses the same covariant notation as used in this thesis and incorporates the proper quantum statistics into the expressions for the transport coefficients. Unfortunately, he does not determine the magnitude of the various relaxation times. This leaves all his expressions for the transport coefficients in terms of this important quantity.

Heinz [21] was the first to derive an expression for the color conductivity of a QGP in the framework of kinetic theory, using the linear response approximation. It is given by

$$\sigma = \tau \Omega_P^2, \quad (3.35)$$

in terms of the relaxation time  $\tau$  and the plasma frequency  $\Omega_P$ . This is the same result as found by Mrówczyński [52], which will be discussed below.

It is interesting to note that the conductivity (3.35) has a  $\alpha_s^{-1}$  dependence on the strong coupling constant, since  $\tau \propto \alpha_s^{-2}$  and  $\Omega_P^2 \propto \alpha_s$ . This is in contrast to our result presented in Chapter 5, we find that  $\sigma \propto \alpha_s^{-2}$ .

Czyż and Florkowski [50] solve the transport equation for quarks and antiquarks (see (2.13)) using the relaxation time method. They follow the procedure of Anderson and Witting [6] for Maxwell Boltzmann type particles to obtain the

baryon and color currents. This enables them to find a generalised version of Ohm's law, thereby explicitly showing the dependence of the color conductivity on thermodynamic quantities. Likewise, they obtain expressions for the other transport coefficients from the study of the non-equilibrium part of the energy momentum tensor.

A very similar analysis to that of Czyż and Florkowski [50] was published by Dyrek and Florkowski [51], the essential difference being the quantum mechanical treatment of color via density matrices, which for finite temperatures gives rise to results different from the classical case.

The color conductivity was studied by Mrówczyński [52] in the relaxation time approximation. One should note that he used the transport cross-section [9]

$$\sigma_t = \frac{10 \pi}{17 T^2} \alpha_s^2 \log(1/\alpha_s) \rightarrow \frac{5}{136 \pi T^2} g^4 \log(1/g^2) \quad (3.36)$$

to obtain an estimate for the relaxation time  $\tau = 1/n \sigma_t$ , and not the full differential cross-section that we use (see Appendix C). His (corrected) color conductivity is then given by

$$\sigma|_M = \frac{17 \pi^2 (N_f + 6) T}{45 (9 N_f + 16) \zeta(3) \alpha_s \log(1/\alpha_s)}. \quad (3.37)$$

It turns out that a comparison with our result from section 5.3 is easier if one writes this result in terms of the number density  $n$  in the Maxwell Boltzmann approximation and takes only quarks and antiquarks into consideration. This gives

$$\sigma|_M = \frac{34 T^4}{45 n \alpha_s \log(1/\alpha_s)}. \quad (3.38)$$

Comparison of (3.38) with our result will be discussed in Chapter 6.

# Chapter 4

## The Chapman Enskog Method

In this Chapter we present the Chapman Enskog method to solve the transport equations derived in Chapter 2, describing simple particle systems, binary mixtures and mixtures in an external field. These transport equations are non-linear integro-differential equations, and are in general, difficult to solve without simplifying assumptions.

The Chapman Enskog method provides a set of rules which make it possible to extract the transport coefficients from the transport equations. The method amounts to the rewriting and solution of the transport equation, such that the phenomenologically motivated linear relations between the thermodynamic forces and flows are recovered. The transport coefficients are the constants of proportionality between the forces and flows, and can thus be obtained by making use of explicit expressions for the forces and flows.

The non-linearity of the collision term is removed by assuming that the system is not far from the equilibrium state. The form of the distribution function is then determined by an expansion around a specific local equilibrium distribution function, which in turn accomplishes the linearisation of the collision term. Then, by using the linear laws for the transport processes between the non-equilibrium manifestations in the system, i.e. the thermodynamic forces and flows, one decomposes the transport equation. The linear subequations obtained by this method can be related to the flows of the system, and an identification of the transport coefficients is then possible.

We now proceed to implement the above program mathematically. In the next section, the solution of (2.16) and (2.17) is presented. It will become apparent, even with the simplifying assumptions to the transport equation (2.13) which led to (2.16) and (2.17), that the task of computing the transport coefficients remains formidable.

## 4.1 Solution

In this section we linearise the transport equation (2.16). Then we rewrite the linearised equation in a form suitable for decomposition, by introducing the thermodynamic forces of the system.

The transport equation to be solved, i.e. the relativistic Boltzmann equation, describing the space-time evolution of the phase space density  $f = f(x, p)$ , is given in eq.(2.16)

$$p^\mu \partial_\mu f = C[f, f]. \quad (4.1)$$

The collision term  $C[f, f]$ , in the Boltzmann approximation, is given by

$$C[f, f] = \frac{1}{2} \int \frac{d^3 p_2}{p_2^0} \frac{d^3 p_3}{p_3^0} \frac{d^3 p_4}{p_4^0} \cdot [ f_3 f_4 (1 + \theta f_1) (1 + \theta f_2) - f_1 f_2 (1 + \theta f_3) (1 + \theta f_4) ] W(p_3 p_4 | p_1 p_2), \quad (4.2)$$

where  $W(p_3 p_4 | p_1 p_2)$  is the transition rate in the collision process

$$p_1 + p_2 \leftrightarrow p_3 + p_4.$$

The constant  $\theta$  can assume different values depending on the type of particles to be described. Fermions have  $\theta = -1$ , bosons  $\theta = +1$  and classical particles (i.e. particles where the equilibrium distribution function is of Maxwell Boltzmann type)  $\theta = 0$ , taking care of the effects of Pauli blocking (fermions) and Bose enhancement (bosons).

At this point a crucial assumption will be made. We will assume that particles are classical and therefore take  $\theta = 0$ . This assumption was made for two reasons:

- In the derivation of the evolution equation (2.13), emphasis has been placed on the fact that particles and their properties are classical. Quantum effects, such as spin, have been neglected.
- The second reason is of a more pragmatic nature and is concerned with the final computability of collision integrals of the type (4.2). For Maxwell Boltzmann-like particles these integrals can still be calculated analytically (as we will show later), whereas for  $\theta \neq 0$  the problem becomes technically much harder.

The kinetic equation (4.1) will now be linearised and solved, employing the Chapman Enskog method [4].

To this end the derivative operator  $\partial^\mu \equiv \partial/\partial x_\mu$  is split into a time-like and a space-like part

$$\partial^\mu \rightarrow U^\mu D + \nabla^\mu, \quad (4.3)$$

such that time- and space-derivatives can be separated. Here,

$$D \equiv U^\nu \partial_\nu \text{ and } \nabla^\mu \equiv \Delta^{\mu\nu} \partial_\nu, \quad (4.4)$$

where  $\nabla^\mu$  is the divergence operator and

$$\Delta^{\mu\nu} \equiv g^{\mu\nu} - U^\mu U^\nu \quad (4.5)$$

is the projection operator.  $U^\mu$  is the hydrodynamic four velocity.

To linearise the collision term (4.2) with  $\theta = 0$ , an expansion of the distribution function  $f$  into an equilibrium part  $f^{(0)}$  and a deviation  $\epsilon f^{(1)}$  is made, i.e.

$$f = f^{(0)} + \epsilon f^{(1)}. \quad (4.6)$$

To order  $\epsilon$ , the transport equation (4.1) then reads

$$p^\mu U_\mu D f_1^{(0)} + p^\mu \nabla_\mu f_1^{(0)} = -f_1^{(0)} L[\phi]. \quad (4.7)$$

$L[\phi]$  is the linearised collision operator found from (4.2) by making use of (4.6) and invoking the principle of detailed balance, i.e.

$$f_1^{(0)} f_2^{(0)} = f_3^{(0)} f_4^{(0)}.$$

Then

$$L[\phi] \equiv \frac{1}{2} \int \frac{d^3 p_2}{p_2^0} \frac{d^3 p_3}{p_3^0} \frac{d^3 p_4}{p_4^0} f_2^{(0)} (\phi_1 + \phi_2 - \phi_3 - \phi_4) W(p_3 p_4 | p_1 p_2) \quad (4.8)$$

where  $\phi_i$  is the ratio  $f_i^{(1)}/f_i^{(0)}$ . The equilibrium distribution functions  $f_i^{(0)}$  are taken to be of the Maxwell Boltzmann (Jüttner) type

$$f_i^{(0)} = \exp\left(\frac{\mu_i(x) - p_i^\nu U_\nu(x)}{T(x)}\right), \quad (4.9)$$

with space-time dependent parameters  $\mu, U^\mu$  and  $T$ . However, the functions  $\mu(x), U^\mu(x)$  and  $T(x)$  as used in (4.9) do not necessarily correspond to the chemical potential, hydrodynamic velocity and temperature of the system. Only by defining certain quantities in terms of these parameters, do they acquire the "normal" meaning. This is accomplished by demanding that the particle density  $n$  and

the energy density  $en$  be determined *solely* by the local equilibrium distribution function (4.9)

$$n \equiv \int \frac{d^3p}{(2\pi)^3 p^0} (p^\mu U_\mu) f^{(0)}, \quad (4.10)$$

$$en \equiv \int \frac{d^3p}{(2\pi)^3 p^0} (p^\mu U_\mu)^2 f^{(0)}, \quad (4.11)$$

or, likewise, in terms of the deviation function

$$\int \frac{d^3p}{p^0} (p^\mu U_\mu) f^{(1)} = \int \frac{d^3p}{p^0} (p^\mu U_\mu)^2 f^{(1)} = 0. \quad (4.12)$$

These are the so-called conditions of fit.

The choice of the distribution function (4.9), together with (4.10) and (4.11) determines the set of independent variables, i.e. the temperature, chemical potential and hydrodynamic velocity. Because of the definition of the particle density in (4.10) it is clear that the set  $(T, \mu, U^\nu)$  can also be translated into the set  $(T, n, U^\nu)$ . This new choice of independent variables is motivated by the desire to derive the Euler equation, as will be done further below. We are now able to implement the Chapman Enskog philosophy by computing the derivatives of the distribution function  $f^{(0)}$ , which by construction is space-time dependent only via its dependence upon the set of independent variables. This leads to

$$\begin{aligned} Df^{(0)} &= \frac{\partial f^{(0)}}{\partial n} Dn + \frac{\partial f^{(0)}}{\partial T} DT + \frac{\partial f^{(0)}}{\partial U^\mu} DU^\mu \\ &= \left[ \frac{\partial \mu}{\partial n} Dn + \left( T^2 \frac{\partial}{\partial T} \left( \frac{\mu}{T} \right) + p^\nu U_\nu \right) D(\log T) - p_\mu DU^\mu \right] \frac{f^{(0)}}{T} \end{aligned} \quad (4.13)$$

and

$$\nabla^\alpha f^{(0)} = \left[ T \nabla^\alpha \left( \frac{\mu}{T} \right) + p^\nu U_\nu \nabla^\alpha \log T - p^\nu \nabla^\alpha U_\nu \right] \frac{f^{(0)}}{T} \quad (4.14)$$

in terms of the density  $n$ , the temperature  $T$ , the hydrodynamic four-velocity  $U^\mu$  and the chemical potential  $\mu$ .

With the conditions of fit (4.12) defining the thermodynamic quantities, one computes the derivatives  $Dn$ ,  $DT$  and  $DU^\mu$  as needed in (4.13). Operating on the linearised transport equation (4.7) with  $\int d^3p/p^0$  one obtains

$$\int \frac{d^3p}{p^0} p^\mu U_\mu Df_1^{(0)} + \int \frac{d^3p}{p^0} p^\mu \nabla_\mu f_1^{(0)} = 0, \quad (4.15)$$

where the right hand side vanishes because of the conservation laws of energy and momentum. Upon substitution of (4.13) and by applying the conditions of fit (4.12), the continuity equation (or Euler equation) is derived

$$Dn = -n \nabla_\mu U^\mu. \quad (4.16)$$

Operating on (4.7) with  $\int d^3p p^\mu/p^0$  and contracting with  $U^\mu$ , gives the energy equation

$$DT = -\frac{T}{c_V} \nabla_\mu U^\mu = -(\gamma - 1) T \nabla_\mu U^\mu, \quad (4.17)$$

where  $c_V$  is the heat capacity per particle at constant volume defined by  $c_V \equiv \frac{\partial e}{\partial T}$ .  $\gamma$  is the ratio of the heat capacities at constant pressure and constant volume, i.e.  $\gamma \equiv c_P/c_V$ ; the ideal equation of state, i.e.  $P = nT$  has also been used (see Appendix E). It should be pointed out that the energy equation (4.17) has its simple form because of the Boltzmann statistics, where the energy per particle  $e = en/n$  is independent of  $\mu$ . When using quantum statistics the expression (4.17) is considerably modified.

After the multiplication of (4.7) by  $\int d^3p p^\mu/p^0$  and contraction with the projection operator  $\Delta_{\mu\nu}$ , the equation of motion is obtained, namely

$$DU^\mu = \frac{1}{wn} \nabla^\mu P. \quad (4.18)$$

Here  $wn$  is the enthalpy density,  $wn = en + P$ , and  $P$  is the pressure.

The respective conservation laws for the particle flow and the energy momentum are also recovered. Operating on (4.1) with  $\int d^3p/p^0$  and  $\int d^3p p^\mu/p^0$ , respectively, we find

$$\partial_\mu N^\mu \equiv \partial_\mu \int \frac{d^3p}{p^0} p^\mu f^{(0)} = 0 \quad \text{and} \quad \partial_\mu T^{\mu\nu} \equiv \partial_\mu \int \frac{d^3p}{p^0} p^\mu p^\nu f^{(0)} = 0. \quad (4.19)$$

These equations express the macroscopic conservation laws for a simple relativistic fluid of classical particles which are spinless and colorless, in terms of the particle flow vector  $N^\mu$  and the energy momentum tensor  $T^{\mu\nu}$ .

The conservation laws (4.16) – (4.19) are well known from ideal relativistic hydrodynamics (perfect fluid theory) and form an important part in the implementation of the Chapman Enskog method. The above procedure of derivation transparently shows the connection between the micro- and macroscopic laws, a feature which makes kinetic theory both an intuitive and useful tool to work with. Also, following a procedure similar to that presented, one easily extends the study to systems in an external field. This will be demonstrated in section 4

of this Chapter.

The linearised transport equation (4.7) can now be rewritten in terms of the thermodynamic forces of the system, which consists of a scalar force, due to the divergence of the hydrodynamic velocity

$$X \equiv -\nabla_\mu U^\mu, \quad (4.20)$$

a vector force, due to the temperature gradient and in relativistic systems the pressure gradient

$$X_q^\mu \equiv \nabla^\mu \log T - \frac{1}{wn} \nabla^\mu P \quad (4.21)$$

and a tensor force (traceless as indicated by the superscript  $o$ ), due to the gradient of the hydrodynamic velocity

$$\overset{o}{X}^{\mu\nu} \equiv \frac{1}{2} \nabla^\mu U^\nu + \frac{1}{2} \nabla^\nu U^\mu - \frac{1}{3} \Delta^{\mu\nu} \nabla_\alpha U^\alpha. \quad (4.22)$$

These thermodynamic forces can be identified, after substituting the conservation laws (4.16) – (4.18) into the derivative  $Df^{(0)}$  in (4.13), and (4.13) and (4.14) into the linearised transport equation (4.7). In terms of these forces, the transport equation is then found to be

$$YX - p_\nu (p^\mu U_\mu - w) X_q^\nu + p_\mu p_\nu \overset{o}{X}^{\mu\nu} = T L[\phi]. \quad (4.23)$$

The abbreviation

$$Y \equiv \left( \frac{4}{3} - \gamma \right) (p^\nu U_\nu)^2 + [(\gamma - 1) w - \gamma T] p^\nu U_\nu - \frac{m^2}{3} \quad (4.24)$$

was introduced and the relativistic Gibbs-Duhem relation

$$T \nabla^\alpha \left( \frac{\mu}{T} \right) = -w \left( \frac{\nabla^\alpha T}{T} - \frac{\nabla^\alpha P}{wn} \right) = -w X_q^\alpha \quad (4.25)$$

was used in the derivation of (4.23).

Equation (4.23) is now in a form suitable for decomposition. This will be further investigated in the next section.

A two component mixture (components labelled by subscripts 1 and 2) is described by an equation very similar to (4.23). Rather than fully derive the

equations which pertain to mixtures, we indicate the few differences which have to be made when extending the derivation of (4.23) to a binary mixture. The analogue of the linearised transport equation (4.7) applicable to mixtures can be written as

$$p_1^\mu U_\mu D f_1^{(0)} + p_1^\mu \nabla_\mu f_1^{(0)} = -f_1^{(0)} \sum_{k=1}^2 L_{1k}[\phi]. \quad (4.26)$$

The right hand side takes collisions of the form  $1 + 1 \rightarrow 1 + 1$  and  $1 + 2 \rightarrow 1 + 2$  into account. The linearised operator  $L_{1k}[\phi]$  is given by

$$L_{1k}[\phi] \equiv \left(1 - \frac{\delta_{1k}}{2}\right) \int \frac{d^3 p_2}{p_2^0} \frac{d^3 p_3}{p_3^0} \frac{d^3 p_4}{p_4^0} f_k^{(0)} (\phi_1 + \phi_2 - \phi_3 - \phi_4) W_{1k}(p_3 p_4 | p_1 p_2). \quad (4.27)$$

The factor  $(1 - \delta_{1k}/2)$  accounts for the correct weighting of the integral in different scattering processes, i.e.  $\delta_{1k} = 0$  for all  $k \neq 1$ . The conservation laws (4.16) – (4.18) are not changed when considering mixtures.

However, a further thermodynamic force, namely the diffusion driving force, given by

$$X_1^\alpha \equiv (\nabla^\alpha \mu_1)_{P,T} - (\nabla^\alpha \mu_2)_{P,T} - \frac{w_1 - w_2}{wn} \nabla^\alpha P, \quad (4.28)$$

has to be introduced when dealing with mixtures. With  $x_i \equiv n_i/(n_1 + n_2)$  being the particle density fraction,  $n_i$  the particle density and  $w_i$  the enthalpy per particle of component  $i$  we find that the energy per particle is given by  $e = \sum_k x_k e_k$  and the entropy per particle given by  $s = (e + P/n - \sum_k x_k \mu_k)/T$ . These relations enable us to find the Gibbs-Duhem relation as valid for binary mixtures

$$T \nabla^\alpha \left(\frac{\mu_k}{T}\right) = -w_k \left(\frac{\nabla^\alpha T}{T}\right) + T \left(\frac{\nabla^\alpha P}{nT}\right) + (\nabla^\alpha \mu_1)_{P,T} - (\nabla^\alpha \mu_2)_{P,T}. \quad (4.29)$$

The further derivation, i.e. the rewriting of the transport equation in terms of the thermodynamic forces, then proceeds analogously to the one leading to eq.(4.23) and we refer the interested reader to p.167(58) and p.177 in the monograph by de Groot et al. [4] where some details useful for the derivation are explained.

For component 1 we then find

$$Y_1 X - p_1^\nu (p_1^\mu U_\mu - w_1) X_{q\nu} - p_1^\mu x_2 X_{1\mu} + p_1^\mu p_1^\nu \overset{\circ}{X}_{\mu\nu} = T \sum_{l=1}^2 L_{1l}[\phi_l]. \quad (4.30)$$

An equation similar to (4.30) holds for component 2.

The linearised form of eq.(4.23) and (4.30) makes it possible to separate the thermodynamic forces and the corresponding flows, thereby obtaining explicit expressions for the transport coefficients. This is our goal in the following sections.

## 4.2 One Component System

In this section we derive the transport coefficients for a simple one component system as described by the transport equation (4.23).

We observe that the thermodynamic forces  $X$ ,  $X_q^\mu$  and  $\overset{\circ}{X}^{\mu\nu}$ , as they appear in (4.23), are linearly independent quantities. This enables one to make a particular choice for the deviation function  $\phi$ , namely

$$\phi \equiv \frac{1}{n \sigma(T)} \left( AX - B_\mu X_q^\mu + C_{\mu\nu} \overset{\circ}{X}^{\mu\nu} \right), \quad (4.31)$$

with a dimensionally suitable constant of proportionality  $1/(n \sigma(T))$ . Here,  $\sigma(T)$  is a typical mean thermal cross-section, and the coefficients  $A$ ,  $B_\mu$  and  $C_{\mu\nu}$  still have to be determined. In other words, the deviation function is a linear combination of the thermodynamic forces  $X$ ,  $X^\mu$  and  $\overset{\circ}{X}^{\mu\nu}$ . The sign of  $B^\mu$  in (4.31) is chosen in accordance with the sign of the vector force in (4.23). Inserting (4.31) into (4.23), the transport equation can be separated into three independent equations, namely

$$Y X = T L \left[ \frac{1}{n \sigma(T)} A X \right], \quad (4.32)$$

$$-(p^\nu U_\nu - w) p_\mu X_q^\mu = T L \left[ -\frac{1}{n \sigma(T)} B_\mu X_q^\mu \right], \quad (4.33)$$

$$p_\mu p_\nu \overset{\circ}{X}^{\mu\nu} = T L \left[ \frac{1}{n \sigma(T)} C_{\mu\nu} \overset{\circ}{X}^{\mu\nu} \right]. \quad (4.34)$$

The next step is the definition of the macroscopic irreversible flows of the simple system, namely the viscous pressure and the heat flow. Generally, flows appear in non-equilibrium situations, and, as such, they are functions of the deviation function  $\phi$ . We define the viscous pressure as

$$\Pi \equiv -\frac{1}{3} \int \frac{d^3 p}{p^0} \Delta_{\mu\nu} p^\mu p^\nu f^{(0)} \phi, \quad (4.35)$$

the heat flow as

$$I_q^\mu \equiv \int \frac{d^3 p}{p^0} \Delta^{\mu\sigma} p_\sigma (p^\nu U_\nu - w) f^{(0)} \phi, \quad (4.36)$$

and the traceless viscous pressure as

$$\overset{\circ}{\Pi}^{\mu\nu} \equiv \int \frac{d^3 p}{p^0} (\Delta_\alpha^\mu \Delta_\delta^\nu - \frac{1}{3} \Delta_{\alpha\delta} \Delta^{\mu\nu}) p^\alpha p^\delta f^{(0)} \phi. \quad (4.37)$$

Through the definition of a dimensionless inner product bracket of the form

$$\begin{aligned} (A, B) &\equiv \frac{T}{n} \int \frac{d^3p}{p^0} A(p) B(p) f^{(0)} \\ &= \frac{1}{4\pi z^2 K_2(z) T^2} \int \frac{d^3p}{p^0} A(p) B(p) e^{-\tau}, \end{aligned} \quad (4.38)$$

where the dimensionless quantities  $z \equiv m/T$  ( $m$  is the particle mass) and  $\tau \equiv p^\nu U_\nu / T$  have been used, the flows can now be rewritten in a more transparent form. With  $\overline{\pi^\mu} \equiv \Delta^{\mu\nu} \pi_\nu$ , where  $\pi^\nu \equiv p^\nu / T$ , the viscous pressure is then found to be given by

$$\Pi = -\frac{1}{3} n T (\overline{\pi^\mu \pi_\mu}, \phi), \quad (4.39)$$

the heat flow is

$$I_q^\mu = n T \left( \overline{\pi^\mu} \left( \tau - \frac{w}{T} \right), \phi \right), \quad (4.40)$$

and the traceless viscous pressure is

$$\overset{\circ}{\Pi}^{\mu\nu} = n T \left( \overset{\circ}{\overline{\pi^\mu \pi^\nu}}, \phi \right). \quad (4.41)$$

Here, the overbar indicates the symmetrisation with respect to the indices, and the superscript  $\circ$  is a reminder that the expression is also traceless by construction. Inserting the deviation function  $\phi$  from (4.31) into (4.39) – (4.41), the flows are written into the form

$$\Pi = \frac{T}{3\sigma(T)} (\overline{\pi^\mu \pi_\mu}, A) \nabla_\nu U^\nu \equiv \eta_\nu X \quad (4.42)$$

$$I_q^\mu = -\frac{T}{\sigma(T)} \left( \overline{\pi^\mu} \left( \tau - \frac{w}{T} \right), B_\nu \right) X_q^\nu \equiv T \lambda_\nu^\mu X_q^\nu, \quad (4.43)$$

and

$$\overset{\circ}{\Pi}^{\mu\nu} = \frac{T}{\sigma(T)} \left( \overset{\circ}{\overline{\pi^\mu \pi^\nu}}, C_{\alpha\beta} \right) \overset{\circ}{X}^{\alpha\beta} \equiv 2\eta \overset{\circ}{\nabla^\mu U^\nu}. \quad (4.44)$$

All other terms in  $\phi$  vanish due to the conditions of fit. These equations clearly illustrate the relationship between the thermodynamic forces and flows, and show how the transport coefficients arise as constants of proportionality between them. This linear relationship is a feature well known [53] from non-equilibrium thermodynamics, where, to first order, the forces in a system (i.e. gradients of thermodynamic quantities) are linearly related to the corresponding flows. As shown, in the

Forces	Transport Coefficients	Flows
$X$ from (4.20)	volume viscosity $\eta_v$	$\Pi$ from (4.35)
$X_q^\mu$ from (4.21)	heat conductivity $\lambda$	$I_q^\mu$ from (4.36)
$\overset{\circ}{X}{}^{\mu\nu}$ from (4.22)	shear viscosity $\eta$	$\overset{\circ}{\Pi}{}^{\mu\nu}$ from (4.37)

Table 4.1: Thermodynamic Forces, Flows and the Transport Coefficients.

Chapman Enskog method this relationship is exploited to obtain the transport coefficients: the volume viscosity  $\eta_v$  is found from (4.42), the heat conductivity  $\lambda \equiv \Delta^{\mu\nu} \lambda_{\mu\nu}/3$  from (4.43) and the shear viscosity  $\eta$  from (4.44). Table 4.1 summarises these linear relationships.

The transport coefficients still contain the unknown functions  $A, B^\mu$  and  $C^{\mu\nu}$ , and some further technical manipulation is required before one arrives at a form useful for computational purposes. The details of this very technical procedure are carried out in Appendix A. Here we shortly summarise what is done: The transport coefficients are written into a positive definite form, as demanded by the H-theorem. This is accomplished by using the separated transport equations (4.32) – (4.34) and the expressions (4.42) – (4.44). A variational method is then used to find the unknown coefficients  $A, B^\mu$  and  $C^{\mu\nu}$ . The resulting expressions for the transport coefficients are conveniently written in terms of so-called square collision brackets such as  $A^{22}, B^{11}$  and  $C^{00}$ . They are given by:

the volume viscosity

$$\eta_v = \frac{T}{\sigma(T)} \frac{(\alpha^2)^2}{A^{22}}, \quad (4.45)$$

the heat conductivity

$$\lambda = \frac{1}{3\sigma(T)} \frac{(\beta^1)^2}{B^{11}}, \quad (4.46)$$

and the shear viscosity

$$\eta = \frac{T}{10\sigma(T)} \frac{(\gamma^0)^2}{C^{00}}. \quad (4.47)$$

The definitions of the symbols  $\alpha^2, \beta^1$  and  $\gamma^0$  and the explicit expressions for

$A^{22}$ ,  $B^{11}$  and  $C^{00}$  are given in Appendix A. These transport coefficients and their numerical values for simple quark and gluon systems will be further investigated in Chapter 5.

### 4.3 Two Component System

We now consider a binary mixture consisting of two components labelled 1 and 2.

The equation that needs to be solved to obtain the transport coefficients for this mixture is given by (4.30). Analogously to the Ansatz for the trial function  $\phi$  in (4.31), a linear combination of the thermodynamic forces of the system is chosen, i.e.

$$\phi_k \equiv \frac{1}{n \sigma(T)} \left( A_k X - B_{k\mu} X_q^\mu - \frac{1}{T} B_{1k}^\mu X_{1\mu} + C_k^{\mu\nu} \overset{\circ}{X}_{\mu\nu} \right). \quad (4.48)$$

The only difference between the deviation function for the simple system (4.31) and  $\phi_k$  is the new force that appears in multi-component systems, namely the diffusion driving force  $X_1^\mu$ . Using the deviation function  $\phi_k$  from (4.48), the linearised transport equation (4.30) separates into

$$Y_1 = \frac{T}{n \sigma(T)} \sum_{l=1}^2 L_{1l} [A_1], \quad (4.49)$$

$$-(p_1^\nu U_\nu - w_1) p_1^\mu = \frac{T}{n \sigma(T)} \sum_{l=1}^2 L_{1l} [-B_1^\mu], \quad (4.50)$$

$$-x_2 p_1^\mu = \frac{T}{n \sigma(T)} \sum_{l=1}^2 L_{1l} \left[ -\frac{1}{T} B_{11}^\mu \right], \quad (4.51)$$

$$p_1^\mu p_1^\nu = \frac{T}{n \sigma(T)} \sum_{l=1}^2 L_{1l} [C_1^{\mu\nu}], \quad (4.52)$$

where, again, the factors  $A_1, B_1^\mu, B_{11}^\mu$  and  $C_1^{\mu\nu}$  are unknown functions to be determined later. It is important to notice that the linear law relating the viscous pressure to the divergence of the hydrodynamic velocity as in (4.42) and the law relating the traceless viscous pressure tensor to the hydrodynamic velocity as in (4.44) do not change their structure in a binary mixture. However, the linear law relating the heat flow to the temperature and pressure gradient, as in (4.43), has to be replaced, as can already be seen from the structure of the trial function (4.48).

In terms of the inner product bracket

$$\begin{aligned} (A_k, B_k) &\equiv \frac{T}{n_k} \int \frac{d^3 p_k}{p_k^0} A_k(p_k) B_k(p_k) f_k^{(0)} \\ &= \frac{1}{4 \pi z_k^2 K_2(z_k) T^2} \int \frac{d^3 p_k}{p_k^0} A_k(p_k) B_k(p_k) e^{-\tau_k}, \end{aligned} \quad (4.53)$$

the new irreversible flow, namely the reduced heat flow, can be written as:

$$\begin{aligned} \bar{I}_q^\mu &\equiv I_q^\mu - (w_1 - w_2) I_1^\mu \\ &= n T \sum_{k=1}^2 x_k \left( \bar{\pi}^\mu_k \left( \tau_k - \frac{w_k}{T} \right), \phi_k \right). \end{aligned} \quad (4.54)$$

Here,  $w_i$  denotes the enthalpy per particle of component  $i$ . Substituting (4.48) into (4.54) then gives

$$\bar{I}_q^\mu = l_{qq} X_q^\mu + l_{q1} X_1^\mu \quad (4.55)$$

where  $X_q^\mu$  is the generalised driving force of heat flow (4.21) and  $X_1^\mu$  the diffusion driving force (4.28), which is the flow due to gradients in the composition of the system. Comparing (4.54), (4.55) and (4.43) one finds the transport coefficients

$$l_{qq} \equiv \lambda T = -\frac{T}{3 \sigma(T)} \sum_{k=1}^2 x_k \left( \bar{\pi}^\mu_k \left( \tau_k - \frac{w_k}{T} \right), B_k \bar{\pi}_{\mu k} \right) \quad (4.56)$$

for the thermal conductivity  $\lambda$ , and

$$l_{q1} \equiv -\frac{1}{3 \sigma(T)} \sum_{k=1}^2 x_k \left( \bar{\pi}^\mu_k \left( \tau_k - \frac{w_k}{T} \right), B_{1k} \bar{\pi}_{\mu k} \right) \quad (4.57)$$

for the Dufour coefficient. This is a coefficient reflecting the heat flow in the presence of composition gradients in the mixture, and is also known as the diffusion thermo-coefficient. In the definition of these coefficients, we follow a convention familiar from non-relativistic studies, see for example de Groot and Mazur [53]. Another new feature in mixtures is the appearance of diffusion flow, given by

$$I_1^\mu = l_{11} X_1^\mu + l_{1q} X_q^\mu, \quad (4.58)$$

giving the diffusion coefficient

$$l_{11} \equiv -\frac{1}{3 T \sigma(T)} \sum_{k=1}^2 (\delta_{1k} - x_1) x_k \left( \bar{\pi}^\mu_k, B_{1k} \bar{\pi}_{\mu k} \right), \quad (4.59)$$

and the thermal diffusion coefficient

$$l_{1q} \equiv -\frac{1}{3\sigma(T)} \sum_{k=1}^2 (\delta_{1k} - x_1) x_k (\bar{\pi}^\mu_k, B_k \bar{\pi}_{\mu k}). \quad (4.60)$$

As a result of the relativistic Onsager relations [54], the thermal diffusion coefficient is equal to the Dufour coefficient in a binary mixture, i.e.

$$l_{1q} = l_{q1}. \quad (4.61)$$

In order to obtain a more intuitive understanding of the reduced heat flow  $I_q^\mu$  and the diffusion flow  $I_1^\mu$ , we now consider a system in mechanical equilibrium, i.e. where the pressure gradients vanish. The thermodynamic forces  $X_q^\mu$  and  $X_1^\mu$  then reduce to

$$X_q^\alpha \rightarrow \frac{1}{T} \nabla^\alpha T, \quad (4.62)$$

$$X_1^\alpha \rightarrow (\nabla^\alpha \mu_1)_{P,T} - (\nabla^\alpha \mu_2)_{P,T}. \quad (4.63)$$

The gradient of the chemical potential is related to the particle density fraction, i.e.  $x_i = n_i/(n_1 + n_2)$  as

$$(\nabla^\alpha \mu_i)_{P,T} = \frac{T}{x_i} \nabla^\alpha x_i. \quad (4.64)$$

In a non-reactive binary mixture, where the particle density fractions  $x_1$  and  $x_2$  are related as

$$x_1 + x_2 = 1, \quad (4.65)$$

the diffusion driving force in mechanical equilibrium can then be written as

$$X_1^\alpha \rightarrow \frac{T}{x_1 x_2} \nabla^\alpha x_1. \quad (4.66)$$

The linear laws (4.55) and (4.58) can thus be written as

$$I_q^\mu = l_{qq} \frac{\nabla^\mu T}{T} + l_{q1} \frac{T \nabla^\mu x_1}{x_1 x_2} \quad (4.67)$$

and

$$I_1^\mu = l_{11} \frac{T \nabla^\mu x_1}{x_1 x_2} + l_{1q} \frac{\nabla^\mu T}{T}. \quad (4.68)$$

The transport coefficients can now, in analogy with their non-relativistic counterparts, be identified: the heat conductivity

$$\lambda \equiv \frac{l_{qq}}{T}, \quad (4.69)$$

the Dufour coefficient

$$D'_T \equiv \frac{l_{q1}}{n x_1 x_2 T}, \quad (4.70)$$

the thermal diffusion coefficient

$$D_T \equiv \frac{l_{1q}}{n x_1 x_2 T}, \quad (4.71)$$

and the diffusion coefficient

$$D_d \equiv \frac{l_{11} T}{n x_1 x_2}. \quad (4.72)$$

These identifications make it possible to rewrite the linear laws relating the forces and flows of a binary mixture with vanishing pressure gradients into a transparent form

$$I_q^{\bar{\mu}} = \lambda \nabla^{\mu} T + P T D'_T \nabla^{\mu} x_1, \quad (4.73)$$

and

$$I_1^{\bar{\mu}} = n D_d \nabla^{\mu} x_1 + n x_1 x_2 D_T \nabla^{\mu} T. \quad (4.74)$$

The method of writing the transport coefficients for the two component mixture into the square collision bracket form is very similar to that for the single component system, as was shown in the previous section. The final expressions, in the lowest order of approximation, in terms of the square collision brackets, are then given by:

the **volume viscosity**

$$\eta_v = \frac{T}{\sigma(T)} x_1 x_2 \frac{\alpha_1^1 \alpha_2^1}{A_{12}^{11}}, \quad (4.75)$$

the **shear viscosity**

$$\eta = \frac{T}{10 \sigma(T) \Delta_c} \left[ (x_1 \gamma_1^0)^2 C_{22}^{00} - 2 x_1 x_2 \gamma_1^0 \gamma_2^0 C_{12}^{00} + (x_2 \gamma_2^0)^2 C_{11}^{00} \right], \quad (4.76)$$

the diffusion coefficient

$$D_d = \frac{1}{3n\sigma(T)} \frac{\beta_{11}^0 \beta_{12}^0}{B_{12}^{00}}, \quad (4.77)$$

the thermal diffusion and Dufour coefficient

$$D_T = D'_T = \frac{1}{3nT\sigma(T)\Delta_B} \left[ \frac{x_1}{x_2} \beta_1^1 \beta_{11}^1 y_2 + \frac{x_2}{x_1} \beta_2^1 \beta_{12}^1 y_3 \right. \\ \left. + (\beta_1^1 \beta_{12}^1 + \beta_2^1 \beta_{11}^1) y_4 + \beta_2^1 \beta_{11}^0 y_5 + \frac{x_1}{x_2} \beta_1^1 \beta_{11}^0 y_6 \right] \quad (4.78)$$

and the heat conductivity

$$\lambda = \frac{1}{3\sigma(T)\Delta_B} \left[ (x_1 \beta_1^1)^2 y_2 + 2x_1 x_2 \beta_1^1 \beta_2^1 y_4 + (x_2 \beta_2^1)^2 y_3 \right]. \quad (4.79)$$

The symbols are explained in Appendix A, and results are provided for the square collision brackets for both the simple quark and gluon systems, and the quark antiquark mixtures. These formulae will be used in the second part of Chapter 5 to calculate the numerical values for a mixture of quarks and antiquarks.

## 4.4 System with Weak External Field

In this section the transport equation (2.17) is solved for particles in an external field, which is expressed in terms of the field strength tensor  $F^{\mu\nu}$ . This field has to be weak enough such that the system can still be considered collision dominated. We present the derivation of the conductivity of the system, as this is the interesting feature appearing when an external field is coupled into the transport equation.

The equation for the evolution of the phase space distribution function was derived in section 2.1 and is given by

$$[p^\mu \partial_\mu - q p^\mu F_{\mu\nu} \partial_p^\nu] f = C[f, f], \quad (4.80)$$

where  $q$  is the “charge” of the particle with  $q = +1$  for particles and  $q = -1$  for antiparticles. The collision term  $C = C[f, f]$  in the Boltzmann approximation with  $\theta = 0$ , is given by (4.2)

$$C[f, f] = \frac{1}{2} \int \frac{d^3 p_2}{p_2^0} \frac{d^3 p_3}{p_3^0} \frac{d^3 p_4}{p_4^0} [f_3 f_4 - f_1 f_2] W(p_3 p_4 | p_1 p_2). \quad (4.81)$$

Following the method of linearisation presented in section 4.1, the following conservation laws are obtained: the Euler equation

$$Dn = -n \nabla_\mu U^\mu, \quad (4.82)$$

which is the same as in a simple one component system. The energy equation remains unchanged

$$DT = -\frac{T}{c_V} \nabla_\mu U^\mu = -(\gamma - 1) T \nabla_\mu U^\mu. \quad (4.83)$$

However, the equation of motion is changed and now reflects the existence of the field

$$DU^\mu = \frac{1}{wn} \nabla^\mu P - \frac{1}{w} F^{\mu\nu} U_\nu \sum_{l=1}^2 q_l x_l. \quad (4.84)$$

Equation (4.82) – (4.84) are now used to find  $Df^{(0)}$ , again as in section 4.1. With the introduction of the thermodynamic forces of a field-free system, namely

$$X \equiv -\nabla_\mu U^\mu, \quad (4.85)$$

$$X_q^\mu \equiv \nabla^\mu \log T - \frac{1}{wn} \nabla^\mu P \quad (4.86)$$

$$\overset{\circ}{X}^{\mu\nu} \equiv \frac{1}{2}\nabla^\mu U^\nu + \frac{1}{2}\nabla^\nu U^\mu - \frac{1}{3}\Delta^{\mu\nu}\nabla_\alpha U^\alpha, \quad (4.87)$$

$$X_1^\alpha \equiv (\nabla^\alpha \mu_1)_{P,T} - (\nabla^\alpha \mu_2)_{P,T} - \frac{w_1 - w_2}{wn} \nabla^\alpha P, \quad (4.88)$$

the linearised transport equation for a two component system in an external field (for species k) is obtained

$$\begin{aligned} Y_k X - p_k^\nu (p_k^\mu U_\mu - w_k) X_{q\nu} - p_k^\mu (\delta_{1k} - x_1) X_{1\mu} + p_1^\mu p_1^\nu \overset{\circ}{X}_{\mu\nu} + q_k p_{k\mu} F^{\mu\nu} U_\nu \\ - p_k^\mu U_\mu \frac{1}{w} p_k^\mu F_{\mu\nu} U^\nu \sum_{l=1}^2 q_l x_l = T \sum_{l=1}^2 L_{1l}[\phi_1]. \end{aligned} \quad (4.89)$$

This transport equation is remarkably similar to the one describing binary mixtures (cf. (4.30)) in a field-free system. This similarity motivates the inclusion of the field effects into the heat- and diffusion driving force, i.e.  $X_q^\mu$  and  $X_1^\mu$ , respectively. It prompts us to make the identifications

$$X_q^\mu|_{\text{field}} \equiv \nabla^\mu \log T - \frac{1}{wn} \nabla^\mu P + \frac{1}{w} F^{\mu\nu} U_\nu \sum_{l=1}^2 q_l x_l, \quad (4.90)$$

$$\begin{aligned} X_1^\alpha|_{\text{field}} \equiv (\nabla^\alpha \mu_1)_{P,T} - (\nabla^\alpha \mu_2)_{P,T} - \frac{w_1 - w_2}{(wn)T} \nabla^\alpha P - (q_1 - q_2) F^{\alpha\nu} U_\nu \\ + \frac{(w_1 - w_2)}{w} F^{\alpha\nu} U_\nu \sum_{l=1}^2 q_l x_l. \end{aligned} \quad (4.91)$$

By demanding that the diffusion flow  $I_1^\mu$  from (4.58), i.e.

$$I_1^\mu = l_{11} X_1^\mu + l_{1q} X_q^\mu, \quad (4.92)$$

in terms of the diffusion coefficient  $l_{11}$  and the thermal diffusion coefficient  $l_{1q}$ , remain in the same overall form when the external field is included, one obtains the new diffusion flows, making the replacement

$$X_q^\mu \rightarrow X_q^\mu|_{\text{field}} \text{ and } X_1^\mu \rightarrow X_1^\mu|_{\text{field}}. \quad (4.93)$$

The new diffusion flow is then, in analogy to (4.92), given by

$$I_1^\mu|_{\text{field}} = l_{11} X_1^\mu|_{\text{field}} + l_{1q} X_q^\mu|_{\text{field}}. \quad (4.94)$$

To make the following analysis more transparent, we now assume that the temperature, pressure and chemical potential (reflecting the composition of the mixture) are constant. Then, by inserting (4.90) and (4.91) into (4.94), this expression can be written as

$$I_1^\mu|_{\text{field}} = l_{11} \left[ \frac{w_1 - w_2}{w} \sum_{l=1}^2 q_l x_l - (q_1 - q_2) \right] F^{\mu\nu} U_\nu + l_{1q} \left[ \frac{1}{w} \sum_{l=1}^2 q_l x_l \right] F^{\mu\nu} U_\nu. \quad (4.95)$$

The diffusion flow  $I_1^\mu|_{\text{field}}$  is now trivially related to the conduction flow  $I_{\text{ch}}^\mu$ , one has

$$I_{\text{ch}}^\mu \equiv -(q_1 - q_2) I_1^\mu|_{\text{field}}, \quad (4.96)$$

which is used to find a generalised version of Ohm's law of the form

$$I_{\text{ch}}^\mu = \sigma F^{\mu\nu} U_\nu. \quad (4.97)$$

One notes that (4.97) would, if one had particles with the additional property of color, change such that  $F^{\mu\nu} \rightarrow F_a^{\mu\nu}$  and  $\sigma \rightarrow \sigma^{ab}$ . Then (4.97) reduces to the form  $I_{\text{ch}}^{\mu a} = \sigma^{ab} F_b^{\mu\nu} U_\nu$  which was first derived for the QGP by Heinz ([20] and [21]).

Comparing (4.95) and (4.96), the conductivity  $\sigma$  is found to be

$$\sigma = (q_1 - q_2) \left[ l_{11} \left( q_1 - q_2 - \frac{w_1 - w_2}{w} \sum_{l=1}^2 q_l x_l \right) - l_{1q} \frac{1}{w} \sum_{l=1}^2 q_l x_l \right]. \quad (4.98)$$

In the quark ( $q_1$ ) antiquark ( $q_2$ ) plasma that we wish to consider, one has  $q_1 - q_2 = 2g$  and  $w_1 = w_2 = 4T$ , also  $\sum_{l=1}^2 q_l x_l = g n_c/n$  where  $n_c \equiv n_1 - n_2$  is a conserved number density related to the "charge"  $q$ . Noting that the coupling constant  $g^2 = 4\pi\alpha_s$ , eq.(4.98) then becomes

$$\sigma = 8\pi\alpha_s \left[ 2l_{11} - \frac{n_c}{wn} l_{1q} \right]. \quad (4.99)$$

In terms of the "phenomenological" transport coefficients  $D_T$  and  $D_d$  introduced in the previous section, i.e. from (4.71) and (4.72), the conductivity can finally be written as

$$\sigma = 8\pi\alpha_s x_1 x_2 \left[ 2 \frac{n}{T} D_d - \frac{n_c T}{w} D_T \right]. \quad (4.100)$$

Expression (4.100) will be used in Chapter 5 to compute the conductivity of a locally colorless quark antiquark mixture.

# Chapter 5

## Results

In this Chapter we present the numerical results for the transport coefficients of various systems, as derived using the Chapman Enskog method, which was presented in Chapter 4. In the following sections, we often refer to “simple systems” – these are understood as systems consisting of only one particle species, for example only quarks or only gluons.

The following particle systems are considered:

- a simple quark system, i.e. a system where only quark-quark scattering is taken into account,
- a simple gluon system, i.e. a system where only gluon-gluon scattering is considered,
- a quark antiquark system, i.e. a system where quark-quark, antiquark-antiquark and quark-antiquark scattering is taken into account,
- a quark-gluon system, i.e. a system where equal numbers of quarks and antiquarks interact with each other and with gluons,
- a quark antiquark system in a weak external field.

In solving for the transport coefficients of a pure gluon system, we assume that gluons can be described by the same transport equation as the quarks, and the only difference distinguishing the two species is the (gauge invariant) scattering cross-section.

Because we used the full cm differential cross-section, and not a parametrisation like some authors (see the discussion in Chapter 3), we faced some technical problems in solving the square collision brackets  $B^{11}$ ,  $C^{00}$ ,  $B_{11}^{00}$ ,  $B_{12}^{00}$ ,  $B_{12}^{01}$ ,  $B_{12}^{10}$ ,  $B_{12}^{11}$ ,  $B_{11}^{11}$ ,  $B_{22}^{11}$ ,  $C_{11}^{00}$ ,  $C_{12}^{00}$  and  $C_{22}^{00}$  as needed in the computation of the transport coefficients. These problems were overcome by calculating the coefficients with the help of the symbolic manipulation routine REDUCE (Version 3.3 (1988), implemented on an Apollo 3500 workstation). This method has several advantages:

- depending on the level of programming, one can check all intermediate results in a purely symbolic form, i.e. in terms of collision brackets (Appendix A) or collision integrals (Appendix B),
- the extension to a binary mixture was possible, even where the full expression for the cm differential cross-section was used. This task would otherwise be almost impossible to carry out, a glance at the results in the next sections will tell why.

Correctness of the written programs and of the presented results was checked in two ways:

- for the simple systems, where most of the analytical work is still manageable, both approaches, i.e. analytic and machine calculations, were performed.
- for the coefficients of the quark antiquark mixture, we first chose a simple parametric form for the cross-sections, the quark antiquark-like system, as discussed in Appendix F, and then calculated the coefficients both analytically and with our REDUCE programs. The code was then used to find the coefficients for a neutrino antineutrino mixture, which could be compared to the results from de Groot and co-workers [4]. We finally performed the full calculations using the complete expressions for the cross-sections for quark-quark and quark antiquark scattering, as derived in Appendix C.

The results for the square collision brackets for the various systems are listed in Appendix A. In the following sections, we summarise our results for the transport coefficients.

## 5.1 One Component Systems

### 5.1.1 Simple Quark System

The transition matrix element for a simple quark system, i.e. a system where the scattering process

$$q q \rightarrow q q$$

is the only scattering mode, is studied in Appendix C. The matrix element squared is given by (C.12). The differential cross-section for this process, in the cm frame, is derived in Appendix C, (C.30). It is used to calculate the transfer cross-section needed in Appendix B (B.31).

Because we are assuming that the quarks are massless, the volume viscosity  $\eta_v$  is zero. This can be shown to hold generally for both ultra-relativistic and non-relativistic particles (cf. [24]).

The only transport processes expected in such a system are the heat conduction and the shear viscous flow. The coefficient of heat conductivity is given by (4.46)

$$\lambda = \frac{1}{3} \frac{(\beta^1)^2}{\sigma(T) B^{11}}, \quad (5.1)$$

and the coefficient of shear viscosity by (4.47)

$$\eta = \frac{T}{10} \frac{(\gamma^0)^2}{\sigma(T) C^{00}}, \quad (5.2)$$

where the result is expressed in terms of the square collision brackets  $B^{11}$  and  $C^{00}$ . From Appendix A, we find that

$$\beta^1 \equiv \frac{3\gamma}{\gamma-1} = 12 \quad \text{and} \quad \gamma^0 \equiv 10 \frac{w}{T} = 40, \quad (5.3)$$

since massless particles have an enthalpy per particle  $w = 4T$ , and the ratio of heat capacities is  $\gamma \equiv c_P/c_V = 4/3$ . With the choice of a characteristic mean cross-section

$$\sigma(T) = \frac{\alpha_s^2}{T^2}, \quad (5.4)$$

one can now calculate both the collision brackets  $B^{11}$  and  $C^{00}$ , as is shown in Appendix A.

The heat conductivity is then given by

$$\lambda = 216 N_f \frac{T^2}{\pi \alpha_s^2 [24 \log \Lambda_c - \Lambda^3 - 37 \Lambda]}. \quad (5.5)$$

The result is expressed in terms of the number of quark flavors  $N_f$ , the temperature  $T$ , the strong coupling constant  $\alpha_s$ , the Coulomb logarithm  $\log \Lambda_c$  and the divergence cut-off  $\Lambda$ . In the limit  $\Lambda \rightarrow 0$ , one finds

$$\lambda = 9 N_f \frac{T^2}{\pi \alpha_s^2 \log \Lambda_c}. \quad (5.6)$$

Similarly, the **shear viscosity** takes the form

$$\eta = 216 N_f \frac{T^3}{\pi \alpha_s^2 [24 \log \Lambda_c - \Lambda^3 - 37 \Lambda]}, \quad (5.7)$$

or, in the limit  $\Lambda \rightarrow 0$ ,

$$\eta = 9 N_f \frac{T^3}{\pi \alpha_s^2 \log \Lambda_c}. \quad (5.8)$$

The Coulomb logarithm appearing in equations (5.5) – (5.8) takes care of the infrared divergences in the scattering matrix element (C.12). Its appearance is a natural consequence of our cut-off procedure, in which the cut-off  $\Lambda$  is introduced at the divergent limits of the scattering integral. This is discussed in more detail in Appendix D. Note that this logarithmic factor is not incorporated in the mean thermal cross-section  $\sigma(T)$  (5.4), in contrast to the treatment of Hosoya and Kajantie [8] or Danielewicz and Gyulassy [9]. It is encouraging that the CE method, together with our cut-off procedure, produces this Coulomb logarithm in a natural manner, whereas it had to be introduced in a rather *ad hoc* way in the other methods of solution discussed in Chapter 3.

Another interesting feature is, that the **Eucken relation**, i.e. the ratio of the heat conductivity to the shear viscosity, turns out to be of the form

$$\frac{\lambda}{\eta} = \frac{1}{T}, \quad (5.9)$$

in contrast to  $5/T$ , the ratio obtained by several other authors (see Chapter 3).

We now compare the magnitudes of the kinetic coefficients (5.6) and (5.8), valid for pure quark systems, to the more commonly encountered values of transport coefficients as determined from experiments with gases under terrestrial conditions [55]. For this purpose we choose some characteristic values as expected in a QGP, i.e. for the temperature  $T = 200 \text{ MeV}$ , the strong coupling constant  $\alpha_s = 0.1$  and the Coulomb logarithm  $\log \Lambda_c \simeq 1$ . With these, the numerical values for the heat conductivity (5.6) and the shear viscosity (5.8) are

$$\lambda = 11.46 \left[ \text{GeV}^2 \right] = 1.21 \cdot 10^{18} \left[ \frac{\text{kg m}}{\text{s}^3 \text{K}} \right], \quad (5.10)$$

$$\eta = 2.29 \text{ [GeV}^3] = 3.16 \cdot 10^{13} \left[ \frac{\text{kg}}{\text{m s}} \right]. \quad (5.11)$$

These are to be compared with the terrestrial values of  $\lambda \simeq 10^{-2} \left[ \frac{\text{kg m}}{\text{s}^3 \text{K}} \right]$  and  $\eta \simeq 10^{-5} \left[ \frac{\text{kg}}{\text{m s}} \right]$ . This shows that quark matter has a heat conductivity coefficient of  $10^{20}$  larger and a viscosity of  $10^{18}$  larger than “ordinary” terrestrial gases !

It is interesting to note that equations (5.6) and (5.8) are similar to the results obtained for a system of quark-like particles ( [56] and [57] ), as discussed in Appendix F. We note however, that the numerical values of the coefficients computed in this section are larger than the corresponding values from Appendix F. This is due to the additional degrees of freedom of “real”, in contrast to the quark-like, quarks, like spin and color. These properties, although not incorporated explicitly in the transport equation leading to the above results, have been taken care of by averaging over initial states and summing over final states in the evaluation of the scattering matrix elements (Appendix C). The quark-like particles considered in Appendix F were assumed spin- and colorless. This is an important difference, and will be reconsidered when we compare the various results in Chapter 6.

## 5.1.2 Simple Gluon System

The only scattering process in a simple gluon system is the process

$$g g \rightarrow g g$$

for which the cm differential cross-section has been calculated in Appendix C. With expressions (4.46) and (4.47) for the heat conductivity and shear viscosity respectively, and the same mean cross-section  $\sigma(T)$  as in (5.4), one obtains, after using the differential cross-section (C.33),  
**the heat conductivity**

$$\lambda = \frac{2560 T^2}{3 \pi \alpha_s^2 [480 \log \Lambda_c - 3 \Lambda^5 - 50 \Lambda^3 - 555 \Lambda]}, \quad (5.12)$$

and, again, letting the infrared divergence cut-off  $\Lambda \rightarrow 0$ , one obtains

$$\lambda = \frac{16}{9} \frac{T^2}{\pi \alpha_s^2 \log \Lambda_c}. \quad (5.13)$$

The **shear viscosity** is found to be

$$\eta = \frac{2560 T^3}{3 \pi \alpha_s^2 [480 \log \Lambda_c - 3 \Lambda^5 - 50 \Lambda^3 - 555 \Lambda]}, \quad (5.14)$$

and, with  $\Lambda \rightarrow 0$ , is given by

$$\eta = \frac{16}{9} \frac{T^3}{\pi \alpha_s^2 \log \Lambda_c}. \quad (5.15)$$

Characteristic values for  $\lambda$  and  $\eta$ , where  $T = 200 \text{ MeV}$ ,  $\alpha_s = 0.1$  and  $\log \Lambda_c \simeq 1$  have been used, are given by

$$\lambda = 2.26 \text{ [GeV}^2\text{]} = 2.41 \cdot 10^{17} \left[ \frac{\text{kg m}}{\text{s}^3 \text{K}} \right], \quad (5.16)$$

$$\eta = 0.45 \text{ [GeV}^3\text{]} = 6.24 \cdot 10^{12} \left[ \frac{\text{kg}}{\text{ms}} \right]. \quad (5.17)$$

The **Eucken relation** is

$$\frac{\lambda}{\eta} = \frac{1}{T}, \quad (5.18)$$

as for the quark system. This should be compared to the value of  $23/10 T$  obtained for a simple neutrino system [4].

It should be noted that the values for the gluon kinetic coefficients are smaller than the corresponding quark coefficients. The ratio, comparing the shear viscosities, is given by

$$\frac{\eta_{\text{quark}}}{\eta_{\text{gluon}}} = \left(\frac{3}{2}\right)^4 N_f \simeq 5.06 N_f. \quad (5.19)$$

This emphasises the importance of including the effects of quarks in a full quark-gluon plasma calculation, and also motivates an investigation of the transport coefficients of a quark antiquark mixture. This is the task set for section 5.2.1.

## 5.2 Two Component System

### 5.2.1 Quark Antiquark System

The formalism presented in Chapter 4 enables us to calculate the transport coefficients for a quark antiquark mixture. The transition matrix element (C.16) for the process

$$q \bar{q} \rightarrow q \bar{q}$$

gives the cm differential cross-section (C.31). It is, together with the cross-sections for quark-quark and antiquark-antiquark scattering processes from (C.30), used to calculate the relevant transfer cross-sections (B.31). These are needed to compute the square collision brackets  $B_{11}^{00}, B_{12}^{00}, B_{12}^{01}, B_{12}^{10}, B_{12}^{11}, B_{11}^{11}, B_{22}^{11}, C_{11}^{00}, C_{12}^{00}$  and  $C_{22}^{00}$ .

We again choose the mean cross-section  $\sigma(T)$ , as needed in the trial function (4.48), to be

$$\sigma(T) = \frac{\alpha_s^2}{T^2}. \quad (5.20)$$

We now list the results for the kinetic coefficients for a mixture of massless ( $\eta_v = 0$ ) quarks (density fraction  $x_1 = n_1/(n_1 + n_2)$ ) and antiquarks (density fraction  $x_2 = n_2/(n_1 + n_2)$ ). The results for  $\Lambda \neq 0$  are unwieldy, there are, for example, 38 terms in the nominator and 92 terms in the denominator of the expression for  $\lambda$ . Consequently, we only present the coefficients for  $\Lambda \rightarrow 0$ .

In this case, the **heat conductivity** is given by

$$\lambda = \frac{576 N_f T^2}{\pi \alpha_s^2} \frac{x_1 x_2 [5760 S + 3186] - 2880 \log \Lambda_{c2} - 1039}{184320 [x_1 x_2 S^2 + G] + x_1 x_2 [132992 S + 17169] - 66496 \log \Lambda_{c1}}, \quad (5.21)$$

and the **thermal diffusion** coefficient is given by

$$D_T = 0. \quad (5.22)$$

The **diffusion coefficient** is found to be

$$D_d = \frac{-2592 N_f T^2}{\pi \alpha_s^2 n [576 \log \Lambda_{c2} + 97]}, \quad (5.23)$$

and the **shear viscosity** takes the form

$$\eta = \frac{576 N_f T^3}{\pi \alpha_s^2} \frac{x_1 x_2 [5760 S + 3186] - 2880 \log \Lambda_{c2} - 1039}{184320 [x_1 x_2 S^2 + G] + x_1 x_2 [132992 S + 17169] - 66496 \log \Lambda_{c1}}. \quad (5.24)$$

Here we have used the abbreviations

$$S \equiv \log \Lambda_{c1} + \log \Lambda_{c2}, \quad (5.25)$$

and

$$G \equiv - \log \Lambda_{c1} \log \Lambda_{c2}, \quad \text{such that } G > 0. \quad (5.26)$$

The logarithmic factors  $\log \Lambda_{c1}$  and  $\log \Lambda_{c2}$  are again, similar to  $\log \Lambda_c$  in the previous sections, Coulomb logarithms. These factors are discussed and evaluated in Appendix D.

The vanishing thermal diffusion coefficient  $D_T$  is an interesting feature of this system. This coefficient tells us about the separation of species in a field-free system in the presence of a temperature, and in relativistic systems also of a pressure, gradient. A consequence of our result is that one can expect that the relative quark and antiquark concentration will not be changed by a temperature gradient. This is in contrast to a neutrino antineutrino system, where this coefficient causes an enhancement of the concentration of the more abundant component in the colder parts of the system.

The thermal diffusion coefficient was found to vanish in all systems interacting via Rutherford-like cross sections. Examples are the “quark-like”-, the quark antiquark- and the proper quark antiquark gluon system. The important difference between the neutrino antineutrino system on the one hand, and for example the quark antiquark system on the other hand is the interaction cross section. The neutrino system is dominated by the weak interaction, the characteristic features of quark system are the infrared divergences due to the Rutherford-like cross sections.

The diffusion coefficient  $D_d$ , which expresses the heat flow due to gradients of concentration, is independent of the particle fractions  $x_1, x_2$ . It is positive (note that  $\log \Lambda_{c2} < 0$ , see Appendix D), which indicates that the flow is directed from a high to a low concentration.

Furthermore, the heat conductivity  $\lambda$  and the shear viscosity  $\eta$  are symmetric with respect to the interchange  $x_1 \leftrightarrow x_2$ , as expected.

From these results we can conclude that there is no mechanism apparent for a separation of quarks and antiquarks in the absence of a (color)-field. If such a

separation is indeed experimentally detected, it must be concluded that it is due to the *color* property of the quarks only, or a joint quark-gluon effect.

Again we recover the **Eucken relation**

$$\frac{\lambda}{\eta} = \frac{1}{T},$$

just as we did for the one component systems.

## 5.2.2 Quark-Gluon System

In this section we present the transport coefficients for a quark-antiquark-gluon system, a quark-gluon plasma. This is a three component system, but to simplify the calculation, we assume that equal numbers of quarks and antiquarks are present, i.e. there is no net baryonnumber.

Four distinct scattering processes occur in this system, namely the

- quark-quark and antiquark-antiquark scattering,
- quark-antiquark and antiquark-quark scattering,
- quark-gluon and antiquark-gluon (and their reverse) scattering,
- and gluon-gluon scattering.

The transition matrix element (C.24) for the process

$$q g \rightarrow q g,$$

which is the same as the process

$$\bar{q} g \rightarrow \bar{q} g,$$

gives the cm differential cross-section (C.32). It is, together with the cross-sections for quark-quark (antiquark-antiquark) and gluon-gluon scattering processes from (C.30) and (C.33) respectively, used to calculate the relevant transfer cross-sections (B.31). Again these are needed to compute the square collision brackets  $B_{11}^{00}, B_{12}^{00}, B_{12}^{01}, B_{12}^{10}, B_{12}^{11}, B_{11}^{11}, B_{22}^{11}, C_{11}^{00}, C_{12}^{00}$  and  $C_{22}^{00}$ .

Note that we completely neglected the reactive processes, such as  $q\bar{q} \rightarrow gg$  and similar. These processes, although probably important for the understanding of the non-equilibrium QGP, introduce a multitude of new problems, and will not be considered in this thesis.

With the choice for the mean cross-section  $\sigma(T)$ , i.e.

$$\sigma(T) = \frac{\alpha_s^2}{T^2}, \tag{5.27}$$

we now calculate the transport coefficients of this interesting system. The quarks and gluons are massless and therefore  $\eta_v = 0$ . Denoting the density fraction of quarks and antiquarks by  $x_{q\bar{q}} \equiv (n_q + n_{\bar{q}})/(n_q + n_{\bar{q}} + n_g)$ , it follows that the gluon density fraction is given by  $x_g \equiv n_g/(n_q + n_{\bar{q}} + n_g)$ . Again, the results for  $\Lambda \neq 0$  are so unwieldy that we only present the coefficients for  $\Lambda \rightarrow 0$ .

In this case, the **heat conductivity** is given by

$$\begin{aligned}
 \lambda = & \frac{288 T^2}{\pi \alpha_s^2 [320 \log \Lambda_2 + 177]} \cdot \\
 & \left[ x_{q\bar{q}} x_g \left( 3732480 \log \Lambda_1^2 + 16992000 \log \Lambda_1 \log \Lambda_2 + 5986980 \log \Lambda_1 \right. \right. \\
 & \quad \left. \left. + 14929920 \log \Lambda_2^2 + 10450944 \log \Lambda_2 + 1273804 \right) + \right. \\
 & \quad \left. x_{q\bar{q}}^2 \left( 1958400 \log \Lambda_1 \log \Lambda_2 + 725220 \log \Lambda_1 \right) - 9331200 \log \Lambda_1 \log \Lambda_2 \right. \\
 & \quad \left. - 3455460 \log \Lambda_1 + 1843200 \log \Lambda_2^2 + 1702080 \log \Lambda_2 + 377541 \right] / \\
 & \left[ 9 \log \Lambda_1 \left( 81 - 162 x_{q\bar{q}} x_g - 17 x_{q\bar{q}}^2 \right) \left( 640 \log \Lambda_2 + 237 \right) \right. \\
 & \quad \left. - 2 x_{q\bar{q}} x_g \left( 93312 \log \Lambda_1^2 + 456192 \log \Lambda_2^2 \right. \right. \\
 & \quad \left. \left. + 352176 \log \Lambda_2 + 56749 \right) \right] \tag{5.28}
 \end{aligned}$$

and the **thermal diffusion coefficient** is given by

$$D_T = 0. \tag{5.29}$$

The **diffusion coefficient** is found to be

$$D_d = \frac{-432 T^2}{\pi \alpha_s^2 n} \cdot \frac{3744 \log \Lambda_2 + 823}{11 [576 \log \Lambda_2 + 97] [48 \log \Lambda_2 + 11]} \tag{5.30}$$

and the shear viscosity takes the form

$$\begin{aligned}
\eta = & \frac{288 T^3}{\pi \alpha_s^2 [320 \log \Lambda_2 + 177]} \cdot \\
& \left[ x_{q\bar{q}} x_g \left( 3732480 \log \Lambda_1^2 + 16992000 \log \Lambda_1 \log \Lambda_2 + 5986980 \log \Lambda_1 \right. \right. \\
& \left. \left. + 14929920 \log \Lambda_2^2 + 10450944 \log \Lambda_2 + 1273804 \right) + \right. \\
& x_{q\bar{q}}^2 \left( 1958400 \log \Lambda_1 \log \Lambda_2 + 725220 \log \Lambda_1 \right) - 9331200 \log \Lambda_1 \log \Lambda_2 \\
& \left. - 3455460 \log \Lambda_1 + 1843200 \log \Lambda_2^2 + 1702080 \log \Lambda_2 + 377541 \right] / \\
& \left[ 9 \log \Lambda_1 (81 - 162 x_{q\bar{q}} x_g - 17 x_{q\bar{q}}^2) (237 + 640 \log \Lambda_2) \right. \\
& \left. - 2 x_{q\bar{q}} x_g \left( 93312 \log \Lambda_1^2 + 456192 \log \Lambda_2^2 \right. \right. \\
& \left. \left. + 352176 \log \Lambda_2 + 56749 \right) \right] \tag{5.31}
\end{aligned}$$

Again, as in the quark antiquark system, the thermal diffusion coefficient  $D_T$  vanishes; and we recover the **Eucken relation**

$$\frac{\lambda}{\eta} = \frac{1}{T}. \tag{5.32}$$

For reasons of comparison, we now make a particular choice for the Coulomb logarithms and the particle fractions in the expression for the shear viscosity (5.31). With

$$\log \Lambda_1 = -\log \Lambda_2 = 5$$

and  $x_{q\bar{q}} = x_g = 0.5$ , one finds

$$\eta = 10.64 \frac{T^3}{\pi \alpha_s^2 \log(1/\alpha_s)}, \tag{5.33}$$

where we have incorporated a factor  $\log(1/\alpha_s)$  with  $\alpha_s = 0.1$  into the numerical factor 10.64.

Comparing (5.33) with the pure quark shear viscosity from (5.8), one finds the ratio

$$\frac{\eta_{qq}}{\eta_{gg}} = \frac{9 N_f \log(1/\alpha_s)}{10.64 \log \Lambda_c} \simeq 1.69 \quad (5.34)$$

for a 2-flavor system.

For the ratio of the pure gluon to the quark-gluon shear viscosity we find from (5.15)

$$\frac{\eta_{gg}}{\eta_{qg}} = \frac{16 \log(1/\alpha_s)}{95.85 \log \Lambda_c} \simeq 0.17. \quad (5.35)$$

### 5.3 Quark Antiquark System in an External Field

For a quark antiquark system in an external field we compute the conductivity coefficient  $\sigma$ .

From (4.100), the expression for the conductivity of a mixture of quarks (density fraction  $x_1$ ) and antiquarks (density fraction  $x_2$ ) is given by

$$\sigma = 8\pi\alpha_s x_1 x_2 \left[ 2 \frac{n}{T} D_d - \frac{n_c T}{w} D_T \right]. \quad (5.36)$$

This expression is given in terms of the diffusion coefficient  $D_d$ , the thermal diffusion coefficient  $D_T$ , the total particle density  $n$ , the total enthalpy per particle  $w$  and the conserved particle density  $n_c$ . From the results presented in the previous section, we know that

$$D_T = 0, \quad (5.37)$$

and

$$D_d = \frac{-2592 N_f T^2}{\pi \alpha_s^2 n [576 \log \Lambda_{c2} + 97]}. \quad (5.38)$$

Inserting these results into (5.36), the conductivity is found to be

$$\sigma = -x_1 x_2 \left[ 16 N_f \frac{2592 T}{\alpha_s [576 \log \Lambda_{c2} + 97]} \right]. \quad (5.39)$$

If we assume the logarithmic factor of the denominator to be the dominant contribution, we finally obtain, noting that  $\log \Lambda_{c2} < 0$  always,

$$\sigma = -x_1 x_2 \left[ 72 N_f \frac{T}{\alpha_s \log \Lambda_{c2}} \right]. \quad (5.40)$$

This expression is now in a form that can be compared with the results from other authors. This will be done in Chapter 6.

i.e.  $(2 * (\text{spin} * \text{flavor} * \text{color}))$ ); and for a QGP one finds  $g = 40$ . One should emphasise that  $g = 40$  overestimates the particle multiplicity in the non-interacting QGP (result  $O_1$ ). But in order to compare that result to some of the others in the literature where for example the antiquark contribution was also not explicitly incorporated, we will use this value throughout the QGP system, i.e. both in  $O_1$  and  $O_2$ .

The transport coefficients obtained by other authors are written into a form such that Maxwell Boltzmann statistics can be used. The authors' names are abbreviated, and we use

- **G** for Gavin [7],
- **HK** for Hosoya and Kajantie [8],
- **DG** for Danielewicz and Gyulassy [9],
- **W** for Weinberg [24],
- **M** for Mrówczyński [31]
- **BMPR** for Baym, Monien, Pethick and Ravenhall [42],
- **HS** for Horsely and Schoenmaker [46],
- **IPS** for Ilyin, Panferov and Sinyukov [47],
- **KW** for Karsch and Wyld [48],
- and **O** for our result.

## 6.1 Simple Gluon System Shear Viscosity

Most authors discussed in Chapter 3 provide expressions for the shear viscosity of a simple gluon system. In this section we therefore provide an interesting study comparing these coefficients, bearing in mind the very different calculational methods used.

Table 6.1 summarises the results for the shear viscosities, and the expressions rewritten in terms of the “viscous” collision time  $\tau_\eta$ . The viscous collision time is multiplied by the temperature, in order to obtain a dimensionless quantity.

Here, we make use of the energy density  $en$  for massless Maxwell Boltzmann particles with a vanishing chemical potential, given by

$$en = g \frac{3}{\pi^2} T^4. \quad (6.3)$$

The gluon relaxation time  $\tau_g$ , needed to compute the shear viscosity for Weinberg’s and Gavin’s result (see Table 6.1), is derived by making use of the relaxation time  $\tau$  as defined by Danielewicz and Gyulassy [9], i.e.

$$\tau \equiv \frac{17 T^2}{10 \pi n \alpha_s^2 \log(1/\alpha_s)}. \quad (6.4)$$

The gluon density, in the Maxwell Boltzmann approximation, is given by  $n = 16 T^3/\pi^2$  with  $\mu = 0$ , and one accordingly finds from (6.4)

$$\tau_g = \frac{17 \pi}{160 T \alpha_s^2 \log(1/\alpha_s)}. \quad (6.5)$$

Also, we make the approximation

$$\log(1/\alpha_s) \simeq \log \Lambda_c \simeq 1, \quad (6.6)$$

to make our results comparable to others. It has to be kept in mind that (6.6) is an approximation, and only a more detailed study (see Appendix D) of the Coulomb logarithm can validate this approximation.

Baym, Monien, Pethick and Ravenhall [42] provide an estimate for the viscous relaxation time. But for reasons of consistency we proceed as indicated above and convert their estimate for the gluon shear viscosity into an expression proportional to the entropy density, as in (6.1), thereby obtaining the viscous relaxation time.

The various values for the viscous relaxation time are displayed in Figure 6.1.

Author(s)	$\eta$	$\tau_\eta T$
W and G	$\frac{4}{15} e n_g \tau_g$	$\frac{17 \pi}{800 \alpha_s^2 \log(1/\alpha_s)}$
HK	$\frac{64 \pi^2}{675} \frac{T^3}{15 \alpha_s^2 \log(1/\alpha_s)}$	$\frac{2}{225 \alpha_s^2 \log(1/\alpha_s)}$
HS	$0.165 \frac{T^3}{\alpha_s^2 \log(1/\alpha_s)}$	$0.165 \frac{\pi^2}{64 \alpha_s^2 \log(1/\alpha_s)}$
IPS	$2.6 \frac{T^3}{\alpha_s}$	$2.6 \frac{\pi^2}{64 \alpha_s}$
KW	$9.5 T^3$	$9.5 \frac{\pi^2}{64}$
BMPR	$0.342 \frac{T^3}{\alpha_s^2 \log(1/\alpha_s)}$	$0.342 \frac{\pi^2}{64 \alpha_s^2 \log(1/\alpha_s)}$
O	$\frac{16}{9} \frac{T^3}{\pi \alpha_s^2 \log \Lambda_c}$	$\frac{\pi}{36 \alpha_s^2 \log \Lambda_c}$

Table 6.1: Shear Viscosities and Viscous Relaxation Times of a Gluon System.

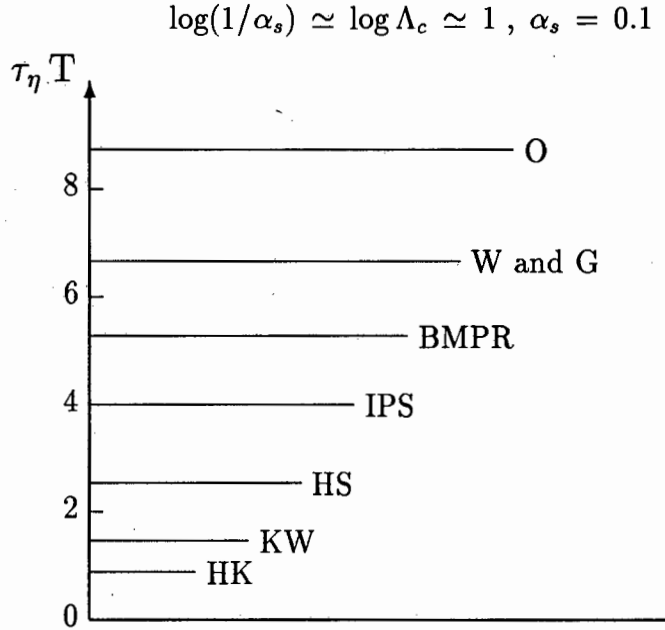


Figure 6.1: Characteristic Viscous Relaxation Times of a Gluon System.

## 6.2 QGP Shear Viscosity

For a system of quarks and gluons, the above procedure of finding viscous relaxation times, is repeated. Our results are presented in two different ways: the result denoted by  $O_1$  is a simple addition of the quark and gluon contributions,

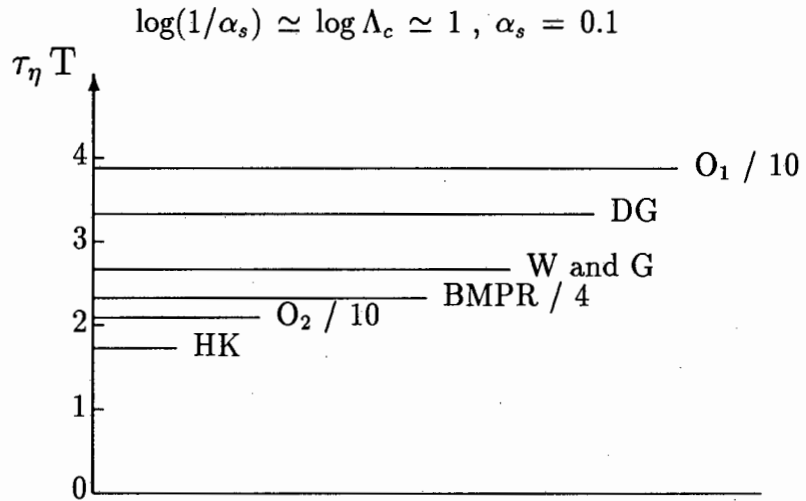


Figure 6.2: Characteristic Viscous Relaxation Times of a QGP.

whereagainst result  $O_2$  is from the quark antiquark symmetric quark gluon system as discussed in chapter 5.2.2.

The results, for a 2-flavor QGP, are plotted in Figure 6.2 and summarised in Table 6.2.

Author(s)	$\eta$	$\tau_\eta T$
W and G	$\frac{4}{15} [en_q \tau_q + en_g \tau_g]$	$\frac{17 \pi}{2000 \alpha_s^2 \log(1/\alpha_s)}$
DG	$17 \frac{T^3}{10 \pi \alpha_s^2 \log(1/\alpha_s)}$	$\frac{17 \pi}{1600 \alpha_s^2 \log(1/\alpha_s)}$
HK	$0.28 \frac{T^3}{\alpha_s^2 \log(1/\alpha_s)}$	$0.28 \frac{\pi^2}{160 \alpha_s^2 \log(1/\alpha_s)}$
BMPR	$1.505 \frac{T^3}{\alpha_s^2 \log(1/\alpha_s)}$	$1.505 \frac{\pi^2}{160 \alpha_s^2 \log(1/\alpha_s)}$
$O_1$	$\frac{178}{9} \frac{T^3}{\pi \alpha_s^2 \log \Lambda_c}$	$\frac{89 \pi}{720 \alpha_s^2 \log \Lambda_c}$
$O_2$	$10.64 \frac{T^3}{\pi \alpha_s^2 \log(1/\alpha_s)}$	$\frac{10.64 \pi}{160 \alpha_s^2 \log(1/\alpha_s)}$

Table 6.2: Shear Viscosities and Characteristic Viscous Relaxation Times of a QGP.

### 6.3 QGP Heat Conductivity

A similar procedure of extracting a characteristic relaxation time is now used to compare the heat conductivities of a non-reactive quark-gluon mixture. We rewrite the expression for the heat conductivity in a form

$$\lambda = \tau_\lambda sn, \quad (6.7)$$

thereby obtaining the characteristic heat conduction relaxation time  $\tau_\lambda$ . Note that we used the enthalpy per particle for massless particles ( $\mu = 0$ ) as

$$w \equiv \frac{en + P}{n} = 4T. \quad (6.8)$$

Again,  $O_1$  denotes the quark plus gluon contribution, and  $O_2$  the quark antiquark symmetric quark gluon plasma.

Table 6.3 summarises the heat conductivities and the various characteristic heat conduction relaxation times.

The characteristic heat conduction relaxation times are plotted in Figure 6.3.

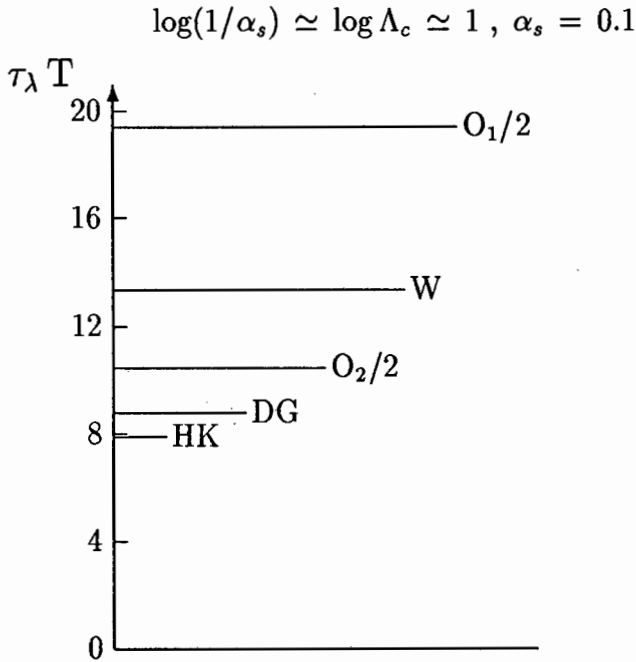


Figure 6.3: Characteristic Heat Conduction Relaxation Times of a QGP.

Author(s)	$\lambda$	$\tau_\lambda T$
W	$\frac{4}{3T} [en_q \tau_q + en_g \tau_g]$	$\frac{17\pi}{400\alpha_s^2 \log(1/\alpha_s)}$
DG	$\frac{2}{3} \tau_q T w^2$	$\frac{17\pi^3}{6000\alpha_s^2 \log(1/\alpha_s)}$
HK	$0.08 \frac{w^2}{\alpha_s^2 \log(1/\alpha_s)}$	$0.008 \frac{\pi^2}{\alpha_s^2 \log(1/\alpha_s)}$
O <sub>1</sub>	$\frac{178}{9} \frac{T^2}{\pi \alpha_s^2 \log \Lambda_c}$	$\frac{89\pi}{720\alpha_s^2 \log \Lambda_c}$
O <sub>2</sub>	$10.64 \frac{T^2}{\pi \alpha_s^2 \log(1/\alpha_s)}$	$\frac{10.64\pi}{160\alpha_s^2 \log(1/\alpha_s)}$

Table 6.3: Heat Conductivities and Heat Conduction Relaxation Times of a QGP.

## 6.4 Quark Antiquark Conductivity

In the case of quark antiquark mixtures, we use Mrówczyński's result of the conductivity to compare to ours. All other coefficients of such a binary system, as computed and presented in Chapter 5, have, to our knowledge, not explicitly been computed before.

For a 2-flavor quark antiquark system, the conductivities, as found by Mrówczyński and by us, are summarised in Table 6.4. Here, the number density  $n$  of massless Maxwell Boltzmann particles with vanishing chemical potential, i.e.

$$n = g \frac{T^3}{\pi^2}, \quad (6.9)$$

has been used, and  $g = 24$  for the quark antiquark mixture, and  $x_1 = x_2 = 1/2$ . The ratio of the results is given by

$$\frac{\sigma|_M}{\sigma|_O} \simeq 0.03. \quad (6.10)$$

We also make the approximation

$$-\log \Lambda_{c2} \simeq \log(1/\alpha_s), \quad (6.11)$$

to make our result readily comparable. Figure 6.4 shows a plot of these results.

Author	$\sigma$
M	$\frac{17 \pi^2 T}{540 \alpha_s \log(1/\alpha_s)}$
O	$36 \frac{T}{\alpha_s \log(1/\alpha_s)}$

Table 6.4: Conductivity of a Quark Antiquark System.

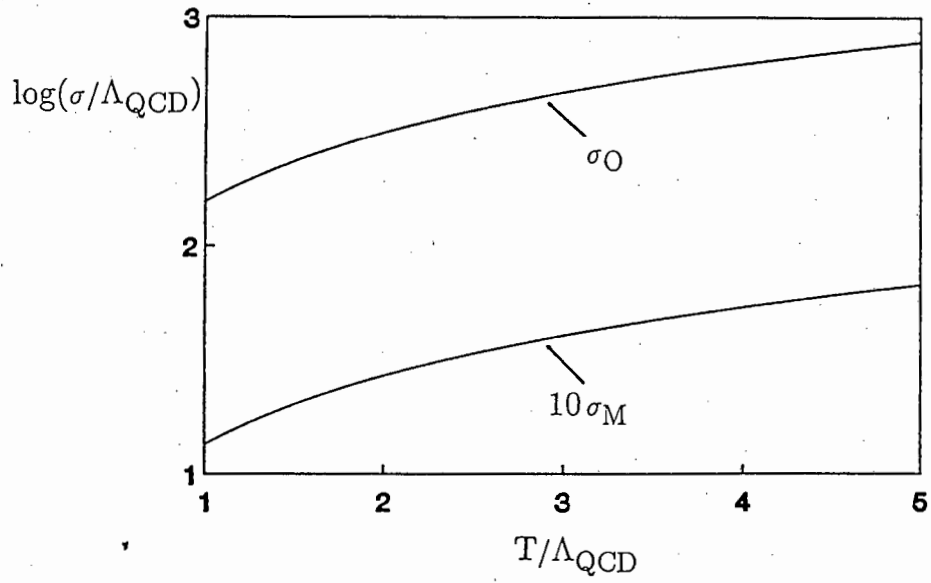


Figure 6.4: Conductivity of a Quark Antiquark System.

## 6.5 Summary

We found that the characteristic viscous relaxation time derived from the shear viscosity of the simple gluon system falls into the range

$$0.88 \leq \tau_\eta|_{\text{gluon}} T \leq 8.73. \quad (6.12)$$

Our result is the largest, probably because we used the full cm differential cross-section, and not a parametrisation. Also, there is an ambiguity connected to the evaluation of the Coulomb logarithm. In the comparison presented in the last sections, we assumed that

$$\log \Lambda_c \simeq \log(1/\alpha_s), \quad (6.13)$$

a relation which overestimates our result (see Appendix D). Another uncertainty introduced in the extraction procedure of the relaxation time is due to the fact that some authors provide results which take the quantum statistics into account. The resulting conversion to Maxwell Boltzmann statistics, which was carried out to make the results more readily comparable to ours, is not always unambiguous.

The results obtained for the characteristic viscous relaxation time of a QGP have a wider range

$$1.73 \leq \tau_\eta|_{\text{QGP}} T \leq 38.83. \quad (6.14)$$

The simple quark plus gluon contribution to the viscous relaxation time, denoted by  $O_1$ , is more than a factor 10 larger than the others in the literature. This discrepancy is due to the quark contribution, which we estimated in Chapter 5 to be a factor  $\sim 5 N_f = 10$  larger than the gluonic contribution. Most authors recognise that quarks contribute significantly to the transport coefficients of a QGP, but obtain a smaller quark to gluon contribution ratio. For example, Danielewicz and Gyulassy [9] estimate, that  $\eta_{\text{quark}}/\eta_{\text{gluon}} = 9/4$  for a 2-flavor plasma. The proper quark-gluon result  $O_2$  is about factor 2 smaller than  $O_1$ , indicating the importance of including antiquarks and the quark- (antiquark)-gluon interactions. Another aspect is, that most authors use a parametrised form of the cross-section, such as  $\sigma_t$  introduced in Chapter 3, (3.36). The quark contribution seems to be underestimated in this method. It is illuminating to see, that the results for quark-like systems, presented in Appendix F, are of the same order of magnitude as the results from Weinberg, Gavin and Danielewicz and Gyulassy. This indicates, that the discrepancy can be ascribed to the properties of spin and color. These have been included in our calculation by making use of the proper quark differential cross-section.

Much the same can be said about the comparison of the heat conduction relaxation times of a QGP. We find the range

$$7.90 \leq \tau_{\lambda}|_{\text{QGP}} T \leq 38.83, \quad (6.15)$$

where the upper limit is given by the simple quark plus gluon contribution, i.e. result  $O_1$ . It is larger by a factor 3 – 5, and the same reasoning as presented above, can be applied to explain the probable cause of this discrepancy in magnitude. Again, the inclusion of antiquarks and gluons reduces the result  $O_1$  to  $O_2$ .

A comparison of the conductivity  $\sigma$  of a quark antiquark mixture shows that

$$3.11 \leq \sigma/T \leq 360, \quad (6.16)$$

again with our result being the largest. This range of values is not satisfactory, and further attention ought to be given to this problem.

We conclude from this comparison, that the results obtained by using the Chapman Enskog method of solution, lead to higher estimates of the transport coefficients. We identified the quarks as the main contributor to transport processes. The study also indicates that the parametrised form of the differential cross-section works reasonably well for gluons, but seems to underestimate the effects due to quarks.

# Chapter 7

## Applications

In this Chapter, the results obtained in the previous Chapters will be applied to relevant physical systems. We shall investigate possible dissipative effects in systems where a quark-gluon plasma exists. These systems are believed to be the early universe and the central region of ultra-relativistic heavy ion collisions. In both scenarios, the quark-gluon phase is only temporary, as this phase is always followed by a transition to a hadron gas. It is expected that some, and possibly even all the signatures of the quark-gluon phase are wiped out in this transition. Nonetheless, it is of importance to study quark-gluon plasma systems, and in particular, to investigate how important non-equilibrium effects like dissipation are. The actual phase transition and its kinetics are complicated separate issues, which will not be considered in this thesis. We refer the reader to the interesting paper by Kajantie and Kurki-Suonio [58], in which the quark-hadron phase transition and possible effects in the context of the early universe are discussed.

The phase diagram of strongly interacting matter in Figure 7.1 shows the phase transition from the QGP to the hadron gas in the plane determined by the temperature and the baryo-chemical potential. Of interest is the evolution trajectory of the early universe, which is the application to be considered in the next section. We note that the ratio of the baryo-chemical potential  $\mu_b$  to the temperature is small,

$$\frac{\mu_b}{T} \simeq 10^{-10}, \quad (7.1)$$

reflecting the near-symmetry between baryons and antibaryons. We observe that the small baryon density and the form of the volume-expansion law (scaling hydrodynamics) are similarities between the “big bang” model of the universe and the central region of a heavy ion collision, also called the “little bang”. Both scenarios will be discussed in the following sections.

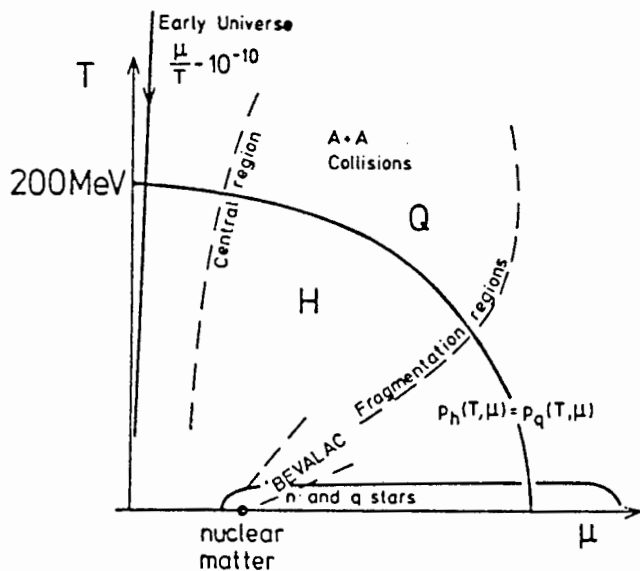


Figure 7.1: QGP-HG Phase Diagram.

## 7.1 Early Universe

In this section we consider the possible effects of viscous matter in the evolution of the early universe. For this purpose, we investigate, how viscous effects can be incorporated into the standard model of cosmology, i.e. the big bang model. A word of explanation concerning the use of “early” as in *early universe* might be in order: here we refer to times, where the universe was in a state so hot and dense, that a quark-gluon plasma was the preferred state. The transition from quarks and gluons to a gas of hot hadrons is believed to have occurred at a time, when the universe was about  $10^{-5}$  s old [59].

There are, of course, a number of papers in the literature, in which viscous phenomena in the early universe are discussed. For completeness, we mention a few: Caderni and Fabbri discuss the entropy production in the early universe, considering neutrino-electron and electron-photon systems [60]. Also, they investigate viscous effects in type 1 Bianchi universes [61]. Murphy [62] discusses viscous fluids and their possible cosmological consequences, such as big bang models without singularities. Hoogeveen et. al. [63] calculate the viscosities of the cosmic fluid in the lepton era. Similarly, van Leeuwen et. al. [64] calculate the transport coefficients of the cosmic proton-electron plasma in a magnetic field. An interest-

ing paper was published by Hageman and van Leeuwen [65], who studied viscous Bianchi type 2 universes. We see that there is an active research interest in this direction, but a detailed discussion of these interesting topics is beyond the scope of this thesis.

The equations governing the macroscopic evolution of the universe are believed to be given by Einstein's field equations [25]

$$R^{\mu\nu} = -8\pi G S^{\mu\nu}, \quad (7.2)$$

in terms of the Ricci or curvature tensor  $R^{\mu\nu}$  and the source term  $S^{\mu\nu}$ , which is given by

$$S^{\mu\nu} \equiv T^{\mu\nu} - \frac{1}{2} g^{\mu\nu} T^\alpha_\alpha. \quad (7.3)$$

Here,  $G$  denotes the gravitational constant,  $T^{\mu\nu}$  is the energy momentum tensor and  $g^{\mu\nu}$  the metric tensor. The metric for a general isotropic, homogeneous space-time is of the Robertson-Walker type, i.e.

$$d\tau^2 \equiv dt^2 - R(t)^2 \left[ \frac{dr^2}{1 - kr^2} + r^2 d\theta^2 + r^2 \sin^2 \theta d\phi^2 \right]. \quad (7.4)$$

The scale parameter  $R(t)$  is an unknown function of time, and  $k$  is the curvature constant.

Assuming that the energy momentum tensor is of the perfect fluid type, i.e.

$$\begin{aligned} T^{\mu\nu} &\equiv (en + P) \dot{U}^\mu U^\nu - P g^{\mu\nu} \\ &= en U^\mu U^\nu - P \Delta^{\mu\nu}, \end{aligned} \quad (7.5)$$

one can, using a usual well known procedure [25], readily obtain the Einstein equation

$$\left( \frac{dR}{dt} \right)^2 + k = \frac{8\pi G}{3} en R^2, \quad (7.6)$$

and the energy conservation equation

$$\frac{d}{dR} (en R^3) = -3 P R^2. \quad (7.7)$$

Here,  $R \equiv R(t)$  refers to the scale parameter. The evolution equations (7.6) and (7.7) have to be complemented by a suitable equation of state,

$$P = P(en), \quad (7.8)$$

in order to be soluble. The cosmological models described by equations (7.4) and (7.6) – (7.7) are known as the Friedmann-Robertson-Walker (FRW) universes. How do the above equations change if dissipative effects are included? This question will now be investigated. The fact that the Robertson-Walker metric (7.4) describes an isotropic space-time already indicates that shear viscosity plays no role in the above FRW models. It can furthermore be shown [25] that the effects of heat conduction are negligible in the FRW models. This leaves the volume viscosity  $\eta_v$  as the only dissipative effect to be considered. The deviation of the energy momentum tensor due to the volume viscosity is given by

$$\Delta T^{\mu\nu} = \eta_v \Delta^{\mu\nu} \partial^\alpha U_\alpha, \quad (7.9)$$

in terms of the hydrodynamic four velocity  $U^\mu$ . By replacing the derivative operator  $\partial^\alpha$  with the covariant derivative  $D^\alpha$ , one extends the validity of (7.9) to space-times with general geometries. For the Robertson-Walker models, one then finds

$$D^\alpha U_\alpha \equiv U_{;\alpha}^\alpha = 3 \frac{1}{R} \frac{dR}{dt}. \quad (7.10)$$

Combining the perfect fluid energy momentum tensor (7.5) with its generalised deviation (7.9), one obtains

$$T^{\mu\nu} = en U^\mu U^\nu - \left( P - 3\eta_v \frac{1}{R} \frac{dR}{dt} \right) \Delta^{\mu\nu}. \quad (7.11)$$

This expression can now be used to find the source term  $S^{\mu\nu}$ , using (7.3). From the field equations (7.2), the new dynamical laws governing the evolution of a viscous universe can be derived

$$\left( \frac{dR}{dt} \right)^2 + k = \frac{8\pi G}{3} en R^2, \quad (7.12)$$

$$\frac{d}{dR} (en R^3) = -3P R^2 + 9\eta_v R \frac{dR}{dt}. \quad (7.13)$$

Throughout our treatment, we have assumed that quarks and gluons are massless. Furthermore, we know that systems of massless particles have a negligible volume viscosity. This leads us to conclude that in an early universe described by the Friedmann-Robertson-Walker model, all entropy producing mechanisms in the quark-gluon phase are negligible. This is understandable if one considers the different time-scales of the problem: the non-equilibrium processes have time-scales of the order of the strong interaction, i.e.  $\tau_s \simeq 10^{-23}$  s, compared to

the inverse Hubble expansion rate with timescales many orders greater than  $\tau_s$ . This concludes the study of the quark-gluon phase.

As the universe expands and cools, its content of quarks and gluons undergoes a transformation to hadronic matter in the form of pions and nucleons. This is the quark-hadron phase transition. In this stage of evolution, our estimates for the transport coefficients of quark-gluon matter become unreliable, since non-perturbative effects are important there. Furthermore, since the kinetics of the phase transition plays an important role, it is well possible that, depending on the type of transition, a considerable amount of entropy may be produced. A possible transition scenario is shown in Figure 7.2. We note that the phase transition time  $\Delta t$  depends on the equation of state of both phases, including possible dissipative effects, the transition temperature and the transition kinetics. It is therefore difficult to make any reliable predictions about the amount of entropy produced without making numerous model-dependent assumptions, such as specifying the equation of state and the order of transition.

After the transition, nearly all the quark-gluon matter is converted into a hot hadronic gas of pions and nucleons. We may now ask what role the pions play in the production of entropy. Pions are massive ( $m_\pi \simeq 140$  MeV), and if the transition temperature is of the order

$$T_c \simeq 200 \text{ MeV}, \quad (7.14)$$

they will contribute to the volume viscosity. Assuming a constant pion cross-section of 20 mb, we can now compute the volume viscosity, using the formalism presented in Chapter 4, which has been adapted for massive particles. We see from Figure 7.3, that pions do indeed contribute to the volume viscosity at temperatures close to the phase transition temperature. Nucleons, on the other hand, with masses of about 1 GeV, are non-relativistic particles, even at  $T \simeq 200$  MeV. Therefore their contribution towards the volume viscosity of the hadronic gas is negligible.

After making the appropriate choice for the equation of state, one can now compute the ‘‘Hubble constant’’  $H \equiv 1/R dR/dt$ , using the Einstein equation (7.12) and the energy conservation equation (7.13). The values obtained can then be used to compare the predictions for the viscous cosmological model (from (7.12) and (7.13)) to those for the non-viscous cosmological model (from (7.6) and (7.7)). It turns out that the rate of expansion decreases if viscous effects are included.

We will now compare the shear viscosity and heat conductivity of the quark-gluon matter to the corresponding quantities in a pion fluid. Repeating the calculations that led to the shear viscosity of quarks for massive pions, we find

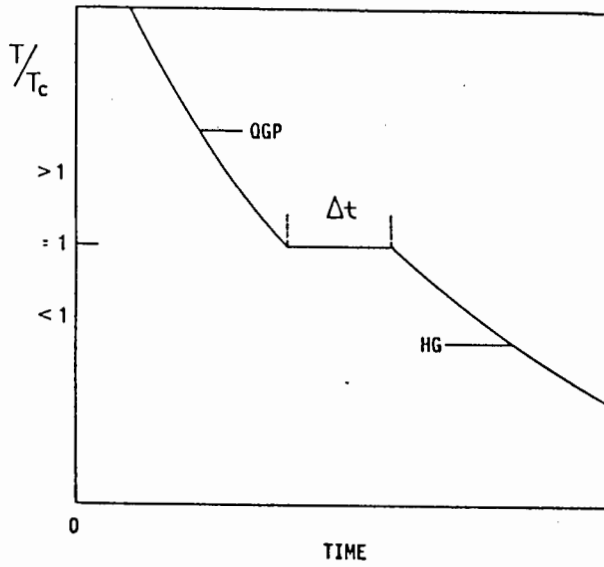


Figure 7.2: Cosmological Phase Transition.

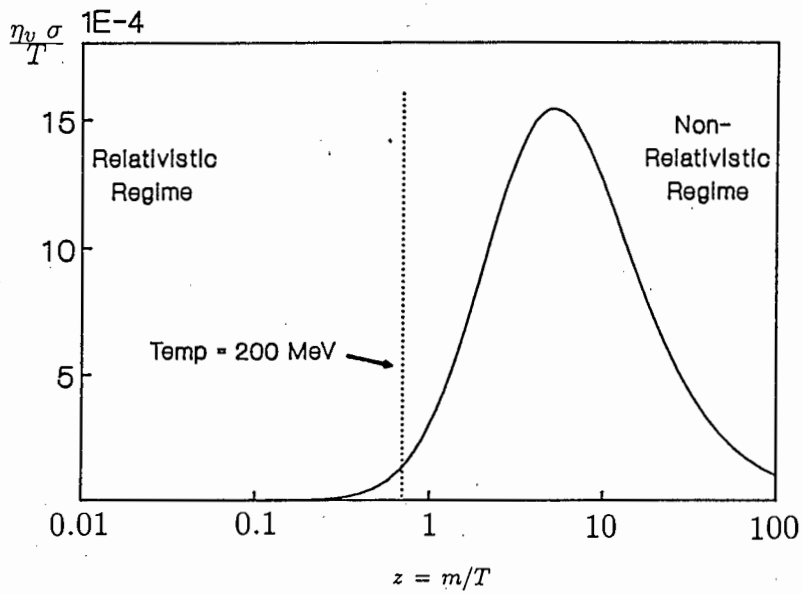


Figure 7.3: Pion Volume Viscosity.

that the pion shear viscosity is a factor  $10^3$  smaller than the corresponding quark-gluon viscosity. Somewhat daringly, we plot both the quark-gluon and pion shear viscosities in a temperature interval centered around the quark-hadron phase transition, bearing in mind that our quark-gluon results are only valid in the perturbative regime, i.e. for  $T \gg \Lambda_{\text{QCD}}$ . The results are displayed in Figure 7.4.

Along the same lines, we find the heat conductivity of the quark-gluon and pion systems. Again we find that the pion heat conductivity is about  $10^3$  smaller than the quark-gluon heat conductivity. This is shown in Figure 7.5.

We conclude this section with the observation, that entropy producing processes can easily be included into the dynamical equations describing the evolution of the early universe. We find that pions are the main contributors towards the volume viscosity in the post-transition phase. The shear viscosity and heat conductivity of the quark-gluon system is much larger than the corresponding quantities in the pion fluid. These coefficients, however, are negligible in a Friedmann-Robertson-Walker universe.

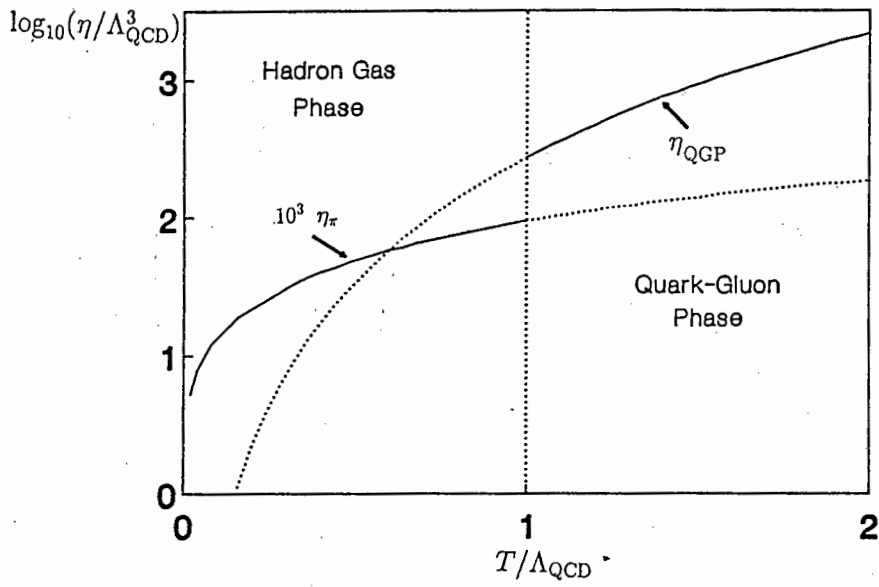


Figure 7.4: Quark-Gluon and Pion Shear Viscosity.

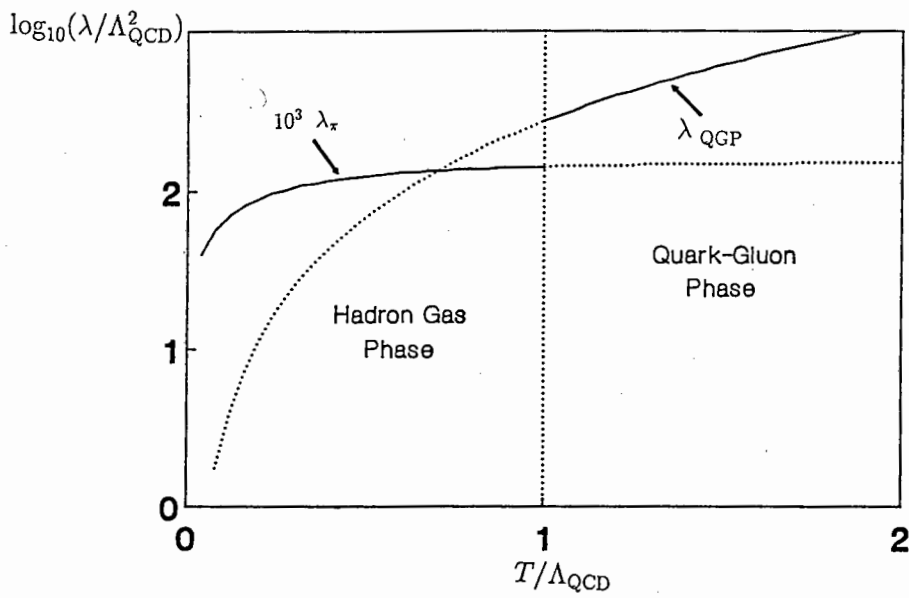


Figure 7.5: Quark-Gluon and Pion Heat Conductivity.

## 7.2 Heavy Ion Collisions

In ultra-relativistic heavy ion collisions, one needs to understand the evolution process of matter from the initial collision until the final state particles reach the detectors. An important diagnostic tool for this purpose is the entropy of the final particle distribution. Entropy measures the degrees of freedom over which the total cm energy is distributed. Because the entropy is essentially conserved during the expansion stage of the excited matter, it serves as a valuable messenger from the initial state. The problem therefore reduces to understanding possible sources of entropy production, hence the preceding study of transport phenomena in quark-gluon matter.

It is important to formulate a model describing the evolution of matter in ultra-relativistic heavy ion collisions. In this thesis, we only discuss one of the more frequently used models, the **Bjorken** space-time picture of the central region of ultra-relativistic heavy ion collisions [66]. In this model, shortly after the projectile-target collision, the partons are viewed as a freely streaming gas. After this initial free expansion phase, interactions become important, leading to a thermalisation of the fluid. This causes a phase of hydrodynamic expansion lasting until the onset of hadronisation, i.e. the quark-hadron transition. In the central rapidity regime, the principal hydrodynamic motion is longitudinal expansion with some transverse rarefaction. Lorentz boost-invariance at small rapidities is assumed. The hydrodynamic equations preserve this Lorentz invariant character which is reflected in the initial conditions in the central regime, such as the energy density  $en = en_0$  and the flow velocity  $v = v_z$  at  $\tau = \tau_0$ . This leads to simple scaling solutions of the thermodynamic quantities, as will be discussed in the following sections.

Figure 7.6 illustrates Bjorken's space-time picture of the central region of heavy ion collisions.

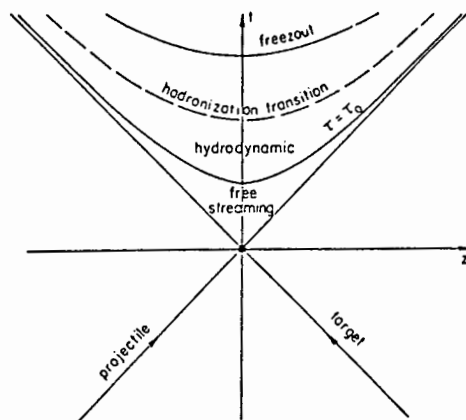


Figure 7.6: Bjorken's Picture of Heavy Ion Collisions.

## 7.2.1 Entropy Evolution

We will now make an estimate of the importance of entropy production during the expansion of the central rapidity region. Here, we follow the Bjorken Ansatz [66] mentioned above, i.e. a scenario where the dominant hydrodynamic motion in the central rapidity regime is a longitudinal expansion.

The entropy density evolution due to the longitudinal expansion obeys the conservation equation

$$\left. \frac{d(sn)}{d\tau} \right|_{\text{long}} + \frac{sn}{\tau} = 0, \quad (7.15)$$

which has the solution

$$sn(\tau) = sn_0 \left( \frac{\tau_0}{\tau} \right). \quad (7.16)$$

If the medium under consideration is viscous, the laws of scaling hydrodynamics demand the inclusion of an entropy production term [67]

$$\left. \frac{\partial(sn(\tau))}{\partial\tau} \right|_{\text{visc}} = \frac{(4/3)\eta + \eta_v}{T} \left( \frac{\partial v}{\partial z} \right)^2 = \frac{(4/3)\eta + \eta_v}{\tau^2 T}. \quad (7.17)$$

The quark-gluon matter is assumed massless, i.e.  $\eta_v = 0$ , so that (7.17) reduces to

$$\left. \frac{\partial(sn(\tau))}{\partial\tau} \right|_{\text{visc}} = \frac{4\eta}{3\tau^2 T}. \quad (7.18)$$

Comparing the longitudinal expansion (7.15) and the entropy production term (7.18), we form a dimensionless ratio of the two contributions, the so-called effective Reynolds number  $Re$  [67]

$$Re(\tau) \equiv \frac{sn}{\tau} \frac{3\tau^2 T}{4\eta} = \frac{3\tau T sn}{4\eta}. \quad (7.19)$$

We will now make use of the concept of a viscous relaxation time  $\tau_\eta$ , as was already introduced in Chapter 6, to rewrite the shear viscosity in terms of the entropy density and  $\tau_\eta$ , i.e.

$$\eta = \tau_\eta T sn. \quad (7.20)$$

The shear viscosity for quark-gluon matter (result O<sub>2</sub>) was found in Chapter 5, i.e.

$$\eta = 10.64 \frac{T^3}{\pi \alpha_s^2 \log(1/\alpha_s)} \quad (7.21)$$

and the entropy density of massless quarks (2 flavors,  $g = 24$ ) and gluons ( $g = 16$ ) is given by

$$sn(T) = 160 \frac{T^3}{\pi^2}. \quad (7.22)$$

Comparing (7.20) with (7.21) and (7.22), one finds the viscous relaxation time  $\tau_\eta$ ,

$$\tau_\eta = \frac{10.64 \pi}{160 T \alpha_s^2 \log(1/\alpha_s)}. \quad (7.23)$$

With appropriate values for a QGP, for example  $T \simeq 200$  MeV,  $\alpha_s \simeq 0.1$  and  $\log(1/\alpha_s) \simeq \log \Lambda_c = 7$ , one finds

$$\begin{aligned} \tau_\eta &\simeq 2.94 \text{ fm} \\ &\simeq 9.8 \cdot 10^{-24} \text{ s}. \end{aligned} \quad (7.24)$$

This value should be compared to Gavin's result [7] discussed in Chapter 3, who obtains

$$\begin{aligned} \tau_\eta &\simeq 3 \text{ fm} \\ &\simeq 10^{-23} \text{ s}. \end{aligned} \quad (7.25)$$

The corresponding value obtained for quark-like systems (for a discussion, see Appendix F) is given by (with  $\log \Lambda_c = 7$ )

$$\begin{aligned} \tau_\eta &\simeq 0.55 \text{ fm} \\ &\simeq 1.8 \cdot 10^{-24} \text{ s}. \end{aligned} \quad (7.26)$$

One should however be careful with the interpretation of this result, as the correct choice of the Coulomb logarithm is essential when comparing the QGP and quark-like system. Because we chose the same value of  $\log \Lambda_c$  for both systems, one obtains the somewhat strange result that the latter system equilibrates faster than the former. The different considerations for the evaluation of the Coulomb logarithm are discussed in greater detail in Appendix D, and we postpone a discussion of this important quantity to that section.

The effective Reynolds number  $Re(\tau)$ , defined in (7.19), can now be found

$$Re(\tau) = \frac{3}{4} \left( \frac{\tau}{\tau_\eta} \right). \quad (7.27)$$

Bearing in mind that Gavin [7] uses a slightly different formula than (7.27), we now compute the effective Reynolds numbers (for  $\tau \simeq 4$  fm), yielding

$$Re(4) \simeq 1.02 \quad (7.28)$$

for our result, Gavin obtains

$$Re(4) \simeq 5, \quad (7.29)$$

and the value for quark-like systems is given by

$$Re(4) \simeq 5.45. \quad (7.30)$$

One should note from the definition (7.19) of the effective Reynolds number that a perfect fluid has an infinite  $Re$ -number. In other words, if the effective Reynolds number is small, viscous effects in the fluid are important. We can therefore conclude that the entropy density in the expansion phase decreases slower relative to the simple scaling solution if the production term (7.18) is included. Viscous effects should therefore be included in hydrodynamical calculations of this nature, if the effective Reynolds number is small.

We will now solve the viscous entropy evolution equation (7.15) with the production term (7.18), i.e.

$$\begin{aligned} \frac{d(sn)}{d\tau} + \frac{sn}{\tau} &= \frac{4\eta}{3\tau^2 T} \\ &= \frac{sn}{\tau} \left( \frac{1}{Re} \right). \end{aligned} \quad (7.31)$$

This equation has the solution

$$sn(\tau) = sn_0(\tau) \left( \frac{\tau}{\tau_0} \right)^{-(1-1/Re)}. \quad (7.32)$$

Figure 7.7 shows a plot of the entropy evolution for the effective Reynolds numbers 1.2, 5, 10 and  $\infty$ .

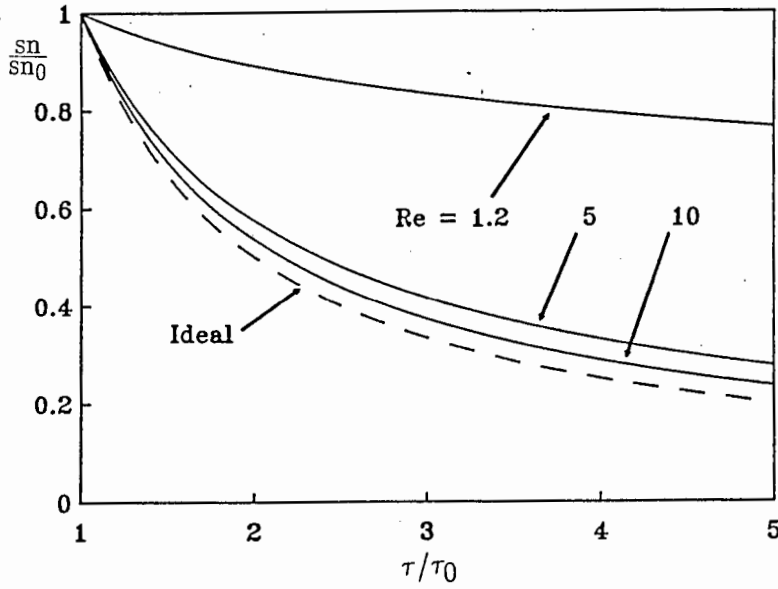


Figure 7.7: Entropy Evolution in Viscous Scaling Hydrodynamics.

### 7.2.2 Energy Density Evolution

As the next example, we investigate the effect of the inclusion of the transport coefficients in the scaling hydrodynamic solution for the energy density.

The conservation equation in scaling hydrodynamics is given by

$$\frac{dn}{d\tau} + \frac{n}{\tau} = 0, \quad (7.33)$$

which has the solution

$$n(\tau) = n_0 \left( \frac{\tau_0}{\tau} \right). \quad (7.34)$$

This equation is now used in conjunction with the viscous entropy evolution equation (7.31) to derive the corresponding energy density evolution equation.

The thermodynamic relation

$$T(sn) = wn - \mu_b n, \quad (7.35)$$

and the first law of thermodynamics

$$T d(sn) = d(en) - \mu_b dn \quad (7.36)$$

simplify in the near baryonless central region, where the scaling solution is applicable. Therefore, with  $\mu_b \simeq 0$  in (7.35) and (7.36), relation (7.31) is trivially rewritten to read

$$\frac{d(en)}{d\tau} + \frac{wn}{\tau} = \frac{wn}{\tau} \left( \frac{1}{Re} \right). \quad (7.37)$$

This equation is easily solved, yielding

$$en(\tau) = en_0 \left( \frac{\tau}{\tau_0} \right)^{-4(1-1/Re)/3}. \quad (7.38)$$

The well-known scaling solution for a perfect fluid is readily recovered, for  $Re \rightarrow \infty$

$$en(\tau)|_{\text{ideal}} = en_0 \left( \frac{\tau}{\tau_0} \right)^{-4/3}. \quad (7.39)$$

We observe here that the inclusion of viscous effects considerably prolongs the time in which the plasma is in a high energy density phase.

Figure 7.8 shows the results for the energy density evolution, using the effective Reynolds numbers of 1.2, 5, 10 and  $\infty$ .

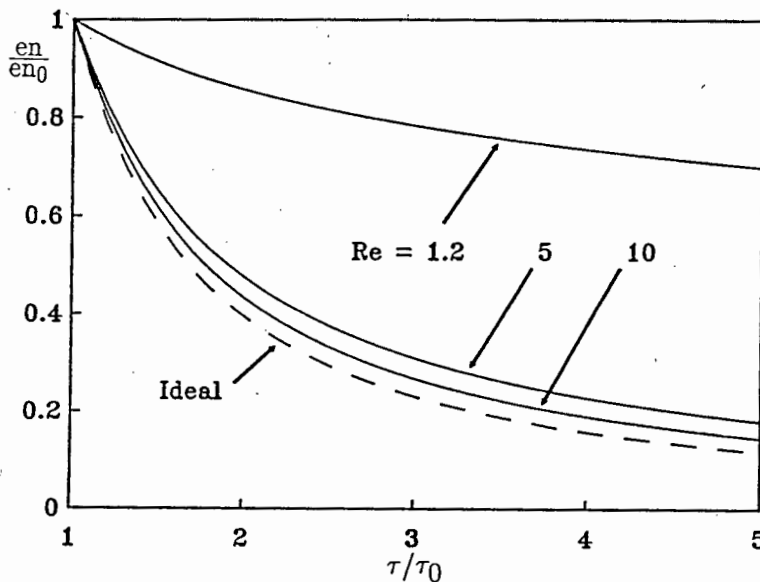


Figure 7.8: Energy Density Evolution in Viscous Scaling Hydrodynamics.

### 7.2.3 Temperature Evolution

As a final example, we investigate the question whether or not viscous effects influence the cooling of the longitudinally expanding central region.

Assuming that the energy density  $en$  and temperature are related by

$$en \propto T^4, \quad (7.40)$$

we immediately find the temperature evolution equation from the energy density evolution equation (7.37)

$$\frac{dT}{d\tau} + \frac{1}{3} \frac{T}{\tau} = \frac{T}{3\tau} \left( \frac{1}{Re} \right). \quad (7.41)$$

Again, this equation is easily solved, yielding

$$T = T_0 \left( \frac{\tau}{\tau_0} \right)^{-(1-1/Re)/3}, \quad (7.42)$$

which, in the limit  $Re \rightarrow \infty$ , reduces to the well-known perfect fluid scaling solution

$$T = T_0 \left( \frac{\tau}{\tau_0} \right)^{-1/3}. \quad (7.43)$$

We plot the results for  $Re = 1.2, 5, 10$  and  $\infty$  in Figure 7.9. It turns out that viscous effects cause the expanding plasma to stay longer in a high temperature phase.

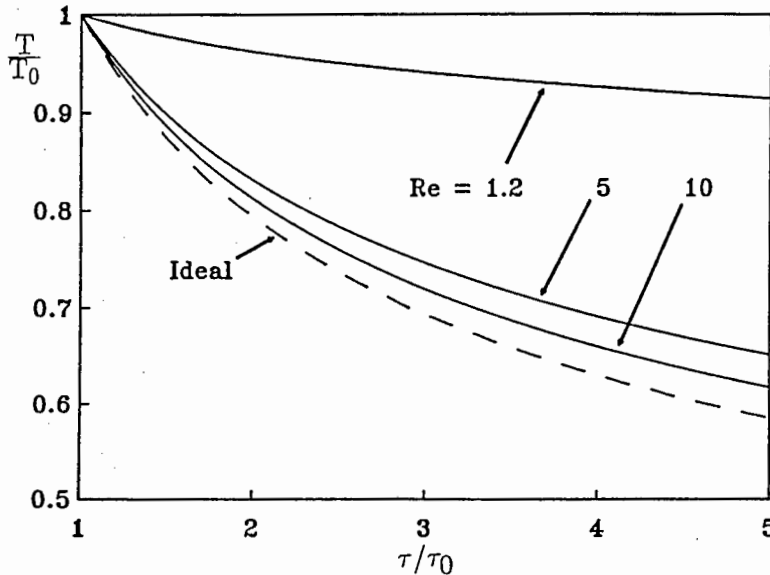


Figure 7.9: Temperature Evolution in Viscous Scaling Hydrodynamics.

### 7.3 Summary

This Chapter saw the discussion of the importance of dissipative effects in quark-gluon plasmas. Two possible scenarios were considered, namely the early universe and the central region of ultra-relativistic heavy ion collisions. It is important to note that predictions were obtained within very specific models, the Friedmann-Robertson-Walker universe on the one hand, and the central region of heavy ion collisions obeying the laws of scaling hydrodynamics on the other.

In the dissipative Friedmann-Robertson-Walker universe it was found that due to the underlying assumption of an isotropic space-time, only viscous, and in particular only effects due to the volume viscosity, played a role. However, massless quarks and gluons imply a vanishing volume viscosity, entropy producing mechanisms in this system are only expected during the phase transition to the hadron gas, and in the post-transition pionic phase.

In the central region of heavy ion collisions, where a longitudinal expansion of the excited matter is dominant, the laws of scaling hydrodynamics were applied. We introduced an effective Reynolds number as a measure of the viscous contribution to the entropy production. This was useful, as it allowed us to find the scaling hydrodynamic solution for viscous matter. The entropy density, energy density and temperature evolution were considered separately. We found that the introduction of viscous effects increases the plasma lifetime, implying a plasma phase with a prolonged time in the high energy density and high temperature state.

# Chapter 8

## Summary

In this thesis we studied the transport coefficients of quarks and gluons.

In the framework of relativistic kinetic theory, we derived a transport equation for quarks and antiquarks as classical, spinless but color carrying particles. Assuming a medium where 2-body collisions are the dominant scattering process, the transport equation could be simplified, yielding a generalised form of the commonly known relativistic Boltzmann equation.

A review of important articles in the literature showed that the relaxation time approximation is the preferred method to solve for the transport coefficients of quarks and gluons. This method, however, has some disadvantages when solving for the transport coefficients of mixtures. The realisation of this problem prompted us to make use of the Chapman Enskog method to calculate the transport coefficients of quarks and gluons. Although more demanding, this method is mathematically rigorous and intuitively appealing. It makes use of the phenomenologically motivated relations connecting the non-equilibrium manifestations of a system, i.e. the thermodynamic forces and flows, to provide the transport coefficients as constants of proportionality between them. For a single species or one component system of massless particles, the transport coefficients are the heat conductivity and shear viscosity. In a binary mixture, we also have the diffusion coefficient, thermal diffusion and Dufour coefficient. Additionally, for a mixture in an external field, the conductivity can be computed.

We have studied various types of systems: a single species quark and gluon system, a binary mixture of quarks and antiquarks, a quark antiquark-gluon mixture and finally a quark antiquark system in an external field. The transport coefficients for the above mentioned systems are summarised in Chapter 5.

Several interesting features are observed. Most of the transport coefficients have a logarithmic dependence on a cut-off. The introduction of the cut-off was made necessary as a cure for the divergent scattering cross-sections. Although the divergence has a physical reason, namely the exchange of (massless) gluons, the resulting long-range interaction is being screened in a plasma. This leads to a limited range interaction, resulting in a logarithmic cut-off dependence of the transport coefficients. The evaluation of this logarithmic factor, traditionally

called the Coulomb logarithm from applications in electron plasmas, is discussed in Appendix D.

We also found that the Eucken relation, i.e. the ratio of the heat conductivity to the shear viscosity, is given by  $1/T$  for all systems studied.

The magnitude of the shear viscosity of a pure gluon systems as obtained in our study is larger by a factor 2 – 7 than that obtained by authors reviewed in Chapter 3. This is probably due to two reasons: most authors use a parametrised interaction cross-section instead of the lowest order perturbation theory scattering matrix elements of QCD to compute the cross-sections as we have done. Secondly, in the comparison of the results in Chapter 6, we made an approximation to the Coulomb logarithm which results in an overestimation of our result.

We found that the contribution to the transport coefficients due to quarks is important, for example, the quark to gluon shear viscosity ratio is given by  $\sim 5N_f$ , where  $N_f$  is the number of quark flavors. This ratio is  $\sim 3$  times larger than previously predicted by other authors. The importance of including quarks prompted us to consider the transport coefficients of a quark antiquark mixture. Here it was found that the thermal diffusion coefficient vanishes. Because this transport coefficient reflects the amount of species separation in a field-free system in the presence of temperature and pressure gradients, the vanishing thereof indicates that there is no quark antiquark separation (as classical particles).

The other system of interest is the quark antiquark-gluon system, the QGP. Here it was found that our results for the transport coefficients are also larger than those obtained by other authors, and when comparing the results for a non-reactive quark-gluon system to the QGP, one finds that the inclusion of antiquarks and the various gluon interactions causes a decrease of the typical relaxation time of the system. But the discrepancy in magnitudes remain, and it was again concluded, that it is due to the different cross-sections used, i.e. parametrised versus the full QCD expression. To substantiate this supposition, we made use of a parametrised interaction cross-section in our study of quark-like systems. It was confirmed that the inclusion of spin and color in the lowest order QCD matrix elements produces a factor  $\sim 9$  difference when comparing the shear viscosities of the real quark to the quark-like systems.

Large characteristic relaxation times imply large transport coefficients. But if the transport coefficients of the QGP produced in a heavy ion collision are considerably larger than previously believed, this plasma may not necessarily be in local equilibrium. In other words, the larger the transport coefficients are, the less likely it becomes that a state of local equilibrium is formed. Many of the signals expected from the QGP rely on the equilibration of the system [3], and should be reexamined in view of the above predictions.

In Chapter 7 we discussed the applications of the above results to systems where a quark-gluon plasma formation is probable. Two scenarios were investi-

gated: the quark-gluon phase and subsequent hadronic phase in the early universe, and the central region of ultra-relativistic heavy ion collisions.

We concluded that in the standard model of cosmology, i.e. the Friedmann-Robertson-Walker model, dissipative effects can only be due to particles exerting viscous pressure, i.e. due to volume viscosity. The pions in the post-transition period are possible candidates for causing such a viscosity.

In the Bjorken model of the central region in heavy ion collisions, where a longitudinal expansion of matter is dominant, we applied the laws of scaling hydrodynamics. Here we made use of an effective Reynolds number as a measure of the importance of non-equilibrium effects. We found that the inclusion of viscous effects causes the expanding plasma to stay in a high energy density and high temperature phase for a considerably longer time in comparison to the perfect fluid scenario. We conclude that viscous effects should be included in more general hydrodynamic calculations, for example to analyse particle distribution spectra.

The main purpose of this thesis was to calculate the transport coefficients of quarks and gluons. Numerous simplifications were made and they should be investigated in future. For example, the explicit color structure of QCD should be incorporated into the method of solution discussed above. Particles should be endowed with the proper quantum statistics, and a reanalysis of the generalised collision integral discussed in Appendix B, along the lines of Baym and Pethick [45], should be attempted. The cut-off problem, and the explicit inclusion of long-range transverse interactions, warrants much further attention. Also, once the quantum mechanical structure of QCD is fully incorporated, different equations are expected, and a basic problem of our calculations is its intrinsically classical nature. A quantum mechanical treatment would describe the scattering of quarks and gluons, as it occurs in the context of heavy ion collisions, as the component-scattering of the nuclear wavefunction. A proper solution of the initial quantum mechanical evolution of a quark-gluon nuclear wavefunction would therefore be useful. Another aspect to be considered in future is the problem of particle creation processes, as studied for example by Eisenberg and Kälbermann [68], which has been ignored entirely in our treatment. In addition, while the results obtained for the transport coefficients provide an estimate of their order of magnitude, and therefore also of the characteristic relaxation times in a quark-gluon plasma, it should be kept in mind that all the results were derived in the weak coupling limit. The relaxation times in the strongly interacting non-perturbative regime, on the other hand, could be considerably shorter and the magnitude of the transport coefficients could be drastically changed.

*Many assumptions and prejudices still have to be reconsidered before a truly realistic picture of the non-equilibrium quark-gluon phase emerges. We express our hope that this work will prove a step into the right direction.*

## Acknowledgements

I would like to thank my supervisor, Prof. Jean Cleymans, for taking me on as a student and for his support in the course of this work.

I am grateful to Prof. Ulrich Heinz for many helpful comments and suggestions. Dr. Derck Smits provided encouragement and I thank him for many useful suggestions and for carefully reading parts of the manuscript.

Prof. Raoul Viollier's continual quest for high-speed-great-memory computers was appreciated.

My thanks also goes to Prof. Jim Reid, who helped me with QCD related topics. I am thankful to Mike O'Connor for introducing me to the intricacies of wine appreciation. Dr. Gary Tupper and my fellow students are thanked for their insights and help.

A special word of thanks goes to Gunhild Schreiber, who endured the synthesis of my thesis, and my quirks. Danke schön !

The financial assistance in the form of a postgraduate student bursary, provided by the Foundation for Research Development of the Council for Scientific and Industrial Research, is gratefully acknowledged.

# Appendix A

## The Collision Bracket

In this Appendix we use a variational method to find the unknown coefficients  $A$ ,  $B^\mu$  and  $C^{\mu\nu}$  as used via the trial function  $\phi$  in the expressions (4.42), (4.43) and (4.44) for the transport coefficients. Our treatment follows the method of solution as used by de Groot, van Leeuwen and van Weert [4]. In this Appendix we therefore concentrate on the principle of solution, and suggest the above-mentioned monograph to be used complimentary.

Consider the equation (4.42) for the volume viscosity of a one component system

$$\eta_v = -\frac{T}{3\sigma(T)} (\overline{\pi^\mu \pi_\mu}, A). \quad (\text{A.1})$$

This transport coefficient is given in terms of the inner product bracket  $(A, B)$ , defined as

$$(A, B) \equiv \frac{1}{4\pi z^2 K_2(z) T^2} \int \frac{d^3 p}{p^0} A(p) B(p) e^{-\tau}. \quad (\text{A.2})$$

In this definition we made use of the dimensionless quantities

$$\tau \equiv \frac{p^\mu U_\mu}{T} \quad \text{and} \quad \pi^\mu \equiv \frac{p^\mu}{T}. \quad (\text{A.3})$$

Also, the overbar in (A.1) denotes a symmetrisation with respect to the space-like part, i.e. the part orthogonal to the hydrodynamic four-velocity  $U^\mu$ , of the vector  $\pi^\mu$ , i.e.

$$\overline{\pi^\mu} \equiv \Delta_\nu^\mu \pi^\nu. \quad (\text{A.4})$$

With the definition (A.4) we find

$$\begin{aligned} \overline{\pi^\mu \pi_\mu} &\equiv \Delta_\alpha^\mu \pi^\alpha \Delta_\mu^\beta \pi_\beta \\ &= \Delta_\alpha^\beta \pi^\alpha \pi_\beta. \end{aligned} \quad (\text{A.5})$$

The unknown coefficient  $A$  appearing in the expression for the volume viscosity (A.1) is the solution of the transport equation (4.32) as found in Chapter 4,

$$Y X = T L \left[ \frac{1}{n\sigma(T)} A X \right]. \quad (\text{A.6})$$

Absorbing all dimensional factors, with

$$Y' \equiv \frac{Y}{T^2} \quad (\text{A.7})$$

and

$$L' [A] \equiv \frac{1}{n T \sigma(T)} L[A], \quad (\text{A.8})$$

we find an equation in terms of the dimensionless, linearised collision operator  $L' [A]$ , given by

$$Y' = L' [A]. \quad (\text{A.9})$$

Here,  $Y'$  is given by

$$Y' \equiv \left( \frac{4}{3} - \gamma \right) \tau^2 + \left[ (\gamma - 1) \frac{w}{T} - \gamma \right] \tau - \frac{1}{3} z^2, \quad (\text{A.10})$$

in terms of the definitions (A.3), (A.7) and

$$z \equiv \frac{m}{T}, \quad (\text{A.11})$$

as from Chapter 4.

It is now useful to define the so-called square bracket operator

$$[B, A] \equiv (L' [B], A), \quad (\text{A.12})$$

in terms of the inner product bracket defined in (A.2) and the dimensionless, linearised collision operator  $L' [A]$ . Inserting  $L' [A]$  in terms of the integral representation of  $L[A]$  from (4.8), into the inner product bracket (A.2), we formulate the definition

$$[A, B] \equiv \frac{1}{2 [4 \pi z^2 K_2(z) T^2] n T \sigma(T)} \cdot \int \frac{d^3 p_1}{p_1^0} \frac{d^3 p_2}{p_2^0} \frac{d^3 p_3}{p_3^0} \frac{d^3 p_4}{p_4^0} e^{-\tau_1} f_2^{(0)} [A_1 + A_2 - A_3 - A_4] B W(p_1 p_2 | p_3 p_4),$$

or,

$$[A, B] \equiv \frac{\beta^6}{2[4\pi z^2 K_2(z)]^2 \sigma(T)} \cdot \int \frac{d^3 p_1}{p_1^0} \frac{d^3 p_2}{p_2^0} \frac{d^3 p_3}{p_3^0} \frac{d^3 p_4}{p_4^0} e^{-\tau_1 - \tau_2} [A_1 + A_2 - A_3 - A_4] B W(p_1 p_2 | p_3 p_4). \quad (\text{A.13})$$

Here we used the traditional notation  $\beta \equiv 1/T$  and assumed an equilibrium distribution function of the Maxwell Boltzmann type.

The volume viscosity (A.1) will now be rewritten in terms of this square bracket operator. To this end we note that (A.1) can be written in terms of the function  $Y'$ , which satisfies the transport equation (A.9), i.e.

$$\eta_v = \frac{T}{\sigma(T)} (Y', A). \quad (\text{A.14})$$

This is a consequence of the conditions of fit mentioned in Chapter 4. But since  $Y'$  is the left-hand-side of the transport equation (A.9), we can now make use of the definition (A.12) to rewrite  $\eta_v$  in (A.14) as

$$\eta_v = \frac{T}{\sigma(T)} [A, A]. \quad (\text{A.15})$$

The particular form of the square collision operator, as defined in (A.13), is motivated by their property

$$[A, B] > 0 \text{ iff } A = B. \quad (\text{A.16})$$

This property can be shown [4] to hold for all non-trivial functions  $A$ . If however, the function  $A$  is chosen to be a summational invariant, the square collision operator  $[A, A]$  vanishes. This is the consequence of energy and momentum conservation, and the conservation of the quantities connected to the respective chemical potentials.

In rewriting the transport coefficient  $\eta_v$  into a positive definite form, i.e. in terms of the square collision operator, we have satisfied an important condition as laid down by Boltzmann's H-theorem. This condition is that the entropy production, or, in other words, the transport coefficients, are always positive or equal to zero. The two other transport coefficients of a simple particle system can likewise be

rewritten in terms of the square collision operators. For the heat conductivity we analogously find

$$\lambda = -\frac{1}{3\sigma(T)} [B\overline{\pi^\mu}, B\overline{\pi_\mu}], \quad (\text{A.17})$$

and the shear viscosity is given by

$$\eta = \frac{T}{10\sigma(T)} \left[ C \frac{\overset{o}{\pi^\mu \pi^\nu}}{\pi^\mu \pi^\nu}, C \frac{\overset{o}{\pi_\mu \pi_\nu}}{\pi_\mu \pi_\nu} \right]. \quad (\text{A.18})$$

As already used in Chapter 4, the overbar in (A.17) and (A.18) denotes the symmetrised space-like part of the specific tensor, and the superscript  $o$  indicates that the tensor is traceless by construction. Note that the sign in (A.17) is a consequence of the metric and ensures that the positive definite character of the square bracket operator (A.16) is preserved.

Now we will address the problem of finding the unknown functions  $A$ ,  $B^\mu$  and  $C^{\mu\nu}$ . In the case of the transport equation (A.9), the exact solution will be denoted by  $\overset{o}{A}$ . Using the norm property

$$|A| \equiv [A, A]^{1/2}, \quad (\text{A.19})$$

and a given trial function  $A$ , then enables us to define a functional

$$F = F[A] \equiv \left| \overset{o}{A} - A \right|^2. \quad (\text{A.20})$$

We can now find the variation of the functional  $F[A]$ , i.e.

$$\begin{aligned} \delta F &= -2 \left( \delta A, L' \left[ \overset{o}{A} - A \right] \right) \\ &= -2 \left( \delta A, L' \left[ \overset{o}{A} \right] - L'[A] \right) \\ &= -2 \left( \delta A, Y' - L'[A] \right) \\ &= 0. \end{aligned} \quad (\text{A.21})$$

Here we made use of the inner product bracket from (A.2). Making an Ansatz for the trial function  $A$ ,

$$A = A(\tau, z) \equiv \sum_{s=0}^u A^s(z) \tau^s \quad (\text{A.22})$$

in terms of the dimensionless quantities  $\tau \equiv (p^\mu U_\mu)/T$  and  $z \equiv m/T$ , one can find its variation

$$\delta A = \sum_{s=0}^u \tau^s \delta A^s. \quad (\text{A.23})$$

The upper limit of the sum, i.e.  $u$ , indicates the order of approximation of  $A$  and determines the degree of the polynomial used for  $\tau^s$ . Inserting equation (A.22) and (A.23) into the minimisation condition (A.21), we find

$$\sum_{s=0}^u \delta A^s (\tau^s, Y') = \sum_{s=0}^u \delta A^s \left( \tau^s, L' \left[ \sum_{r=0}^u A^r \tau^r \right] \right). \quad (\text{A.24})$$

Now making use of the square bracket operator defined in (A.13), one finds

$$\begin{aligned} \alpha^s \equiv (\tau^s, Y') &= \sum_{r=0}^u A^r [\tau^s, \tau^r] \\ &\equiv \sum_{r=0}^u A^r A^{rs}. \end{aligned} \quad (\text{A.25})$$

The function  $\alpha^s$  is known, since both  $Y'$ , as from (A.10), and  $(\tau^s, 1)$ , as from (A.2), can be calculated.

Inserting the Ansatz for  $A$ , i.e. (A.22), into the expression for  $\eta_v$  from (A.15), we obtain

$$\begin{aligned} \eta_v &= \frac{T}{\sigma(T)} \sum_{r=0}^u \sum_{s=0}^u [A^r \tau^r, A^s \tau^s] \\ &= \frac{T}{\sigma(T)} \sum_{r,s=0}^u A^r A^s A^{rs}. \end{aligned} \quad (\text{A.26})$$

This equation is simplified by making use of the algebraic equation (A.25), i.e.

$$\eta_v = \frac{T}{\sigma(T)} \sum_{s=0}^u \alpha^s A^s. \quad (\text{A.27})$$

In the lowest non-vanishing order of approximation, i.e. for  $u = 2$ , (A.27) is given by

$$\eta_v = \frac{T}{\sigma(T)} \alpha^2 A^2. \quad (\text{A.28})$$

It is easily verified that  $\alpha^0 = \alpha^1 = 0$ . This realisation leads to

$$\alpha^2 = A^2 A^{22} \quad (\text{A.29})$$

from (A.25). Inserting (A.29) into (A.28), one finally obtains, in the lowest order of approximation, an expression for the volume viscosity

$$\eta_v = \frac{T}{\sigma(T)} \frac{(\alpha^2)^2}{A^{22}}. \quad (\text{A.30})$$

This expression is in terms of the square collision bracket  $A^{rs} \equiv [\tau^r, \tau^s]$  introduced in (A.26).

Rather than repeat the similar procedure for the heat conductivity and the shear viscosity (and the extra coefficients for mixtures), we briefly state the philosophy of the above mentioned variational approach:

1. rewrite the transport coefficient in terms of the square bracket operator, such as in (A.15),
2. choose a trial function for the unknown coefficients  $B^\mu$  or  $C^{\mu\nu}$ , such as (A.22),
3. insert into minimization condition (A.21),
4. obtain the algebraic equations, such as (A.25),
5. use 2) and 4) in the square bracket expression of the coefficient, such as in (A.15),
6. solve 4) and 5) to specific order of approximation, for example the first order, such as in (A.28).

Following this procedure, one arrives at the lowest order approximations for the heat conductivity

$$\lambda = \frac{1}{3\sigma(T)} \frac{(\beta^1)^2}{B^{11}}, \quad (\text{A.31})$$

and the shear viscosity

$$\eta = \frac{T}{10\sigma(T)} \frac{(\gamma^0)^2}{C^{00}}. \quad (\text{A.32})$$

Summarising, we collect the various factors needed in the computation of the transport coefficients.

The square collision brackets are given by

$$A^{rs} \equiv [\tau^r, \tau^s], \quad (\text{A.33})$$

$$B^{rs} \equiv - [\tau^r \bar{\pi}^\mu, \tau^s \bar{\pi}_\mu], \quad (\text{A.34})$$

$$C^{rs} \equiv \left[ \tau^r \frac{\circ}{\pi^\mu \pi^\nu}, \tau^s \frac{\circ}{\pi_\mu \pi_\nu} \right]. \quad (\text{A.35})$$

Note that the sign in (A.34) is a consequence of the metric and ensures that the square collision bracket  $B^{rs} > 0$  for all permissible  $r, s$ .

Also, the constants  $\alpha^r$ ,  $\beta^r$  and  $\gamma^r$  are given by

$$\begin{aligned} \alpha^r &\equiv (\tau^r, Y') \\ &= \left( \frac{4}{3} - \gamma \right) (1, \tau^{r+2}) + \left[ (\gamma - 1) \frac{w}{T} - \gamma \right] (1, \tau^{r+1}) - \frac{1}{3} z^2 (1, \tau^r) \end{aligned} \quad (\text{A.36})$$

$$\begin{aligned} \beta^r &\equiv - \left( \tau^r \bar{\pi}^\mu, \left( \tau - \frac{w}{T} \right) \bar{\pi}_\mu \right) \\ &= \frac{1}{z^2 K_2(z)} \left[ \int_z^\infty d\tau (\tau^2 - z^2)^{3/2} \tau^{r+1} e^{-\tau} - \frac{w}{T} \int_z^\infty d\tau (\tau^2 - z^2)^{3/2} \tau^r e^{-\tau} \right], \end{aligned} \quad (\text{A.37})$$

$$\begin{aligned} \gamma^r &\equiv \left( \tau^r \frac{\circ}{\pi^\mu \pi^\nu}, \frac{\circ}{\pi_\mu \pi_\nu} \right) \\ &= \frac{2}{3 z^2 K_2(z)} \left[ \int_z^\infty d\tau (\tau^2 - z^2)^{5/2} \tau^r e^{-\tau} \right], \end{aligned} \quad (\text{A.38})$$

and  $(1, \tau^r)$  is given by

$$(1, \tau^r) = \frac{1}{z^2 K_2(z)} \int_z^\infty d\tau (\tau^2 - z^2)^{1/2} \tau^r e^{-\tau}. \quad (\text{A.39})$$

Thus, with  $\gamma \equiv c_P/c_V = 1/c_V + 1$  (see Appendix E), one obtains the factors needed in the lowest order of approximation of the transport coefficients, i.e. for expressions (A.30), (A.31) and (A.32). They are

$$\alpha^2 = 5 \frac{w}{T} - 3\gamma \left( 1 + \frac{w}{T} \right) \quad (\text{A.40})$$

$$\beta^1 = \frac{3\gamma}{\gamma - 1}, \quad (\text{A.41})$$

$$\gamma^0 = 10 \frac{w}{T}. \quad (\text{A.42})$$

It remains to be shown how the square collision brackets (A.33) – (A.35) are computed.

To this end one writes the total momenta  $P^\mu$  and  $P'^\mu$  as

$$P^\mu \equiv p_1^\mu + p_2^\mu \quad \text{and} \quad P'^\mu \equiv p_3^\mu + p_4^\mu, \quad (\text{A.43})$$

and the relative momenta  $Q^\mu$  and  $Q'^\mu$  as

$$Q^\mu \equiv p_1^\mu - p_2^\mu \quad \text{and} \quad Q'^\mu \equiv p_3^\mu - p_4^\mu. \quad (\text{A.44})$$

With these we find  $\tau_1^r, \tau_2^r, \tau_3^r$  and  $\tau_4^r$ . Making a binomial expansion of  $\tau_1$ , and noting that

$$P \cdot U \equiv P^\mu U_\mu \quad \text{and} \quad P \cdot P \equiv (P)^2, \quad (\text{A.45})$$

we find

$$\begin{aligned} \tau_1^r &\equiv \left( \frac{p_1^\mu U_\mu}{T} \right)^r = \left( \frac{1}{2} \beta (P \cdot U + Q \cdot U) \right)^r \\ &= \left( \frac{1}{2} \right)^r \sum_{u=0}^r \binom{r}{u} (\beta P \cdot U)^{r-u} (\beta Q \cdot U)^u. \end{aligned} \quad (\text{A.46})$$

Similarly, a binomial expansion can be found for  $\tau_2^r, \tau_3^r$  and  $\tau_4^r$ . Combined into a form as needed to compute the square collision bracket  $A^{rs}$ , one finds

$$\begin{aligned} (\tau_1^r + \tau_2^r - \tau_3^r - \tau_4^r) \tau_1^s &= \left( \frac{1}{2} \right)^{r+s-1} \sum_{u,v=\text{even}}^{r,s} \binom{r}{u} \binom{s}{v} (\beta P \cdot U)^{r+s-v-u} \\ &\quad \cdot (\beta Q \cdot U)^v [(\beta Q \cdot U)^u - (\beta Q' \cdot U)^u]. \end{aligned} \quad (\text{A.47})$$

It is now useful to define a general 12-fold collision integral of the form

$$\begin{aligned} C^{[a,b,c,d,e]} &\equiv \frac{\beta^6}{2[4\pi z^2 K_2(z)]^2 \sigma(T)} \int \frac{d^3 p_1}{p_1^0} \frac{d^3 p_2}{p_2^0} \frac{d^3 p_3}{p_3^0} \frac{d^3 p_4}{p_4^0} e^{-\beta P \cdot U} (\beta P)^{2a} (\beta P \cdot U)^b \\ &\quad \cdot (\beta Q \cdot U)^c (\beta Q' \cdot U)^d (-\beta^2 Q' \cdot Q)^e W(p_3 p_4 | p_1 p_2), \end{aligned} \quad (\text{A.48})$$

and a combination of this integral, i.e.

$$C^{*[a,b,c,d,e]} \equiv C^{[a,b,c+d,0,e]} - C^{[a,b,c,d,e]}. \quad (\text{A.49})$$

Making use of (A.47) in the collision bracket  $A^{rs}$ , we find, using (A.48), (A.49) and the definition of  $A^{rs}$  from (A.33)

$$\begin{aligned} A^{rs} &\equiv [\tau^r, \tau^s] \\ &= \left(\frac{1}{2}\right)^{r+s-1} \sum_{u,v=\text{even}}^{r,s} \binom{r}{u} \binom{s}{v} C^{*[0,r+s-v-u,v,u,0]}. \end{aligned} \quad (\text{A.50})$$

In order to calculate  $B^{rs}$ , one needs the combination

$$(\tau_1^r \overline{\pi}_1^\mu + \tau_2^r \overline{\pi}_2^\mu - \tau_3^r \overline{\pi}_3^\mu - \tau_4^r \overline{\pi}_4^\mu) \tau_1^s \overline{\pi}_1^\mu. \quad (\text{A.51})$$

A binomial expansion, similar to the one made in (A.46), gives

$$\begin{aligned} \tau_3^r \overline{\pi}_3^\mu \tau_1^s \overline{\pi}_1^\mu &= -\tau_3^{r+1} \tau_1^{s+1} + \left(\frac{1}{2}\right)^{r+s+2} \sum_{u,v=0}^{r,s} \binom{r}{u} \binom{s}{v} (\beta P \cdot U)^{r+s-v-u} \\ &\quad \cdot (\beta Q \cdot U)^v (\beta Q' \cdot U)^u [(\beta P)^2 - (-\beta Q' \cdot Q)]. \end{aligned} \quad (\text{A.52})$$

Likewise, all other terms needed to find (A.51) are expanded. Then, regrouping the various sums and using the collision integral (A.48) and (A.49), one finally obtains

$$\begin{aligned} B^{rs} &\equiv -[\tau^r \overline{\pi}^\mu, \tau^s \overline{\pi}_\mu] \\ &= A^{r+1,s+1} + \left(\frac{1}{2}\right)^{r+s+1} \left[ \sum_{u,v=\text{odd}}^{r,s} \binom{r}{u} \binom{s}{v} C^{*[0,r+s-v-u,v,u,1]} \right. \\ &\quad \left. - \sum_{u,v=\text{even}}^{r,s} \binom{r}{u} \binom{s}{v} C^{*[1,r+s-v-u,v,u,0]} \right]. \end{aligned} \quad (\text{A.53})$$

The bracket expression for  $C^{rs}$  is obtained in a similar manner, one obtains

$$\begin{aligned}
C^{rs} &\equiv \left[ \tau^r \frac{o}{\pi^\mu \pi^\nu}, \tau^s \frac{o}{\pi_\mu \pi_\nu} \right] \\
&= -\frac{4}{3} A^{r+2,s+2} + \frac{z^2}{3} (A^{r+2,s} + A^{r,s+2}) - \frac{z^4}{3} A^{r,s} + 2B^{r+1,s+1} \\
&+ \left( \frac{1}{2} \right)^{r+s+3} \left[ \sum_{u,v=\text{even}}^{r,s} \binom{r}{u} \binom{s}{v} (C^{*[2,r+s-v-u,v,u,0]} + C^{*[0,r+s-v-u,v,u,2]}) \right] \\
&- \left( \frac{1}{2} \right)^{r+s+2} \sum_{u,v=\text{odd}}^{r,s} \binom{r}{u} \binom{s}{v} C^{*[1,r+s-v-u,v,u,1]}. \tag{A.54}
\end{aligned}$$

Note that the sign of the term  $2B^{r+1,s+1}$  in (A.54) needs to be corrected in [4] if the definition (A.34) and (A.53) is used consistently. The final answer is insensitive to the change  $u \leftrightarrow v$ .

The above expressions, i.e. (A.50), (A.53) and (A.54) enable us to calculate the bracket terms as needed in the transport coefficients (A.30), (A.31) and (A.32).

For a binary mixture, very similar expressions are found for the square collision brackets. Here we present the final results [4].

$$A_{kl}^{rs} \equiv x_k x_l [\tau^r, \tau_1^s]_{kl} + \delta_{kl} x_k \sum_{m=1}^2 x_m [\tau^r, \tau^s]_{km}, \tag{A.55}$$

$$B_{kl}^{rs} \equiv -x_k x_l [\tau^r \overline{\pi^\mu}, \tau_1^s \overline{\pi_{1\mu}}]_{kl} - \delta_{kl} x_k \sum_{m=1}^2 x_m [\tau^r \overline{\pi^\mu}, \tau^s \overline{\pi_\mu}]_{km}, \tag{A.56}$$

$$C_{kl}^{rs} \equiv x_k x_l \left[ \tau^r \frac{o}{\pi^\mu \pi^\nu}, \tau_1^s \frac{o}{\pi_{1\mu} \pi_{1\nu}} \right]_{kl} + \delta_{kl} x_k \sum_{m=1}^2 x_m \left[ \tau^r \frac{o}{\pi^\mu \pi^\nu}, \tau^s \frac{o}{\pi_\mu \pi_\nu} \right]_{km}. \tag{A.57}$$

With the generalised 12-fold collision integral given by

$$C_{kl}^{[a,b,c,d,e]} \equiv \gamma_{kl} \frac{\beta^6}{[8\pi]^2 \sigma(T)} \int \frac{d^3 p_k}{p_k^0} \frac{d^3 p_l}{p_l^0} \frac{d^3 p_i}{p_i^0} \frac{d^3 p_j}{p_j^0} e^{-\beta P \cdot U} (\beta P)^{2a} (\beta P \cdot U)^b (\beta Q \cdot U)^c (\beta Q' \cdot U)^d (-\beta^2 Q' \cdot Q)^e W_{kl}(p_i p_j | p_k p_l), \quad (\text{A.58})$$

where  $\gamma_{kl} \equiv 1 - \delta_{kl}/2$ , a factor introduced to avoid double counting when  $k = l$ , and making use of the combination

$$C_{kl}^{*[a,b,c,d,e]} \equiv C_{kl}^{[a,b,c+d,0,e]} - C_{kl}^{[a,b,c,d,e]}, \quad (\text{A.59})$$

we find the collision brackets as needed in (A.55) – (A.57). They are given by

$$[\tau^r, \tau_1^s]_{kl} \equiv \left(\frac{1}{2}\right)^{r+s} \sum_{u,v=1}^{r,s} (-1)^v \binom{r}{u} \binom{s}{v} C_{kl}^{*[0,r+s-u-v,u,v,0]}, \quad (\text{A.60})$$

$$[\tau^r, \tau^s]_{kl} \equiv \left(\frac{1}{2}\right)^{r+s} \sum_{u,v=1}^{r,s} \binom{r}{u} \binom{s}{v} C_{kl}^{*[0,r+s-u-v,u,v,0]}. \quad (\text{A.61})$$

The collision brackets needed in (A.56) are given by

$$\begin{aligned} [\tau^r \overline{\pi^\mu}, \tau_1^s \overline{\pi_{1\mu}}]_{kl} &\equiv -[\tau^{r+1}, \tau_1^{s+1}]_{kl} \\ &+ \left(\frac{1}{2}\right)^{r+s+2} \sum_{u,v=0}^{r,s} (-1)^v \binom{r}{u} \binom{s}{v} [C_{kl}^{*[1,r+s-u-v,u,v,0]} \\ &\quad + C_{kl}^{*[0,r+s-u-v,u,v,1]}] \end{aligned} \quad (\text{A.62})$$

$$\begin{aligned} [\tau^r \overline{\pi^\mu}, \tau^s \overline{\pi_\mu}]_{kl} &\equiv -[\tau^{r+1}, \tau^{s+1}]_{kl} \\ &+ \left(\frac{1}{2}\right)^{r+s+2} \sum_{u,v=0}^{r,s} \binom{r}{u} \binom{s}{v} [C_{kl}^{*[1,r+s-u-v,u,v,0]} \\ &\quad - C_{kl}^{*[0,r+s-u-v,u,v,1]}]. \end{aligned} \quad (\text{A.63})$$

Also, the collision brackets, as needed in (A.57) are given by

$$\begin{aligned}
\left[ \tau^r \frac{o}{\pi^\mu \pi^\nu}, \tau_1^s \frac{o}{\pi_{1\mu} \pi_{1\nu}} \right]_{kl} &\equiv -\frac{4}{3} \left[ \tau^{r+2}, \tau_1^{s+2} \right]_{kl} - 2 \left[ \tau^{r+1} \overline{\pi^\mu}, \tau_1^{s+1} \overline{\pi_{1\mu}} \right]_{kl} \\
&+ \left( \frac{1}{2} \right)^{r+s+4} \sum_{u,v=0}^{r,s} (-1)^v \binom{r}{u} \binom{s}{v} \left[ C_{kl}^{*[2,r+s-u-v,u,v,0]} \right. \\
&\quad \left. + 2 C_{kl}^{*[1,r+s-u-v,u,v,1]} + C_{kl}^{*[0,r+s-u-v,u,v,2]} \right] \quad (\text{A.64})
\end{aligned}$$

$$\begin{aligned}
\left[ \tau^r \frac{o}{\pi^\mu \pi^\nu}, \tau^s \frac{o}{\pi_\mu \pi_\nu} \right]_{kl} &\equiv -\frac{4}{3} \left[ \tau^{r+2}, \tau^{s+2} \right]_{kl} - 2 \left[ \tau^{r+1} \overline{\pi^\mu}, \tau^{s+1} \overline{\pi_\mu} \right]_{kl} \\
&+ \left( \frac{1}{2} \right)^{r+s+4} \sum_{u,v=0}^{r,s} \binom{r}{u} \binom{s}{v} \left[ C_{kl}^{*[2,r+s-u-v,u,v,0]} \right. \\
&\quad \left. - 2 C_{kl}^{*[1,r+s-u-v,u,v,1]} + C_{kl}^{*[0,r+s-u-v,u,v,2]} \right] \quad (\text{A.65})
\end{aligned}$$

Note that the results quoted for a binary mixture only hold for massless particles, expressions for massive particle mixtures are similarly obtained but more complicated in structure [4].

What remains to be done is the evaluation of the generalised collision integral. This task is carried out in Appendix B.

## A.1 Results for Square Collision Brackets

The square collision brackets  $B^{11}$  and  $C^{00}$  for simple systems of quarks and gluons, which, together with the constants in (A.36) – (A.38) are used in the expressions for the transport coefficients presented in Chapter 5, are listed below.

For the simple quark system we obtain

$$B^{11}|_{\text{quark}} = \pi \left( \frac{16}{3} \log \Lambda_c - \frac{2}{9} \Lambda^3 - \frac{74}{9} \Lambda \right), \quad (\text{A.66})$$

$$C^{00}|_{\text{quark}} = \pi \left( \frac{160}{9} \log \Lambda_c - \frac{20}{27} \Lambda^3 - \frac{740}{27} \Lambda \right). \quad (\text{A.67})$$

For the simple gluon system, using the differential cross-section (C.33), we find

$$B^{11}|_{\text{gluon}} = \pi \left( 27 \log \Lambda_c - \frac{27}{160} \Lambda^5 - \frac{45}{16} \Lambda^3 - \frac{999}{32} \Lambda \right), \quad (\text{A.68})$$

$$C^{00}|_{\text{gluon}} = \pi \left( 90 \log \Lambda_c - \frac{9}{16} \Lambda^5 - \frac{75}{8} \Lambda^3 - \frac{1665}{16} \Lambda \right). \quad (\text{A.69})$$

Note that the logarithmic terms and the terms proportional to  $\Lambda^5$  would have the same numerical coefficients if we used the factor 51/16 instead of 3 in the gluon scattering cross-section, as was discussed in Appendix C.

For the quark antiquark mixture, we use the expressions for the square collision brackets  $A_{kl}^{rs}$ ,  $B_{kl}^{rs}$  and  $C_{kl}^{rs}$ . Below we present the constants and square collision brackets needed to compute the transport coefficients (4.75) – (4.79) for such a mixture.

$$\alpha_1^1 = \alpha_2^1 = 0, \quad (\text{A.70})$$

$$\beta_1^1 = \beta_2^1 = 12, \quad (\text{A.71})$$

$$\gamma_1^0 = \gamma_2^0 = 10 \frac{w}{T} = 40, \quad (\text{A.72})$$

$$\beta_{11}^0 = 3x_2, \quad \beta_{12}^0 = -3x_1, \quad (\text{A.73})$$

$$\beta_{11}^1 = 12x_2, \quad \beta_{12}^1 = -12x_1, \quad (\text{A.74})$$

The square collision brackets needed to compute the first order approximation to the shear viscosity, the diffusion coefficient, the thermal diffusion and heat conductivity are found to be

$$\begin{aligned} B_{11}^{11} = & -\pi x_1 \left( 16x_2 \log \Lambda_{c2} + \frac{x_2 \Lambda^5}{60} + \frac{7x_2 \Lambda^4}{36} - \frac{25x_2 \Lambda^3}{54} + \frac{17x_2 \Lambda^2}{18} + \frac{191x_2 \Lambda}{36} \right. \\ & \left. + \frac{2009x_2}{540} - \frac{16x_1 \log \Lambda_{c1}}{3} + \frac{2x_1 \Lambda^3}{9} + \frac{74x_1 \Lambda}{9} \right) \end{aligned} \quad (\text{A.75})$$

$$B_{12}^{00} = \pi x_1 x_2 \left( \frac{2 \log \Lambda_{c2}}{3} + \frac{\Lambda^4}{96} - \frac{5\Lambda^3}{216} + \frac{5\Lambda^2}{144} + \frac{13\Lambda}{72} + \frac{97}{864} \right) \quad (\text{A.76})$$

$$B_{12}^{01} = \pi x_1 x_2 \left( \frac{8 \log \Lambda_{c2}}{3} + \frac{\Lambda^4}{24} - \frac{5\Lambda^3}{54} + \frac{5\Lambda^2}{36} + \frac{13\Lambda}{18} + \frac{97}{216} \right) \quad (\text{A.77})$$

$$B_{12}^{10} = \pi x_1 x_2 \left( \frac{8 \log \Lambda_{c2}}{3} + \frac{\Lambda^4}{24} - \frac{5\Lambda^3}{54} + \frac{5\Lambda^2}{36} + \frac{13\Lambda}{18} + \frac{97}{216} \right) \quad (\text{A.78})$$

$$B_{12}^{11} = \pi x_1 x_2 \left( \frac{32 \log \Lambda_{c2}}{3} - \frac{\Lambda^5}{60} + \frac{2\Lambda^4}{9} - \frac{25\Lambda^3}{54} + \frac{4\Lambda^2}{9} + \frac{23\Lambda}{12} + \frac{104}{135} \right) \quad (\text{A.79})$$

$$\begin{aligned} B_{22}^{11} = & \pi x_2 \left( \frac{16x_2 \log \Lambda_{c1}}{3} - \frac{2x_2 \Lambda^3}{9} - \frac{74x_2 \Lambda}{9} - 16x_1 \log \Lambda_{c2} - \frac{x_1 \Lambda^5}{60} \right. \\ & \left. - \frac{7x_1 \Lambda^4}{36} + \frac{25x_1 \Lambda^3}{54} - \frac{17x_1 \Lambda^2}{18} - \frac{191x_1 \Lambda}{36} - \frac{2009x_1}{540} \right) \end{aligned} \quad (\text{A.80})$$

$$C_{11}^{00} = -\pi x_1 \left( \frac{160x_2 \log \Lambda_{c2}}{9} + \frac{x_2 \Lambda^5}{18} + \frac{5x_2 \Lambda^4}{54} - \frac{25x_2 \Lambda^3}{81} + \frac{35x_2 \Lambda^2}{27} + \frac{145x_2 \Lambda}{18} \right. \\ \left. + \frac{1039x_2}{162} - \frac{160x_1 \log \Lambda_{c1}}{9} + \frac{20x_1 \Lambda^3}{27} + \frac{740x_1 \Lambda}{27} \right) \quad (\text{A.81})$$

$$C_{12}^{00} = -\pi x_1 x_2 \left( \frac{\Lambda^5}{18} - \frac{5\Lambda^4}{27} + \frac{25\Lambda^3}{81} + \frac{10\Lambda^2}{27} + \frac{175\Lambda}{54} + \frac{277}{81} \right) \quad (\text{A.82})$$

$$C_{22}^{00} = \pi x_2 \left( \frac{160x_2 \log \Lambda_{c1}}{9} - \frac{20x_2 \Lambda^3}{27} - \frac{740x_2 \Lambda}{27} - \frac{160x_1 \log \Lambda_{c2}}{9} - \frac{x_1 \Lambda^5}{18} \right. \\ \left. - \frac{5x_1 \Lambda^4}{54} + \frac{25x_1 \Lambda^3}{81} - \frac{35x_1 \Lambda^2}{27} - \frac{145x_1 \Lambda}{18} - \frac{1039x_1}{162} \right) \quad (\text{A.83})$$

The denominator determinants  $\Delta_B$  and  $\Delta_c$  are given in terms of the above collision brackets

$$\Delta_B \equiv -B_{12}^{00} y_1 - B_{12}^{10} y_6 + B_{12}^{01} y_5, \quad (\text{A.84})$$

$$\Delta_c \equiv C_{11}^{00} C_{22}^{00} - (C_{12}^{00})^2. \quad (\text{A.85})$$

The coefficients needed for some of the transport coefficients are

$$y_1 \equiv B_{11}^{11} B_{22}^{11} - (B_{12}^{11})^2, \quad (\text{A.86})$$

$$y_2 \equiv -B_{12}^{00} B_{22}^{11} - (B_{12}^{01})^2, \quad (\text{A.87})$$

$$y_3 \equiv -B_{12}^{00} B_{11}^{11} - (B_{12}^{10})^2, \quad (\text{A.88})$$

$$y_4 \equiv -B_{12}^{01} B_{12}^{10} + B_{12}^{00} B_{12}^{11}, \quad (\text{A.89})$$

$$y_5 \equiv -B_{12}^{10} B_{12}^{11} - B_{12}^{01} B_{11}^{11}, \quad (\text{A.90})$$

$$y_6 \equiv B_{12}^{01} B_{12}^{11} + B_{12}^{10} B_{22}^{11}. \quad (\text{A.91})$$

The above factors and square collision brackets are used in the formulae (4.75) to (4.79) for the transport coefficients of a massless quark antiquark mixture. The final results for the transport coefficients are presented in Chapter 5.

# Appendix B

## The Collision Integral

In this Appendix we solve the generalised 12-fold collision integral (A.48) following the treatment by Israel [17], van Erkelens and van Leeuwen [69] and by de Groot and co-workers [4]. The integral to be solved is given by

$$C^{[a,b,c,d,e]} \equiv \frac{\beta^6}{2[4\pi z^2 K_2(z)]^2 \sigma(T)} \int \frac{d^3 p_1}{p_1^0} \frac{d^3 p_2}{p_2^0} \frac{d^3 p_3}{p_3^0} \frac{d^3 p_4}{p_4^0} e^{-\beta P \cdot U} (\beta P)^{2a} (\beta P \cdot U)^b \cdot (\beta Q \cdot U)^c (\beta Q' \cdot U)^d (-\beta^2 Q' \cdot Q)^e W(p_3 p_4 | p_1 p_2). \quad (\text{B.1})$$

Here we made use of the total four-momenta

$$P^\mu \equiv p_1^\mu + p_2^\mu \text{ and } P'^\mu \equiv p_3^\mu + p_4^\mu, \quad (\text{B.2})$$

and relative four-momenta

$$Q^\mu \equiv \Delta_P^{\mu\nu} (p_{\nu 1} - p_{\nu 2}) \text{ and } Q'^\mu \equiv \Delta_{P'}^{\mu\nu} (p_{\nu 3} - p_{\nu 4}), \quad (\text{B.3})$$

where the projector  $\Delta_P^{\mu\nu}$  is defined as

$$\Delta_P^{\mu\nu} \equiv g^{\mu\nu} - \frac{P^\mu P^\nu}{P^2}. \quad (\text{B.4})$$

The definitions (B.2) and (B.3) ensure the orthogonality

$$P^\mu U_\mu \equiv P \cdot Q = 0 = P \cdot Q'. \quad (\text{B.5})$$

The first step in the general solution of (B.1) will be to write the integral measures in a manifestly covariant form. To this end, consider the integral

$$I \equiv \int \delta^{(4)}(p_1 + p_2 - p_3 - p_4) \frac{d^3 p_1}{p_1^0} \frac{d^3 p_2}{p_2^0}. \quad (\text{B.6})$$

This is integrated over  $\vec{p}_2$  to give

$$I = \int \delta(p_1^0 + p_2^0 - p_3^0 - p_4^0) \frac{d^3 p_1}{p_1^0 p_2^0}, \quad (\text{B.7})$$

which, in the cm-frame, is given by

$$I = \int \delta(P^0 - P'^0) \frac{|\vec{p}|_{\text{cm}}}{(P^0)^2} P^0 dP^0 d\Omega_{\text{cm}} \quad (\text{B.8})$$

in terms of the four-momenta and the angular integration measure  $d\Omega_{\text{cm}}$ . By introducing dummy integrations over  $Q^0$  and  $\vec{P}$ , (B.8) is written as

$$I = \frac{1}{2} \int dQ^0 d^4 P d\Omega_{\text{cm}} \delta^{(4)}(P - P') \delta(P \cdot Q) |\vec{Q}|, \quad (\text{B.9})$$

where the orthogonality condition  $P \cdot Q = 0$  has been used. The magnitude of the relative momentum vector  $Q^\mu$  is given by

$$Q^2 = 2(m_1^2 + m_2^2) - (1 + \alpha_{12}^2) P^2 \quad (\text{B.10})$$

where  $\alpha_{12} \equiv (m_1^2 - m_2^2)/P^2$ . This relation is used to introduce a dummy integration over  $\vec{Q}$  in the cm-frame, and (B.9) is finally given by

$$I = \int d^4 P d^4 Q \delta^{(4)}(P - P') \delta(P \cdot Q) \delta(Q^2 + (1 + \alpha_{12}^2) P^2 - 2(m_1^2 + m_2^2)), \quad (\text{B.11})$$

which is manifestly covariant.

Comparing (B.6) with (B.11), one similarly rewrites the collision integral (B.1). Making use of the  $\delta$ -function from the transition element, i.e.

$$\begin{aligned} W(p_3 p_4 | p_1 p_2) &\equiv s \sigma(s, \theta) \delta^{(4)}(p_1 + p_2 - p_3 - p_4) \\ &= P^2 \sigma(s, x) \delta^{(4)}(P - P') \end{aligned} \quad (\text{B.12})$$

in terms of the differential cross-section  $\sigma(s, x)$ , which is a function of the total cm-energy  $s$  and the cm-scattering angle  $x = \cos \theta$ , one finds

$$\begin{aligned}
C^{[a,b,c,d,e]} &= \frac{\beta^4}{2[4\pi z^2 K_2(z)]^2} \int d^4 P e^{-\beta P \cdot U} (\beta P)^{2a} (\beta P \cdot U)^b \\
&\cdot \frac{(\beta P)^2}{\sigma(T)} \int d^4 Q d^4 Q' \delta(P \cdot Q) \delta(P \cdot Q') \\
&\cdot \delta(Q^2 - 2(m_1^2 + m_2^2) + (1 + \alpha_{12}^2) P^2) \\
&\cdot \delta(Q'^2 - 2(m_3^2 + m_4^2) + (1 + \alpha_{34}^2) P^2) \\
&\cdot (\beta Q \cdot U)^c (\beta Q' \cdot U)^d (-\beta^2 Q' \cdot Q)^e \sigma(s, x). \tag{B.13}
\end{aligned}$$

The second part of (B.13) is easily integrated in the cm-frame over  $Q^0, Q'^0$ , which gets rid of the  $\delta$ -functions  $\delta(P \cdot Q)$  and  $\delta(P \cdot Q')$ . With the unit vectors

$$\hat{Q}^\mu \equiv \frac{Q^\mu}{(-Q^2)^{1/2}} \quad \text{and} \quad \hat{Q}'^\mu \equiv \frac{Q'^\mu}{(-Q'^2)^{1/2}}, \tag{B.14}$$

the second part of (B.13) is then written as

$$\begin{aligned}
C^{(c,d,e)} &\equiv \frac{\beta^{2+c+d+2e}}{\sigma(T)} \int d|\vec{Q}| d|\vec{Q}'| d\Omega d\Omega' |\vec{Q}|^2 |\vec{Q}'|^2 (-Q^2)^{(c+e)/2} \\
&\cdot \delta(Q^2 - 2(m_1^2 + m_2^2) + (1 + \alpha_{12}^2) P^2) \\
&\cdot \delta(Q'^2 - 2(m_3^2 + m_4^2) + (1 + \alpha_{34}^2) P^2) \\
&\cdot (-Q'^2)^{(d+e)/2} (\hat{Q} \cdot U)^c (\hat{Q}' \cdot U)^d (-\hat{Q}' \cdot \hat{Q})^e \sigma(s, -\hat{Q}' \cdot \hat{Q}). \tag{B.15}
\end{aligned}$$

This expression is simplified by integrating out the two remaining  $\delta$ -functions in the cm-frame (assuming that the particles are massless), giving

$$\begin{aligned}
C^{(c,d,e)} &= \frac{1}{4\sigma(T)} (\beta^2 P^2)^{(c+e+1)/2} (\beta^2 P'^2)^{(d+e+1)/2} \\
&\cdot \int d\Omega d\Omega' (-\hat{\vec{Q}} \cdot \vec{U})^c (-\hat{\vec{Q}}' \cdot \vec{U})^d (\hat{\vec{Q}}' \cdot \hat{\vec{Q}})^e \sigma(s, \hat{\vec{Q}}' \cdot \hat{\vec{Q}}). \tag{B.16}
\end{aligned}$$

To perform the remaining integral in (B.16), a frame is chosen such that  $\vec{U} = \vec{U}_z$ , and  $\hat{\vec{Q}} \cdot \vec{U} = U_z \cos \theta$ , and thus

$$U_z = \left( \frac{(P \cdot U)^2 - P^2}{P^2} \right)^{1/2}. \tag{B.17}$$

Now we make use of the properties of the properties of Legendre polynomials, see for example Arfken [70], then

$$\begin{aligned} f(x) &\equiv \frac{1}{\sigma(T)} \left( \hat{\vec{Q}} \cdot \hat{\vec{Q}}' \right)^e \sigma \left( P, \hat{\vec{Q}} \cdot \hat{\vec{Q}}' \right) \\ &= \sum_{n=0}^{\infty} a_n P_n(x). \end{aligned} \quad (\text{B.18})$$

Also, the orthogonality of Legendre polynomials is given by

$$\int_{-1}^{+1} dx P_n(x) P_m(x) = \frac{2}{2n+1} \delta_{nm}, \quad (\text{B.19})$$

and (B.18) can thus be expressed as

$$\frac{1}{\sigma(T)} \left( \hat{\vec{Q}} \cdot \hat{\vec{Q}}' \right)^e \sigma \left( P, \hat{\vec{Q}} \cdot \hat{\vec{Q}}' \right) = \sum_{n=0}^{\infty} \sigma^{(e,n)} P_n(\cos \Theta). \quad (\text{B.20})$$

Here,  $x = \cos \Theta$ , and

$$\sigma^{(e,n)} \equiv \frac{2n+1}{2\sigma(T)} \int_{-1}^{+1} dx x^e P_n(x) \sigma(P, x). \quad (\text{B.21})$$

Substituting (B.21) into (B.16) yields

$$\begin{aligned} C^{(c,d,e)} &= \frac{1}{4} \left( \beta^2 P^2 \right)^{(c+e+1)/2} \left( \beta^2 P'^2 \right)^{(d+e+1)/2} \\ &\cdot \int d\Omega d\Omega' (U_z)^{c+d} (-\cos \theta)^c (-\cos \theta')^d \sum_{n=0}^{\infty} \sigma^{(e,n)} P_n(x). \end{aligned} \quad (\text{B.22})$$

But the integral appearing in (B.22), i.e.

$$K(c, d, n) \equiv \frac{1}{(4\pi)^2} \int d\Omega d\Omega' (-\cos \theta)^c (-\cos \theta')^d P_n(\cos \Theta), \quad (\text{B.23})$$

can be solved, see for example Arfken [70], and is given by

$$K(c, d, n) = \frac{c! d!}{(c-n)!! (c+n+1)!! (d-n)!! (d+n+1)!!}. \quad (\text{B.24})$$

Substituting (B.24) into (B.22), and (B.17) into (B.13) gives

$$\begin{aligned}
C^{[a,b,c,d,e]} &= \frac{\beta^4}{8[z^2 K_2(z)]^2} \sum_{n=0}^{\min(c,d)} K(c,d,n) \\
&\cdot \int d^4 P e^{-\beta P \cdot U} (\beta P)^{2a-(c+d)} (\beta P \cdot U)^b [(\beta P \cdot U)^2 - (\beta P)^2]^{(c+d)/2} \\
&\cdot (\beta^2 P^2)^{(c+e+1)/2} (\beta^2 P'^2)^{(d+e+1)/2} \sigma^{(e,n)}. \tag{B.25}
\end{aligned}$$

The change of variables

$$\beta P^\mu = \left( \tau, \begin{matrix} \longrightarrow \\ (\tau^2 - v^2)^{1/2} \end{matrix} \right), \tag{B.26}$$

where

$$\beta^2 P^2 \equiv v^2 = \tau^2 - (\beta \vec{P})^2,$$

enables one to write

$$\beta^4 d^4 P = d\tau v dv d\Omega (\tau^2 - v^2)^{1/2}. \tag{B.27}$$

Using the magnitude  $Q^2$  of the relative four-momentum  $Q^\mu$  from (B.10), and a similar expression for  $Q'^2$ , one finally has

$$\begin{aligned}
C^{[a,b,c,d,e]} &= \frac{\pi}{2[z^2 K_2(z)]^2} \sum_{n=0}^{\min(c,d)} K(c,d,n) \int_{2z}^{\infty} dv \int_v^{\infty} d\tau \tau^b (\tau^2 - v^2)^{(c+d+1)/2} e^{-\tau} \\
&\cdot v^{2a-(c+d)+1} [v^2 - 4z^2]^{(c+d+2e+2)/2} \sigma^{(e,n)}. \tag{B.28}
\end{aligned}$$

Since we are dealing with massless particles only in this thesis, one conveniently rewrites (B.28), using the property of the modified Bessel functions, i.e.  $\lim_{z \rightarrow 0} z^2 K_2(z) = 2$ , and obtains

$$\begin{aligned}
C^{[a,b,c,d,e]} &= \frac{\pi}{8} \sum_{n=0}^{\min(c,d)} K(c,d,n) \\
&\cdot \int_0^{\infty} dv \int_v^{\infty} d\tau \tau^b (\tau^2 - v^2)^{(c+d+1)/2} e^{-\tau} v^{2a+2e+3} \sigma^{(e,n)}. \tag{B.29}
\end{aligned}$$

The particular form of the collision integral, as needed in Appendix A, prompts

us to introduce the transfer cross-section, which after the substitution  $u \equiv v/\tau$ , gives

$$\begin{aligned}
 C^{*[a,b,c,d,e]} &\equiv C[a,b,c+d,0,e] - C[a,b,c,d,e] \\
 &= \frac{\pi}{8(c+d+1)} \int_0^\infty d\tau \tau^{2(a+e+2)+b+c+d+1} e^{-\tau} \\
 &\quad \cdot \int_0^1 du u^{2(a+e+1)+1} (1-u^2)^{(c+d+1)/2} \sigma^{(c,d,e)}, \quad (\text{B.30})
 \end{aligned}$$

where the transfer cross-section  $\sigma^{(c,d,e)}$  is given by

$$\begin{aligned}
 \sigma^{(c,d,e)} &\equiv \frac{1}{2\sigma(T)} \int_{-1}^{+1} dx [1 - (c+d+1) \\
 &\quad \cdot \sum_{n=0}^{\min(c,d)} K(c,d,n) (2n+1) x^e P_n(x)] \sigma(s,x). \quad (\text{B.31})
 \end{aligned}$$

Once the differential cross-section  $\sigma(s,x)$  is known (rewritten as a function of  $u$  and  $\tau$ ), see Appendix C, the collision integral  $C^{*[a,b,c,d,e]}$  in (B.30) can be integrated.

Two integrals which are usually needed in the above calculations are the gamma function  $\Gamma(n)$

$$\begin{aligned}
 \Gamma(n) &\equiv \int_0^\infty d\tau \tau^{n-1} e^{-\tau} \\
 &= (n-1)!, \quad (\text{B.32})
 \end{aligned}$$

and the beta function  $B(n,m)$

$$\begin{aligned}
 B(n,m) &\equiv 2 \int_0^1 du (1-u^2)^{m-1} u^{2n-1} \\
 &= \frac{\Gamma(n)\Gamma(m)}{\Gamma(n+m)}. \quad (\text{B.33})
 \end{aligned}$$

# Appendix C

## The Matrix Elements

In this Appendix we examine the scattering diagrams (to lowest order in the perturbation expansion) for the processes

$$q q \rightarrow q q \tag{C.1}$$

$$q \bar{q} \rightarrow q \bar{q} \tag{C.2}$$

$$q g \rightarrow q g \tag{C.3}$$

and

$$g g \rightarrow g g. \tag{C.4}$$

All particles are considered to be massless.

Process (C.1) can generally be written as

$$q_{\alpha}^i q_{\beta}^k \rightarrow q_{\alpha}^j q_{\beta}^l$$

where  $\alpha, \beta$  is the quark flavor index, and  $i, j, k, l$  the quark color index  $i, j, k, l = 1, 2, 3$ . The notation used is such, that the index  $a, b$  is the gluon color index,  $a, b = 1, 2, \dots, 8$ , the Bjorken and Drell notation [38] is used throughout. We use the Feynman rules in the Feynman gauge, as listed in Table C.1.

The channels available in process (C.1) are the t- and the u-channel, as shown in Figure C.1 and Figure C.2, respectively. The t-channel matrix element in Figure C.1 then gives:

gluon		$-i \delta^{ab} \frac{g_{\mu\nu}}{k^2}$
ghost		$-i \delta^{ab} \frac{1}{k^2}$
quark		$i \delta^{ij} \frac{\not{p}}{p^2 + i\epsilon}$
quark-gluon vertex		$-i g \gamma^\mu \left(\frac{\lambda^a}{2}\right)_{ij}$
three-gluon vertex		$-g f_{abc} [(p - q)_\nu g_{\lambda\mu} + (q - r)_\lambda g_{\mu\nu} + (r - p)_\mu g_{\nu\lambda}]$
four-gluon vertex		$-i g^2 f_{abc} f_{cde} (g_{\lambda\nu} g_{\mu\sigma} - g_{\lambda\sigma} g_{\mu\nu})$ $-i g^2 f_{ace} f_{bde} (g_{\lambda\mu} g_{\nu\sigma} - g_{\lambda\sigma} g_{\mu\nu})$ $-i g^2 f_{ade} f_{cbe} (g_{\lambda\nu} g_{\mu\sigma} - g_{\lambda\mu} g_{\sigma\nu})$
ghost-gluon vertex		$g f_{abc} p^\mu$

Table C.1: Feynman Rules of QCD in the Feynman Gauge.

$$|M_t|^2 = \frac{g^4}{t^2} (T_{ij}^a T_{kl}^a)^2 \left[ (\bar{u}_\alpha^j \gamma^\mu u_\alpha^i) (\bar{u}_\beta^l \gamma_\mu u_\beta^k) (\bar{u}_\alpha^i \gamma^\nu u_\alpha^j) (\bar{u}_\beta^k \gamma_\nu u_\beta^l) \right], \quad (\text{C.5})$$

and for the u-channel matrix element from Figure C.2 we find

$$|M_u|^2 = \frac{g^4}{u^2} (T_{il}^a T_{jk}^a)^2 \delta_{\alpha\beta} \left[ (\bar{u}_\beta^l \gamma^\mu u_\alpha^i) (\bar{u}_\alpha^j \gamma_\mu u_\beta^k) (\bar{u}_\alpha^i \gamma^\nu u_\beta^l) (\bar{u}_\beta^k \gamma_\nu u_\alpha^j) \right]. \quad (\text{C.6})$$

Here, t and u are the Mandelstam variables such that

$$\begin{aligned} s &\equiv (p_1 + p_2)^2 = (p_3 + p_4)^2, \\ t &\equiv (p_1 - p_4)^2 = (p_2 - p_3)^2, \\ u &\equiv (p_1 - p_3)^2 = (p_2 - p_4)^2. \end{aligned} \quad (\text{C.7})$$

The color matrices  $T_{ij}^a$  are written as  $T_{ij}^a \equiv \frac{1}{2} \lambda_{ij}^a$ , where  $\lambda_{ij}^a$  are the Gell-Mann matrices.  $g$  is the coupling constant such that  $g^2 = 4 \pi \alpha_s$  in terms of the strong coupling constant  $\alpha_s$ .

Averaging over initial states of spin and color and summing over the final states gives, after the extensive use of the well-known trace relations and color sums from Table C.2,

$$|M_t|^2 = \frac{4}{9} g^4 \left( \frac{s^2 + u^2}{t^2} \right) \quad (\text{C.8})$$

and

$$|M_u|^2 = \frac{4}{9} g^4 \left( \frac{s^2 + t^2}{u^2} \right) \delta_{\alpha\beta}. \quad (\text{C.9})$$

The cross-channel, i.e. the matrix elements

$$|M_t M_u^*| \quad \text{and} \quad |M_u M_t^*|,$$

is found from Figure C.1 and Figure C.2. It is given by

$$|M_t M_u^*| = -\frac{g^4}{u t} (T_{ij}^a T_{kl}^a T_{il}^b T_{kj}^b) \delta_{\alpha\beta} \left[ (\bar{u}_\alpha^j \gamma^\mu u_\alpha^i) (\bar{u}_\beta^l \gamma_\mu u_\beta^k) (\bar{u}_\alpha^i \gamma^\nu u_\beta^l) (\bar{u}_\beta^k \gamma_\nu u_\alpha^j) \right], \quad (\text{C.10})$$

which, after the use of some trace relations, reduces to

$$|M_t M_u^*| = -\frac{4}{27} g^4 \delta_{\alpha\beta} \left( \frac{s^2}{u t} \right). \quad (\text{C.11})$$

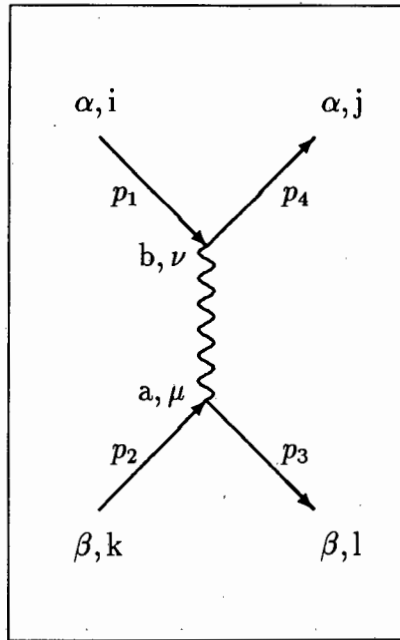


Figure C.1: t-Channel Diagram for Quark-Quark Scattering.

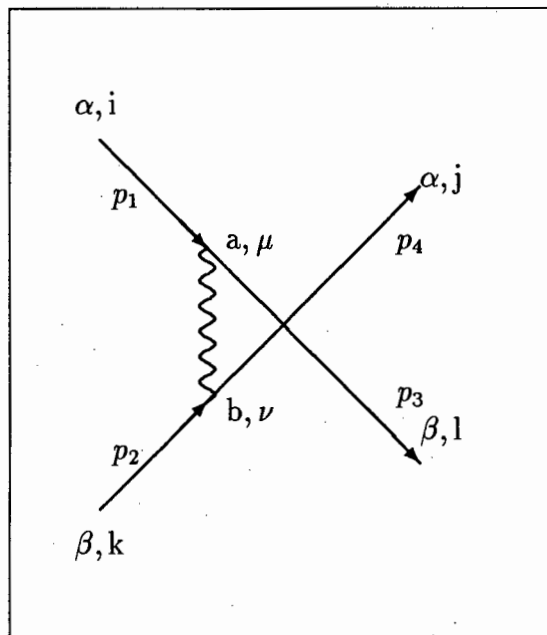


Figure C.2: u-Channel Diagram for Quark-Quark Scattering.

The matrix element  $|M_u M_t^*|$  is the same as (C.11), so that the final matrix element squared for the process (C.1) is the sum of (C.8), (C.9) and  $2*(C.11)$ :

$$|M_{q_\alpha^i q_\alpha^k \rightarrow q_\alpha^j q_\alpha^l}|^2 = \frac{4}{9} g^4 \left[ \frac{s^2 + u^2}{t^2} + \frac{s^2 + t^2}{u^2} - \left(\frac{2}{3}\right) \frac{s^2}{u t} \right]. \quad (C.12)$$

The expression (C.12) applies to processes for which the quark flavor (index  $\alpha$  and  $\beta$ ) is the same in the in- and outgoing channel; we only describe single flavor systems. It also holds for the process  $\bar{q} \bar{q} \rightarrow \bar{q} \bar{q}$ .

The next scattering matrix element to be considered is for the quark-antiquark process (C.2), generally written as

$$q_\alpha^i \bar{q}_\beta^k \rightarrow q_\delta^j \bar{q}_\gamma^l$$

where the indices have the same meaning as in the previous process. Channels available for this process are the s- and t-channel:

The s-channel matrix element, from Figure C.3, is given by

$$|M_s|^2 = \frac{g^4}{s^2} (T_{ik}^a T_{jl}^a)^2 \left[ (\bar{v}_\beta^k \gamma^\mu u_\alpha^i) (\bar{u}_\delta^j \gamma_\mu v_\gamma^l) (\bar{u}_\alpha^i \gamma^\nu v_\beta^k) (\bar{v}_\gamma^l \gamma_\nu u_\delta^j) \right] \quad (C.13)$$

and the t-channel from Figure C.4 is found to be

$$|M_t|^2 = \frac{g^4}{t^2} (T_{ij}^a T_{kl}^a)^2 \left[ (\bar{u}_\delta^j \gamma^\mu u_\alpha^i) (\bar{v}_\beta^k \gamma_\mu v_\gamma^l) (\bar{u}_\alpha^i \gamma^\nu u_\delta^j) (\bar{v}_\gamma^l \gamma_\nu v_\beta^k) \right]. \quad (C.14)$$

The cross-channel is given by

$$|M_t M_s^*| = -\frac{g^4}{s t} (T_{ij}^a T_{kl}^a) (T_{ik}^a T_{jl}^a) \left[ (\bar{u}_\delta^j \gamma^\mu u_\alpha^i) (\bar{v}_\beta^k \gamma_\mu v_\gamma^l) (\bar{u}_\alpha^i \gamma^\nu v_\beta^k) (\bar{v}_\gamma^l \gamma_\nu u_\delta^j) \right]. \quad (C.15)$$

After averaging over the initial states and summing over the final states, one obtains (again restricted to a single flavor scattering event) from (C.13) – (C.15), the matrix element squared:

$$|M_{q_\alpha^i \bar{q}_\alpha^k \rightarrow q_\alpha^j \bar{q}_\alpha^l}|^2 = \frac{4}{9} g^4 \left[ \frac{s^2 + u^2}{t^2} + \frac{t^2 + u^2}{s^2} - \left(\frac{2}{3}\right) \frac{u^2}{s t} \right]. \quad (C.16)$$

$$g^{\mu\nu} g_{\mu\nu} = \gamma^\mu \gamma_\mu = \text{Tr}(1) = 4$$

$$s + t + u = 0 \text{ and } s^3 + t^3 + u^3 = 3 s t u$$

$$\sum_{\text{spin}} u^{(s)}(p) \bar{u}^{(s)}(p) = \not{p} = \sum_{\text{spin}} v^{(s)}(p) \bar{v}^{(s)}(p)$$

$$\text{Tr}(\not{a} \not{b}) = \text{Tr}(\not{b} \not{a}) = 4 a \cdot b$$

$$\text{Tr}(\not{a} \not{b} \not{c} \not{d}) = \text{Tr}(\not{b} \not{c} \not{d} \not{a}) = 4 [a \cdot b c \cdot d - a \cdot c b \cdot d + a \cdot d b \cdot c]$$

Trace of an odd number of  $\gamma^\mu$ 's vanish.

$$\gamma^\mu \not{a} \gamma_\mu = -2 \not{a}$$

$$\gamma^\mu \not{a} \not{b} \gamma_\mu = 4 a \cdot b$$

$$\gamma^\mu \not{a} \not{b} \not{c} \gamma_\mu = -2 \not{c} \not{b} \not{a}$$

$$T_{ij}^a T_{kl}^a = \frac{1}{2} [\delta_{il} \delta_{jk} - \frac{1}{3} \delta_{ij} \delta_{kl}]$$

$$(T_{ij}^a T_{kl}^a)^2 = 2$$

$$T_{ij}^a T_{kl}^a T_{il}^a T_{kj}^a = -\frac{2}{3}$$

$$\text{Tr}(T^a) = 0$$

$$\text{Tr}(T^a T^b) = \frac{1}{2} \delta_{ab}$$

$$\text{Tr}(T^a T^b T^a T^c) = -\frac{1}{12} \delta_{bc}$$

$$f_{abb} = 0 \text{ and } f_{abc} = -f_{acb} = f_{cab} = -f_{cba}$$

$$f_{abc} f_{dbc} = 3 \delta_{ab}$$

$$f_{abe} f_{cde} f_{dae} f_{ebc} = -f_{dae} f_{ebc} f_{ace} f_{bde} = 72/2$$

$$f_{dae} f_{ebc} f_{ade} f_{cbe} = 72$$

Table C.2: Trace Relations and Color Sums.

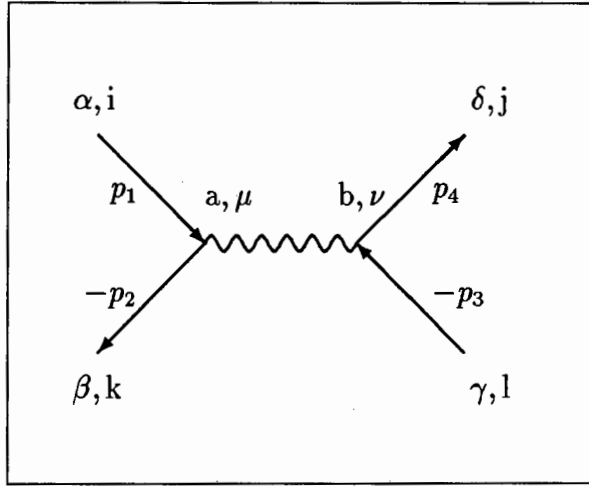


Figure C.3: s-Channel Diagram for Quark-Antiquark Scattering.

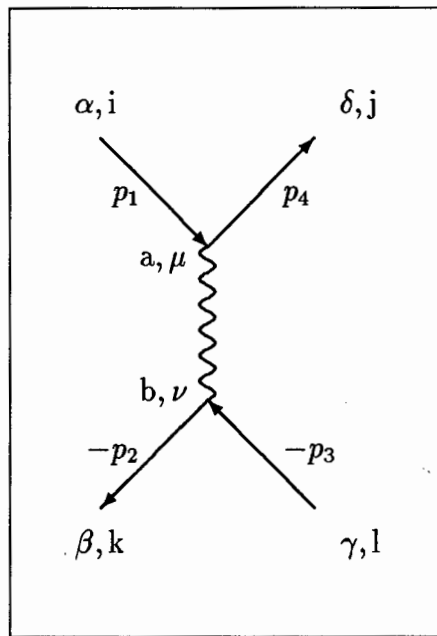


Figure C.4: t-Channel Diagram for Quark-Antiquark Scattering.

Now we consider the quark-gluon scattering process (C.3), the available channels are the s-, t- and u-channel as shown in Figures C.5, C.6 and C.7 respectively.

The s-channel (Figure C.5) matrix element squared is, after the application of the Feynman rules, given by

$$|M_s|^2 = -g^4 \left( \frac{4u}{9s} \right). \quad (\text{C.17})$$

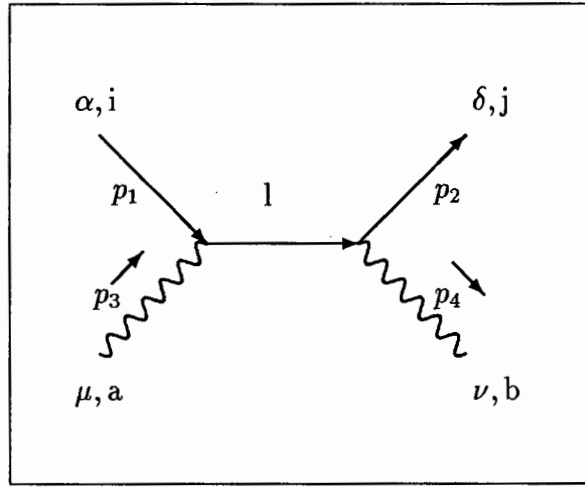


Figure C.5: s-Channel Diagram for Quark-Gluon Scattering.

The t-channel matrix element squared, from Figure C.6, is given by

$$|M_t|^2 = 2g^4 \left( 1 - \frac{us}{t^2} \right). \quad (\text{C.18})$$

The u-channel matrix element squared, from Figure C.7, is given by

$$|M_u|^2 = -g^4 \left( \frac{4s}{9u} \right). \quad (\text{C.19})$$

The s-t cross-channel is given by

$$|M_s M_t^*| = g^4 \left( \frac{s}{2t} \right), \quad (\text{C.20})$$

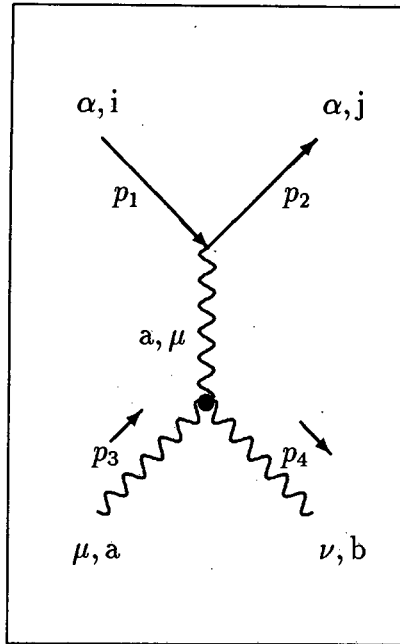


Figure C.6: t-Channel Diagram for Quark-Gluon Scattering.

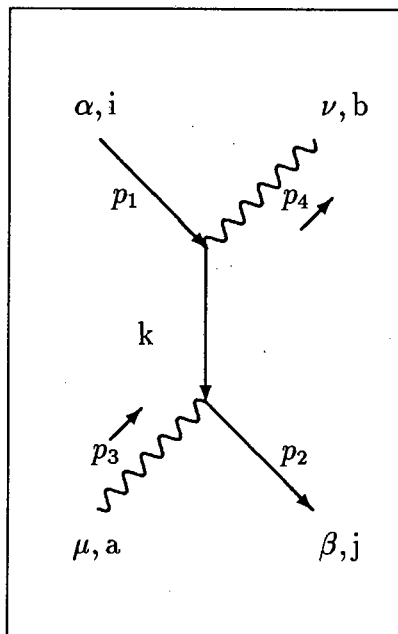


Figure C.7: u-Channel Diagram for Quark-Gluon Scattering.

and similarly, by exchange of  $s \rightarrow u$ , one finds

$$|M_u M_t^*| = g^4 \left( \frac{u}{2t} \right). \quad (\text{C.21})$$

The  $s$ - $u$  cross-channel vanishes on account of the relation  $s + t + u = 0$  which holds since both quarks and gluons are assumed to be massless, thus

$$|M_s M_u^*| = 0. \quad (\text{C.22})$$

After noting that

$$|M_u M_t^*| + |M_s M_t^*| = \frac{g^4}{2} \left( \frac{u}{t} + \frac{s}{t} \right) = -\frac{g^4}{2}, \quad (\text{C.23})$$

we find the total quark-gluon matrix element squared as a sum of (C.17), (C.18), (C.19) and 2\*(C.23), i.e.

$$|M_{q g \rightarrow q g}|^2 = g^4 \left[ 2 \left( 1 - \frac{us}{t^2} \right) - \frac{4}{9} \left( \frac{s}{u} + \frac{u}{s} \right) - 1 \right]. \quad (\text{C.24})$$

As a consequence of time-reversal invariance, the matrix element squared describing the antiquark-gluon scattering is the same as (C.24).

The gluon-gluon scattering matrix element for process (C.4), is the final calculation presented in this Appendix. In this scattering process, one has to consider four reaction channels, namely the s-, t-, and u-channel and the so-called “sea-gull-” or “4-point”-channel. These are shown in Figures C.8 to C.11.

The method used in the evaluation of the gluon-gluon scattering diagrams differs from the one presented above. Following Owens et. al. [75], we make use of the substitution

$$\sum_{\text{spins}} \epsilon_1^\mu \epsilon_1^{\nu*} \Rightarrow -g^{\mu\nu} + \frac{2}{s} (k_1^\mu k_2^\nu + k_2^\mu k_1^\nu) \quad (\text{C.25})$$

instead of using the replacement  $\sum_{\text{spins}} \epsilon^\mu \epsilon^{\nu*} \Rightarrow -g^{\mu\nu}$  as used in the Feynman gauge. Here, the  $\epsilon^\mu$ 's are the polarisation vectors and the  $k^\mu$ 's are the four momentum vectors in the gluon scattering process

$$k_1(\epsilon_1) + k_2(\epsilon_2) \rightarrow k_3(\epsilon_3) + k_4(\epsilon_4). \quad (\text{C.26})$$

The Fadeev-Popov ghost method, as used in the previous calculations of the matrix elements, follows a strategy, whereby the longitudinal polarisation states of the physical gluons, i.e. the external lines, which appeared due to the set of Feynman rules (Table C.1) used, are removed. This operation is performed by replacing all physical gluons by Fadeev-Popov ghosts, and evaluating the diagrams constructed in this way. The Fadeev-Popov method however produces an incorrect result for the gluon-gluon scattering, as was mentioned (but not explained) by Cutler and Sivers [71] and Owens et. al. [75]. The substitution (C.25), although resulting in a very lengthy calculation, has the advantage of avoiding the Fadeev-Popov ghost prescription.

The total matrix element squared for gluon-gluon scattering is then given by

$$|M_{g g \rightarrow g g}|^2 = \frac{9}{2} g^4 \left[ 3 - \frac{us}{t^2} - \frac{st}{u^2} - \frac{ut}{s^2} \right]. \quad (\text{C.27})$$

This result is in agreement with Shuryak [73], Combridge et. al. [74] and Owens et. al. [75], but as mentioned above, Cutler and Sivers [71] and Leader and Predazzi [72] obtained a different result. Their first term in (C.27) is 51/16 instead of 3. However it should be noted that the leading order terms of the collision brackets, i.e. the logarithmic terms, and therefore the transport coefficients, are insensitive to this small discrepancy in the matrix elements.

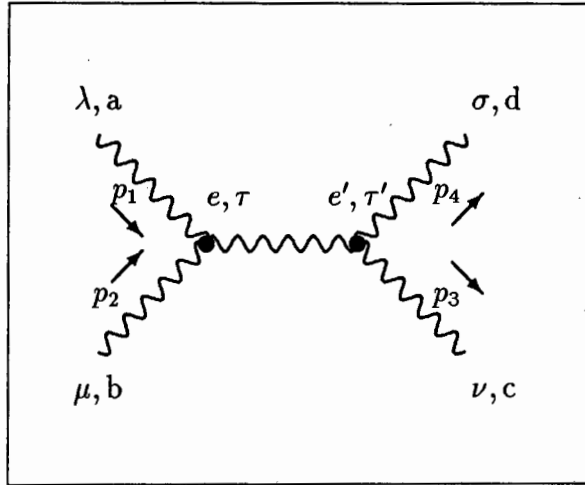


Figure C.8: s-Channel Diagram for Gluon-Gluon Scattering.

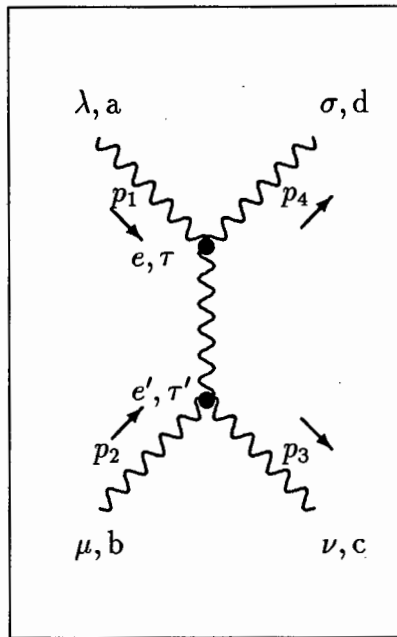


Figure C.9: t-Channel Diagram for Gluon-Gluon Scattering.

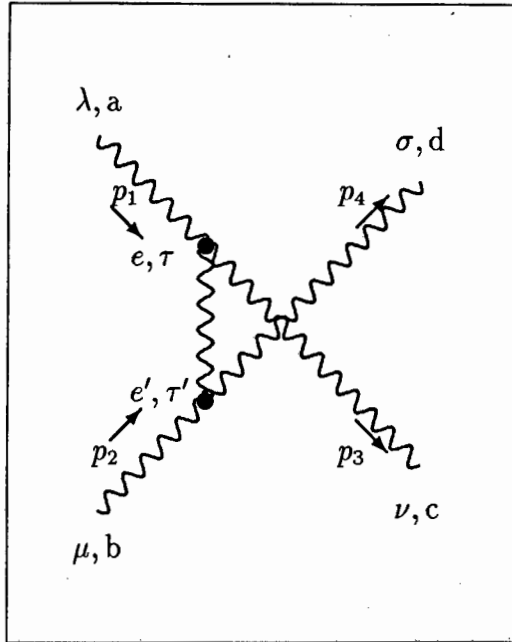


Figure C.10: u-Channel Diagram for Gluon-Gluon Scattering.

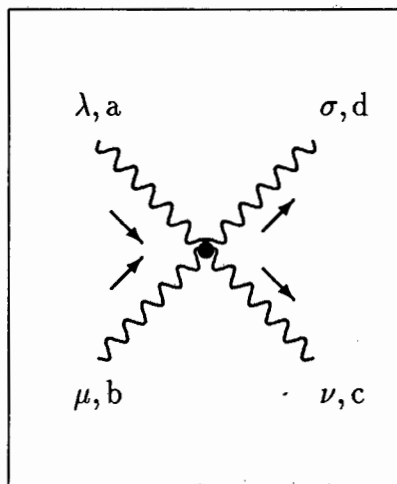


Figure C.11: 4-Point Diagram for Gluon-Gluon Scattering.

## C.1 Differential Cross-Sections

We still need to find the differential cross-sections for the processes (C.1) – (C.4). To this end, we make use of the connection between the transition rate  $W(p_3 p_4 | p_1 p_2)$ , as used in the transport equation, the centre of momentum differential cross-section  $\sigma(s, \theta)$  and the transition matrix element squared  $|M|^2$  [76]:

$$\begin{aligned} W(p_3 p_4 | p_1 p_2) &\equiv s \sigma(s, \theta) \delta^{(4)}(p_1 + p_2 - p_3 - p_4) \\ &= \frac{1}{(8\pi)^2} \delta^{(4)}(p_1 + p_2 - p_3 - p_4) |M_{p_1+p_2 \rightarrow p_3+p_4}|^2. \end{aligned} \quad (\text{C.28})$$

Furthermore, in the cm-frame, one rewrites the Mandelstam variables (C.7) for massless particles as

$$\begin{aligned} s &= 4|\vec{p}|^2, \\ t &= -2|\vec{p}|^2(1-x), \\ u &= -2|\vec{p}|^2(1+x), \end{aligned} \quad (\text{C.29})$$

where  $x = \cos \theta$  is the cm scattering angle. Using (C.28) and (C.29), one finds the cm differential cross-section for the quark-quark scattering process (C.1) from the scattering matrix element (C.12):

$$\sigma_{\text{cm}}(s, x) |_{\text{qq}} = \frac{\alpha_s^2}{9s} \left[ \frac{4 + (1+x)^2}{(1-x)^2} + \frac{4 + (1-x)^2}{(1+x)^2} - \left(\frac{2}{3}\right) \frac{4}{1-x^2} \right]. \quad (\text{C.30})$$

For the quark-antiquark scattering process (C.2), where the matrix element squared is given by (C.16), one obtains

$$\sigma_{\text{cm}}(s, x) |_{\text{q}\bar{\text{q}}} = \frac{\alpha_s^2}{9s} \left[ \frac{4 + (1+x)^2}{(1-x)^2} + \frac{(1-x)^2 + (1+x)^2}{4} + \left(\frac{1}{3}\right) \frac{(1+x)^2}{(1-x)} \right]. \quad (\text{C.31})$$

For the quark-gluon scattering process (C.3), where the matrix element squared is given by (C.24), one obtains

$$\sigma_{\text{cm}}(s, x)|_{\text{qg}} = \frac{\alpha_s^2}{4s} \left[ 2 \left( 1 + 2 \frac{1+x}{(1-x)^2} \right) + \frac{4}{9} \left( \frac{1+x}{2} + \frac{2}{1+x} \right) - 1 \right]. \quad (\text{C.32})$$

Finally, for the gluon-gluon scattering process (C.4), we find from (C.27)

$$\sigma_{\text{cm}}(s, x)|_{\text{gg}} = \frac{9\alpha_s^2}{8s} \left[ 3 + 2 \frac{(1+x)}{(1-x)^2} + 2 \frac{(1-x)}{(1+x)^2} - \frac{1-x^2}{4} \right]. \quad (\text{C.33})$$

The cm cross-sections (C.30) – (C.33) are used in Appendix B to compute the transfer cross-sections. In Appendix D we discuss the resulting divergences of (C.30) – (C.33) for values  $x = +1$  and  $x = -1$ , and how they are taken care of in a plasma.

# Appendix D

## The Cut-off Problem

As we have seen, the scattering matrix elements for the scattering processes involving quarks and gluons, are divergent. How do we deal with these divergences when evaluating physical quantities such as the total cross-section ? Answering this question is the topic of this Appendix.

Because of its purely Abelian interactions, an electron plasma can serve as a first step towards understanding the plasma properties of the more complex non-Abelian plasmas. Obviously, any extrapolation from the QED plasma properties to QCD plasmas must be performed under careful scrutiny, bearing in mind the fundamentally different physical properties of the two systems.

Generally speaking, the exchange of massless particles, i.e. the photons in QED and the gluons in QCD, leads to divergent cross-sections. For example, in an electron system in which Coulomb scattering processes take place, the interaction cross-section displays the familiar divergent Rutherford behaviour at small momentum  $q$  transfers. In transport processes, such small angle scatterings have an important effect on the transport properties: in fact they are more important than the rare large-deflection collisions. This feature is reflected in the relevance that we attach to the resulting logarithmically divergent parts of the transport coefficients. Traditionally (see for example [40], [77] and [78]), this realisation has led to the formulation of the so-called transport cross-section  $\sigma_t$ , in which the scattering angles occurring in the cross section are weighted with appropriate factors, such as  $1 - \cos \theta$ . From the Coulomb cross-section, i.e.

$$\frac{d\sigma}{d\Omega} \propto g^4 \frac{1}{q^4}, \quad (\text{D.1})$$

one would then calculate the total cross-section as

$$\sigma_t \equiv \int \frac{d\sigma}{d\Omega} (1 - \cos \theta) d\Omega, \quad (\text{D.2})$$

yielding for the transport cross-section

$$\sigma_t \propto \left(\frac{g^2}{T}\right)^2 \log\left(\frac{T}{q_D}\right), \quad (\text{D.3})$$

where  $\log(T/q_D)$  is the so-called Coulomb logarithm and  $q_D$  is some appropriate cut-off parameter. We observe that the cross-section diverges logarithmically. When looked at naively, such a logarithmically divergent factor would lead to vanishing transport coefficients, because, as we saw in Chapter 5, these logarithmic factors occur in the denominator of the transport coefficients. The vanishing of the transport coefficients is clearly unsatisfactory and for non-equilibrium conditions even unphysical, and it is therefore crucial to obtain reliable estimates of the magnitude of this logarithmic quantity.

The realisation that the logarithmic factor, or Coulomb logarithm, is dependent on some parameters of the plasma, leads us to a study of the characteristic scales in a plasma. Here, we wish to emphasise the high temperature aspect of the plasma, because the temperature is the only remaining natural scale in systems in which the temperature is much larger than the particle masses, i.e.

$$T \gg m. \quad (\text{D.4})$$

We proceed to discuss the important length-scales of a plasma (see also [79] and [80]). These are

- the Landau length  $\lambda_L$ , which is the typical length-scale determined by the point of balance between the electrostatic energy of a charged particle and its kinetic energy, i.e.

$$\lambda_L \equiv \frac{\alpha}{T}. \quad (\text{D.5})$$

- The thermal wavelength  $\lambda_t$  for a particle in a medium in which  $T \gg m$  is given by

$$\lambda_t \equiv \frac{1}{T}. \quad (\text{D.6})$$

In a relativistic plasma, this quantity represents the typical distance of closest approach.

- The Debye length  $\lambda_D$  is the typical distance from a charge, at which its potential has decreased by a factor  $e^{-1}$  due to the screening of other charges in the neighbourhood.
- The interparticle spacing  $\lambda_p$  is proportional to the inverse cubic root of the particle density, i.e.

$$\lambda_p \equiv n^{-1/3}. \quad (\text{D.7})$$

- The mean free path of particles is given by

$$\lambda \simeq \frac{1}{n \sigma}. \quad (\text{D.8})$$

However, since the cross-section  $\sigma$  in (D.8) is divergent, we isolate the divergence by replacing  $\sigma$  by the product of a typical mean thermal cross-section  $\sigma(T)$  and a logarithmic factor, the Coulomb logarithm  $\log \Lambda_c$ . The mean free path can then (using Maxwell Boltzmann statistics,  $g$  is the particle multiplicity) be written as

$$\begin{aligned} \lambda &\simeq \frac{1}{n \sigma(T) \log \Lambda_c} = \frac{\pi^2 T^2}{g T^3 \alpha^2 \log \Lambda_c} \\ &= \frac{\pi^2}{g T \alpha^2 \log \Lambda_c}. \end{aligned} \quad (\text{D.9})$$

It is instructive to arrange these length-scales in decreasing order of magnitude

$$\lambda_L < \lambda_t < \lambda_p < \lambda_D < \lambda. \quad (\text{D.10})$$

Alternatively, these scales can be written in terms of the temperature, strong coupling constant and Coulomb logarithm as

$$\frac{\alpha}{T} < \frac{1}{T} < n^{-1/3} \simeq \# \frac{1}{T} < \frac{1}{\alpha^{1/2} T} < \frac{1}{\alpha^2 T}. \quad (\text{D.11})$$

Using the density of particles within a sphere of radius  $\lambda_D$ , one can now compute the plasma parameter  $\mathcal{P}$  which determines whether or not the system is a plasma. If the system can indeed be considered to be a plasma, i.e. if effects such as screening are important, this means the condition

$$\frac{4\pi}{3} \lambda_D^3 n \gg 1, \quad (\text{D.12})$$

applies. This condition can be used to define the plasma parameter  $\mathcal{P}$

$$\mathcal{P} \equiv \frac{1}{n \lambda_D^3} \ll 1. \quad (\text{D.13})$$

In other words, if  $\mathcal{P} \ll 1$ , the system under consideration is a plasma.

Traditionally [40], the Coulomb logarithm of a plasma is given by

$$\log \Lambda_c \equiv \log \left( \frac{\lambda_D}{\lambda_L} \right). \quad (\text{D.14})$$

Since the Debye length is given by

$$\lambda_D^2 = \frac{T}{4\pi\alpha n}, \quad (\text{D.15})$$

and the Landau length by

$$\lambda_L = \frac{\alpha}{T}, \quad (\text{D.16})$$

one arrives at

$$\begin{aligned} \frac{\lambda_D}{\lambda_L} &= \left( \frac{T^3}{4\pi\alpha^3 n} \right)^{1/2} \\ &\simeq \alpha^{-3/2}. \end{aligned} \quad (\text{D.17})$$

On the other hand, from the comparison of length-scales (D.10) we observe that in a relativistic plasma, the thermal wavelength  $\lambda_t$  is larger than the Landau length  $\lambda_L$

$$\frac{\lambda_L}{\lambda_t} \propto \left( \frac{\alpha}{T} \right) T = \alpha. \quad (\text{D.18})$$

This suggests that the Coulomb logarithm in high temperature plasmas should rather be defined as

$$\log \Lambda_c \equiv \log \left( \frac{\lambda_D}{\lambda_t} \right). \quad (\text{D.19})$$

From (D.6) and (D.15) one obtains

$$\begin{aligned} \frac{\lambda_D}{\lambda_t} &= \left( \frac{T^3}{4\pi\alpha n} \right)^{1/2} \\ &\simeq \alpha^{-1/2}. \end{aligned} \quad (\text{D.20})$$

This is the value that we shall use in what follows.

We see that in relativistic electron plasmas, the Rutherford divergence is screened, thereby effectively replacing the Coulomb interaction with a modified interaction. This results in a finite Coulomb logarithm which is related to the plasma properties, and the previously divergent transport cross-sections become finite.

After these introductory remarks regarding the divergences and their cures in QED plasmas, we will now consider the effects in QCD plasmas. Here an effect

occurs for the electric part of the QCD interaction which is analogous to the Debye screening already discussed. This effect is due to the interactions associated with the longitudinal gluons. For a plasma of massless quarks, the Debye screening length is proportional to the coupling constant squared times the excitation density and inversely proportional to the excitation energy, so that the characteristic screening length is of the order  $1/gT$ , or  $g^{-1}$  times the typical inter-quark separation [81].

But the effects due to transverse gluons are different to those from longitudinal gluons, and the dynamical behaviour of the plasma must be investigated in order to understand how the divergences due to these interactions can be removed. Intuitively the difference between these two kinds of gluons and their different interactions is easy to understand: while long wavelength electric fields are screened out by mobile charges, this is not the case for the long wavelength magnetic fields. Baym et. al. ([42] and [82]) showed that in QCD plasmas, the magnetic interactions at finite frequencies and temperature are screened at large distances, due to the Landau damping of the gluons, the exchange of which produces the transverse interactions (see also [43] and [44]). The effect of the magnetic mass is in this case only of order  $\sim g^2$  and does therefore not contribute significantly to the logarithmic factors. The conclusion is, that static magnetic fields are not screened, but finite frequency ones are. This is therefore a dynamical screening effect; an analogy is the anomalous skin effect in pure metals.

Another important aspect of quark-gluon plasma screening has been discussed by Bialas and co-workers [83]. They found that in the early stages of the evolution of the plasma, the expansion of the plasma significantly reduces the Debye length as compared to the static scenario. This means that screening is more efficient in the dynamic than in the static case.

Baym et. al. [42] also showed that one can calculate the leading terms of the transport coefficients by using a bare interaction cut-off, without the necessity of explicitly decomposing the interaction into longitudinal and transverse parts. This is remarkable insofar as the underlying physics is very different in the two cases. It also motivates us to proceed in our calculation by simply introducing cut-offs in the various divergent integrals and then relating these cut-offs to the plasma parameters.

Let us summarise the above: The many-particle correlations which provide the Debye shielding in a plasma are not included in the transport equation. However, one can take these collective effects into consideration by introducing a cut-off at around the Debye length. This procedure is correct as long as the plasma condition  $\mathcal{P} \ll 1$  is met. This indicates that there are a certain number of particles in the Debye sphere which are responsible for the screening effect.

In the deconfining phase, color electric forces are screened, but not necessarily the color magnetic forces. The amount of electric screening can be computed from the so-called electric mass, or the inverse Debye screening length. In a high temperature plasma, the color electric fields are weak. This is due to the onset of asymptotic freedom at short distances on the one hand and due to the overall plasma screening effect at large distances on the other hand. One possible effect of this screening is, for example, the expected suppression of charmonium in a QGP. This is because the Debye screening would be larger than the  $c\bar{c}$  binding potential (see for example [84] – [87]).

After these qualitative remarks, we will now adopt a pragmatic view to compute the magnitude of the Coulomb logarithm. We will be guided by the analogy to electron plasmas discussed earlier. Here we utilise the length-scales of the quark-gluon plasma to find this important logarithmic factor. If the particles are massless Maxwell Boltzmann particles and their chemical potential can be neglected, their density is given by

$$n = g \frac{T^3}{\pi^2}. \quad (\text{D.21})$$

Furthermore, the Debye length  $\lambda_D$  for electrical plasmas is given by (D.15). Assuming that a similar formula holds for QCD systems, i.e. letting  $\alpha \rightarrow \alpha_s$ , we arrive at

$$\lambda_D^2 = \frac{T}{4\pi\alpha_s n}. \quad (\text{D.22})$$

The plasma parameter  $\mathcal{P}$  can now be computed. From (D.21) and (D.22) we find

$$\mathcal{P} = \left( \pi g (4\alpha_s)^3 \right)^{1/2}. \quad (\text{D.23})$$

The function  $\mathcal{P} = \mathcal{P}(\alpha_s)$  is plotted in Figure D.1 for the values  $g = 5, 20, 50$ . This indicates the possible combinations of values for the multiplicity  $g$  and the strong coupling constant  $\alpha_s$ .

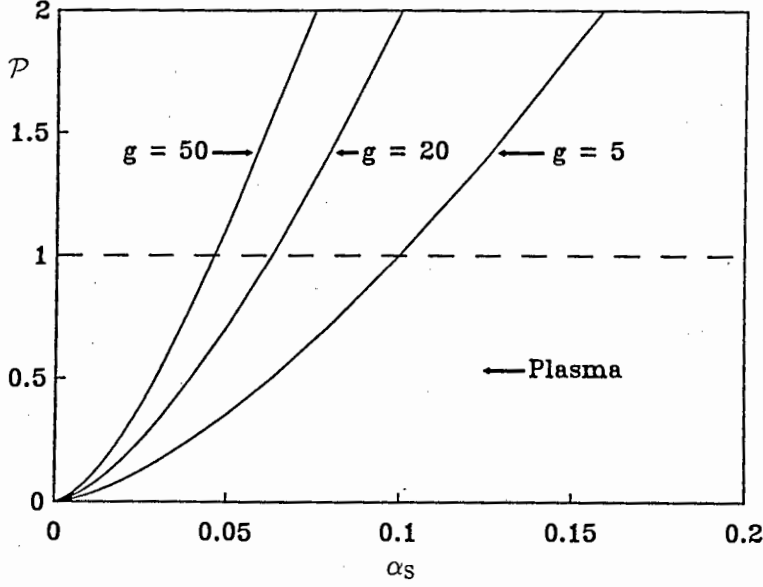


Figure D.1: Plasma Parameter  $\mathcal{P}$  for a QGP.

Finally we turn to the actual computation of the Coulomb logarithm. In order to solve the divergent scattering integrals, we introduce a cut-off  $\Lambda$  at the divergent limit. Typical integrals encountered are of the type

$$\int_{-1}^{+1} dx \frac{x^p}{(1+x)^2} \rightarrow \int_{-\Lambda}^{+1} dx \frac{x^p}{(1+x)^2}, \quad (\text{D.24})$$

$$\int_{-1}^{+1} dx \frac{x^p}{(1-x)^2} \rightarrow \int_{-1}^{+\Lambda} dx \frac{x^p}{(1-x)^2}, \quad (\text{D.25})$$

$$\int_{-1}^{+1} dx \frac{x^p}{1-x^2} \rightarrow \int_{-\Lambda}^{+\Lambda} dx \frac{x^p}{1-x^2}. \quad (\text{D.26})$$

The cut-off  $\Lambda$  is now related to the physical system. On solving the integrals (D.24) – (D.26), one obtains two distinct logarithmic factors, i.e.

$$\log \left( \frac{1+\Lambda}{1-\Lambda} \right) \equiv \log \Lambda_{c1} > 0, \quad (\text{D.27})$$

and

$$\log \left( \frac{1-\Lambda}{2} \right) \equiv \log \Lambda_{c2} < 0. \quad (\text{D.28})$$

The physical origin of these divergences has been discussed above.

Now in order to relate the cut-off  $\Lambda$  to the plasma parameters, we make use of the characteristic plasma length-scales from (D.10), namely

- the Debye screening length  $\lambda_D$  and
- the thermal wavelength  $\lambda_t$ .

From the integrals (D.24) – (D.26) it can be seen that the identification

$$\log \Lambda_c \simeq \log \Lambda_{c1} \quad (\text{D.29})$$

is justified. This identification gives us an estimate for the cut-off  $\Lambda$ , if the definition of the Coulomb logarithm from (D.19) is applied. We recall

$$\begin{aligned} \log \Lambda_c &\equiv \log \left( \frac{\lambda_D}{\lambda_t} \right) \\ &= \frac{1}{2} \log \left( \frac{T^3}{4 \pi \alpha_s n} \right). \end{aligned} \quad (\text{D.30})$$

As expected, the cut-off turns out to be a function of the particle multiplicity and the strong coupling constant. Using (D.21) we arrive at

$$\begin{aligned} \log \Lambda_{c1} &= \frac{1}{2} \log \left( \frac{\pi}{4 \alpha_s g} \right) \\ &= \log \left( \frac{4 \pi \alpha_s}{\mathcal{P}} \right), \end{aligned} \quad (\text{D.31})$$

which is now in terms of the plasma parameter  $\mathcal{P}$  computed in (D.23). Introducing the variable  $C$ , defined as

$$C \equiv \frac{4 \pi \alpha_s}{\mathcal{P}}, \quad (\text{D.32})$$

and making the identification (D.27), we find the cut-off  $\Lambda$

$$\log \Lambda_{c1} \equiv \log C \Rightarrow \Lambda \equiv \frac{C - 1}{C + 1}. \quad (\text{D.33})$$

Some typical values for  $\mathcal{P}$ ,  $\alpha_s$ , the resulting cut-off  $\Lambda$  and the Coulomb logarithms  $\log \Lambda_{c1}$  and  $\log \Lambda_{c2}$  are summarised in Table D.1.

$\mathcal{P}$	$\alpha_s$	C	$\Lambda$	$\log \Lambda_{c1}$	$-\log \Lambda_{c2}$
0.1	0.05	6.28	0.73	1.84	2.00
0.01	0.01	12.57	0.85	2.53	2.59
0.01	0.05	62.83	0.97	4.14	4.20

Table D.1: Plasma Parameters and Coulomb Logarithms.

The Coulomb logarithms  $\log \Lambda_{c1}$  and  $-\log \Lambda_{c2}$  in Table D.1 are to be compared to more common values from applications in plasma physics, where a range of

$$1 < \log \Lambda_c < 30 \quad (\text{D.34})$$

is found for plasma systems (see for example Chen [88]). However, although the cut-off depends on the density and the temperature of the system, and these factors can indeed be large, the resulting logarithm, i.e. the Coulomb logarithm, is relatively insensitive to the exact values of the plasma parameters.

We have to keep in mind that the above calculations are a simple analogy from QED applied to QCD, and should in future be analysed more carefully. The underlying non-Abelian character and the resulting non-linearities of a proper quark-gluon plasma could change these predictions considerably. It is however beyond the scope of this thesis to pursue this matter in greater detail.

We conclude by remarking that more detailed calculations of the Coulomb logarithms and the resulting rates and transport coefficients of a quark-gluon plasma must await a better understanding of the nature of the interactions and in collective properties of such plasmas.

# Appendix E

## Useful Relations

In this Appendix we collect the most important thermodynamic relations and provide conversion factors and other quantities used in this thesis.

### E.1 Thermodynamic Quantities and Relations

Using Maxwell Boltzmann statistics, the particle density  $n$  is given by

$$\begin{aligned} n &\equiv g \int \frac{d^3p}{(2\pi)^3} \exp\left(\frac{\mu - E}{T}\right) \\ &= \frac{g}{2\pi^2} T^3 z^2 K_2(z) \exp(\mu/T) \end{aligned} \quad (\text{E.1})$$

where  $E = (|\vec{p}|^2 + m^2)^{1/2}$  and  $z \equiv m/T$ ,  $g$  is the particle multiplicity.  $K_2$  is the modified Bessel function of the second kind [89], defined by

$$K_n(z) \equiv \frac{2^n n!}{(2n)!} z^{-n} \int_z^\infty dx (x^2 - z^2)^{(2n-1)/2} \exp(-x). \quad (\text{E.2})$$

Similarly, the energy density  $en$  is given by

$$\begin{aligned} en &\equiv g \int \frac{d^3p}{(2\pi)^3} E \exp\left(\frac{\mu - E}{T}\right) \\ &= \frac{g}{2\pi^2} T^4 \left[ z^3 K_1(z) + 3z^2 K_2(z) \right] \exp(\mu/T) \end{aligned} \quad (\text{E.3})$$

and the pressure  $P$  by

$$\begin{aligned} P &\equiv \frac{g}{3} \int \frac{d^3p}{(2\pi)^3} \frac{|\vec{p}|^2}{E} \exp\left(\frac{\mu - E}{T}\right) \\ &= \frac{g}{2\pi^2} T^4 z^2 K_2(z) \exp(\mu/T). \end{aligned} \quad (\text{E.4})$$

Comparing the expression for the particle density  $n$  (E.1) and the pressure  $P$  (E.4), the equation of state for a perfect gas is recovered, i.e.

$$P = nT. \quad (\text{E.5})$$

The enthalpy density  $wn$  is given by

$$wn = en + P \quad (\text{E.6})$$

and therefore

$$wn = \frac{g}{2\pi^2} T^4 \left[ z^3 K_1(z) + 4z^2 K_2(z) \right] \exp(\mu/T). \quad (\text{E.7})$$

The recurrence relation for the modified Bessel functions is given by

$$K_{n+1}(z) = K_{n-1}(z) + \frac{2n}{z} K_n(z) \quad (\text{E.8})$$

which is used to find the energy per particle  $e$  from (E.1) and (E.3)

$$e \equiv \frac{en}{n} = 3T + m \frac{K_1(z)}{K_2(z)}, \quad (\text{E.9})$$

and the enthalpy per particle

$$w \equiv \frac{wn}{n} = 4T + m \frac{K_1(z)}{K_2(z)}. \quad (\text{E.10})$$

The total density of a particle antiparticle system is given by

$$\begin{aligned} n_T &\equiv \frac{g}{2\pi^2} T^3 z^2 K_2(z) [\exp(\mu/T) + \exp(-\mu/T)] \\ &= \frac{g}{\pi^2} z^2 K_2(z) T^3 \cosh(\mu/T), \end{aligned} \quad (\text{E.11})$$

and the conserved number of particles  $n_c$ , for example the baryon number, is given by

$$\begin{aligned} n_c &\equiv \frac{g}{2\pi^2} T^3 z^2 K_2(z) [\exp(\mu/T) - \exp(-\mu/T)] \\ &= \frac{g}{\pi^2} z^2 K_2(z) T^3 \sinh(\mu/T). \end{aligned} \quad (\text{E.12})$$

In this thesis we have mainly used the thermodynamic quantities for massless particles. The asymptotic behaviour of the modified Bessel functions is given by

$$\lim_{z \rightarrow 0} z^n K_n(z) \rightarrow 2^{n-1} (n-1)!, \quad (\text{E.13})$$

so that the relation for the density of massless particles is then found from (E.1)

$$n = g \frac{T^3}{\pi^2} \exp(\mu/T), \quad (\text{E.14})$$

the energy density  $en$  from (E.3), making use of (E.8), is given by

$$en = g \frac{3}{\pi^2} T^4 \exp(\mu/T), \quad (\text{E.15})$$

and the pressure  $P$  from (E.4)

$$P = \frac{g}{\pi^2} T^4 \exp(\mu/T) = \frac{1}{3} en. \quad (\text{E.16})$$

The energy per particle  $e$  (massless) is thus given by

$$e = 3T \quad (\text{E.17})$$

and the enthalpy per particle  $w$  (massless) by

$$w \equiv e + \frac{P}{n} = e + T = 4T, \quad (\text{E.18})$$

which is also directly evident from (E.9) and (E.10), respectively.

The entropy density  $sn$  for  $\mu = 0$  can now be found, since

$$\begin{aligned} sn &= \frac{1}{T} (en + P) = \frac{4}{3T} en \\ &= g \frac{4}{\pi^2} T^3, \end{aligned} \quad (\text{E.19})$$

and the entropy per particle  $s$  (massless) is given by

$$s \equiv \frac{sn}{n} = 4. \quad (\text{E.20})$$

We find the heat capacity per particle at constant volume  $c_V$  and constant pressure  $c_P$  from their definition

$$c_V \equiv \left( \frac{\partial e}{\partial T} \right)_V \quad \text{and} \quad c_P \equiv \left( \frac{\partial w}{\partial T} \right)_P. \quad (\text{E.21})$$

From (E.9) we find

$$c_V = 3 + \frac{\partial}{\partial z^{-1}} \left( \frac{K_1(z)}{K_2(z)} \right), \quad (\text{E.22})$$

and from (E.10)

$$c_P = 4 + \frac{\partial}{\partial z^{-1}} \left( \frac{K_1(z)}{K_2(z)} \right), \quad (\text{E.23})$$

which can also be written as

$$c_V = c_P - 1. \quad (\text{E.24})$$

For massless particles, we find the heat capacities from (E.17) and (E.18)

$$c_V = 3 \quad \text{and} \quad c_P = 4. \quad (\text{E.25})$$

The ratio  $\gamma$  of the heat capacities is defined by

$$\begin{aligned} \gamma \equiv \frac{c_P}{c_V} &= 1 + \frac{1}{c_V} \\ &= \frac{4}{3}. \end{aligned} \quad (\text{E.26})$$

## E.2 Constants

The following constants and conversion factors are useful in our calculations.

$$\hbar c = 197.327 \text{ [MeV fm]} \quad (\text{E.27})$$

$$k_B = 8.617 \cdot 10^{-11} \text{ [MeV K}^{-1}\text{]} \quad (\text{E.28})$$

$$c = 2.997 \cdot 10^{23} \text{ [fm s}^{-1}\text{]} \quad (\text{E.29})$$

$$\begin{aligned} \text{GeV}^2 &= 1.063 \cdot 10^{17} \left[ \frac{\text{kg m}}{\text{K s}^3} \right] \text{ or } \left[ \frac{\text{J}}{\text{m K s}} \right] \\ &= 1.063 \cdot 10^{22} \left[ \frac{\text{g cm}}{\text{K s}^3} \right] \end{aligned} \quad (\text{E.30})$$

$$\text{GeV}^3 = 1.373 \cdot 10^{13} \left[ \frac{\text{kg}}{\text{m s}} \right] \quad (\text{E.31})$$

$$\text{GeV}^{-1} = 5.916 \cdot 10^{-8} \left[ \frac{\text{m}^2}{\text{s}} \right] \quad (\text{E.32})$$

$$\text{MeV} = 1.602 \cdot 10^{-13} \text{ [J]} \quad (\text{E.33})$$

$$G = 6.707 \cdot 10^{-39} \text{ [GeV}^{-2}\text{]} \quad (\text{E.34})$$

$$\text{fm} = 10^{-15} \text{ [m]} \quad (\text{E.35})$$

$$\text{fm}^2 = 10 \text{ [mb]} \quad (\text{E.36})$$

$$\Lambda_{QCD} \simeq 200 \text{ [MeV]} \quad (\text{E.37})$$

# Appendix F

## Quark-like Systems

In this Appendix we present the transport coefficients of a quark-like system [56]. The particles considered are called quark-like, because their interaction is similar to the quark-quark interaction. They are, however, considered spinless and colorless. The cm differential cross-section  $\sigma(s, x)$ , describing the interaction of this model system, is entirely motivated by its similarity to the quark cm cross-section (Appendix C). It has the characteristic infrared divergence, reflected by the Coulomb logarithm appearing in the results, and is expected to produce the correct high temperature behaviour.

### F.1 Simple Quark-like System

As a first case we are considering massless, spinless particles, colliding elastically only. Since the particles are massless, the volume viscosity vanishes.

For the differential cross-section, we choose an expression similar to the well-known  $e^- - e^-$  cross-section for spinless electrons [76], i.e.

$$\sigma(s, x) = \frac{\alpha^2}{s} \left( \frac{3 + x^2}{1 - x^2} \right)^2. \quad (\text{F.1})$$

This expression is in terms of the cm scattering angle  $x = \cos \theta$ , the coupling constant  $\alpha$  and the total cm energy  $s$ .

The square collision brackets needed to compute the heat conductivity and shear viscosity are  $B^{11}$  and  $C^{00}$ . Using the formalism presented in Appendix A, we find

$$B^{11} = \pi \left[ 24 \log \Lambda_c - \Lambda^3 - 21 \Lambda \right], \quad (\text{F.2})$$

$$C^{00} = \pi \left[ 80 \log \Lambda_c - \frac{10}{3} \Lambda^3 - 70 \Lambda \right], \quad (\text{F.3})$$

where  $\beta^1 \equiv 3\gamma/(\gamma - 1) = 12$  and  $\gamma^0 \equiv 10w/T = 40$ , and the only transfer cross-sections

$$\sigma^{(111)} \equiv 16 \log \Lambda_c, \quad (\text{F.4})$$

$$\sigma^{(220)} \equiv \frac{32}{3} \log \Lambda_c, \quad (\text{F.5})$$

$$\sigma^{(002)} \equiv 16 \log \Lambda_c, \quad (\text{F.6})$$

have been used.

Using the formulae for the heat conductivity (4.46) and shear viscosity (4.47), as derived in Chapter 4, we then find the **heat conductivity**

$$\lambda = \frac{48 T^2}{\pi \alpha^2 [24 \log \Lambda_c - \Lambda^3 - 21 \Lambda]}, \quad (\text{F.7})$$

or, for  $\Lambda \rightarrow 0$ ,

$$\lambda = 2 \frac{T^2}{\pi \alpha^2 \log \Lambda_c}. \quad (\text{F.8})$$

Similarly, the **shear viscosity** is found to be

$$\eta = \frac{48 T^3}{\pi \alpha^2 [24 \log \Lambda_c - \Lambda^3 - 21 \Lambda]}, \quad (\text{F.9})$$

or, for  $\Lambda \rightarrow 0$ ,

$$\eta = 2 \frac{T^3}{\pi \alpha^2 \log \Lambda_c}. \quad (\text{F.10})$$

The results (F.8) and (F.10) are similar to their “real quark” counterparts describing a simple quark system, see Chapter 5. However, the square collision brackets  $B^{11}$  and  $C^{00}$  needed to compute  $\lambda$  and  $\eta$  are considerably easier to calculate analytically, and of course, with our REDUCE programs. The results have essential features such as the Coulomb logarithm and the expected high temperature behaviour, and can therefore be considered suited as a model describing a simple quark system. Also, the ratio of the heat conductivity to the shear viscosity again reproduces the **Eucken relation** as previously found, i.e.

$$\frac{\lambda}{\eta} = \frac{1}{T}. \quad (\text{F.11})$$

A more detailed discussion of the quark-like system was published by us [56]; the system should be considered as an instructive first attempt to describe real quark matter only.

## F.2 Quark Antiquark-like System

Similar to the quark-like system studied in the previous section, we consider the simplest possible model of interaction capable of describing a quark antiquark mixture [56]. Again we are led by the interactions of a relativistic electron system. In the model gas under consideration, we use differential cross-sections similar to those in spinless  $e^- - e^-$  and  $e^- - e^+$  scatterings. Labelling the components of the mixture by 1 and 2, respectively, the differential cross-sections are given by [76]

$$\sigma_{11}(s, x) = \sigma_{22}(s, x) = \frac{\alpha^2}{s} \left( \frac{3 + x^2}{1 - x^2} \right)^2, \quad (\text{F.12})$$

and

$$\sigma_{12}(s, x) = \sigma_{21}(s, x) = \frac{\alpha^2}{4s} \left( \frac{3 + x^2}{1 - x} \right)^2, \quad (\text{F.13})$$

in terms of the cm scattering angle  $x = \cos \theta$ , the coupling constant  $\alpha$  and the total cm energy  $s$ . To simplify matters even further, we take only the logarithmic dependence of the square collision brackets into account (i.e. all constant terms and those proportional to  $\Lambda$  vanish). This is equivalent as making the following choice for the transfer cross sections

$$\sigma_{11}^{(001)} \equiv \sigma_{11}^{(110)} \equiv 0, \quad (\text{F.14})$$

$$\sigma_{11}^{(002)} \equiv \sigma_{11}^{(111)} \equiv \frac{2}{3} \sigma_{11}^{(220)} \equiv 16 \log \Lambda_{c1}, \quad (\text{F.15})$$

$$\sigma_{12}^{(001)} \equiv \sigma_{12}^{(110)} \equiv -16 \log \Lambda_{c2}, \quad (\text{F.16})$$

$$\sigma_{12}^{(002)} \equiv \sigma_{12}^{(111)} \equiv \frac{2}{3} \sigma_{12}^{(220)} \equiv -32 \log \Lambda_{c2}. \quad (\text{F.17})$$

These transfer cross-sections are in terms of the Coulomb logarithms

$$\begin{aligned} \log \Lambda_{c1} &\equiv \log \left( \frac{1 + \Lambda}{1 - \Lambda} \right) > 0, \\ \log \Lambda_{c2} &\equiv \log \left( \frac{1 - \Lambda}{2} \right) < 0, \end{aligned} \quad (\text{F.18})$$

in terms of the infrared divergence cut-off  $\Lambda$ . They are now used to find the square collision brackets  $B_{12}^{00}, B_{12}^{01}, B_{12}^{10}, B_{11}^{11}, B_{12}^{11}, B_{22}^{11}, C_{11}^{00}, C_{12}^{00}$  and  $C_{22}^{00}$ . The collision brackets are given by

$$B_{12}^{00} = 6 \pi x_1 x_2 \log \Lambda_{c2} \quad (\text{F.19})$$

$$B_{12}^{01} = 24 \pi x_1 x_2 \log \Lambda_{c2} \quad (\text{F.20})$$

$$B_{12}^{10} = 24 \pi x_1 x_2 \log \Lambda_{c2} \quad (\text{F.21})$$

$$B_{11}^{11} = 48 \pi x_1 [x_1 \log \Lambda_{c1} - 3 x_2 \log \Lambda_{c2}] \quad (\text{F.22})$$

$$B_{12}^{11} = 96 \pi x_1 x_2 \log \Lambda_{c2} \quad (\text{F.23})$$

$$B_{22}^{11} = 48 \pi x_2 [x_2 \log \Lambda_{c1} - 3 x_1 \log \Lambda_{c2}] \quad (\text{F.24})$$

$$C_{11}^{00} = 160 \pi x_1 [x_1 \log \Lambda_{c1} - x_2 \log \Lambda_{c2}] \quad (\text{F.25})$$

$$C_{12}^{00} = 0 \quad (\text{F.26})$$

$$C_{22}^{00} = 160 \pi x_2 [x_2 \log \Lambda_{c1} - x_1 \log \Lambda_{c2}]. \quad (\text{F.27})$$

We can now calculate the transport coefficients for this quark antiquark-like mixture. The heat conductivity is then given by

$$\begin{aligned} \lambda &= \frac{2T^2}{\pi\alpha^2} \frac{x_1^2 \log \Lambda_{c2} - 2x_1 x_2 \log \Lambda_{c1} + x_2^2 \log \Lambda_{c2}}{(x_2 \log \Lambda_{c1} - x_1 \log \Lambda_{c2})(x_2 \log \Lambda_{c2} - x_1 \log \Lambda_{c1})} \\ &= \frac{2T^2}{\pi\alpha^2} \frac{\log \Lambda_{c2} - 2x_1 x_2 [\log \Lambda_{c1} + \log \Lambda_{c2}]}{\log \Lambda_{c1} \log \Lambda_{c2} - x_1 x_2 [\log \Lambda_{c1} + \log \Lambda_{c2}]^2} \\ &= \frac{2T^2}{\pi\alpha^2} \frac{\log \Lambda_{c2} - 2x_1 x_2 S}{\log \Lambda_{c1} \log \Lambda_{c2} - x_1 x_2 S^2} \\ &= \frac{2T^2}{\pi\alpha^2} \frac{2x_1 x_2 S - \log \Lambda_{c2}}{G + x_1 x_2 S^2}, \end{aligned} \quad (\text{F.28})$$

the **thermal diffusion** coefficient is given by

$$D_T = 0, \quad (\text{F.29})$$

the **diffusion** coefficient is given by

$$D_d = -\frac{T^2}{\pi \alpha^2 n \log \Lambda_{c2}}, \quad (\text{F.30})$$

and the **shear viscosity** is found to be

$$\begin{aligned} \eta &= \frac{2T^3}{\pi \alpha^2} \frac{\log \Lambda_{c2} - 2x_1 x_2 S}{\log \Lambda_{c1} \log \Lambda_{c2} - x_1 x_2 S^2} \\ &= \frac{2T^3}{\pi \alpha^2} \frac{2x_1 x_2 S - \log \Lambda_{c2}}{G + x_1 x_2 S^2}. \end{aligned} \quad (\text{F.31})$$

Here, as in the quark antiquark system discussed in Chapter 5, we made use of the abbreviations

$$S \equiv \log \Lambda_{c1} + \log \Lambda_{c2}, \quad (\text{F.32})$$

and

$$G \equiv -\log \Lambda_{c1} \log \Lambda_{c2} > 0. \quad (\text{F.33})$$

Noting that  $\log \Lambda_{c1} > 0$  and  $\log \Lambda_{c2} < 0$ , it is again easy to show that all the above transport coefficients are positive, as is needed for the validity of the H-theorem.

When comparing the results from this section with those from the quark antiquark system, it is clear that a multi-component system is complex. The proposed differential cross-sections (F.12) and (F.13) are therefore a useful first approximation to the real quark antiquark interaction. Again, they model some of the quark antiquark properties, such as infrared divergence and the expected high temperature behaviour, but are less complicated in structure. The resulting transfer cross-sections and square collision brackets can be calculated analytically with relative ease, in contrast to the quantities for the “real” system. Also, the same **Eucken relation** as obtained previously is recovered.

Comparing the shear viscosity of the simple quark system to the result for that coefficient found in this Appendix, i.e. from (F.10),

$$\eta_{\text{real quark}} = 9 N_f \frac{T^3}{\pi \alpha_s^2 \log \Lambda_c}, \quad (\text{F.34})$$

$$\eta_{\text{quark-like}} = 2 \frac{T^3}{\pi \alpha^2 \log \Lambda_c}, \quad (\text{F.35})$$

one observes, that the “real” quark viscosity is larger by a factor

$$\frac{\eta_{\text{real quark}}}{\eta_{\text{quark-like}}} = \frac{9}{2} N_f, \quad (\text{F.36})$$

assuming that  $\alpha_s = \alpha$ . This factor is due to the different cross-sections used, and due to the color and spin property of “real” quarks, which, although not taken care of explicitly, were accounted for in the evaluation of the scattering matrix elements. For a 2-flavor system, this ratio is 9, which is about the factor by which our results differ from others in the literature. Note however, that the value of the Coulomb logarithm is of crucial importance, also for the results obtained above, and, a change in this value will always influence the final magnitude of the transport coefficients.

# Bibliography

- [1] J.Cleymans, R.V. Gavai and E. Suhonen, Phys.Rep. **130** (1986) 217,  
*Quarks and Gluons at High Temperatures and Densities*
- [2] K. Kajantie and L. McLerran, Ann.Rev.Nucl.Part.Sci. **37** (1987) 293  
*Probes of the Quark Gluon Plasma in High Energy Collisions*
- [3] Quark Matter 1988, Lenox, Mass. (USA), Nucl.Phys. **A498** (1989)  
Quark Matter 1990, Menton (France), to appear in Nucl.Phys. **A**
- [4] S.R. de Groot, W.A. van Leeuwen and C.G. van Weert,  
*“Relativistic Kinetic Theory”*, North-Holland 1980
- [5] J.M. Stewart, *“Non-Equilibrium Relativistic Kinetic Theory”*, Lecture Notes in  
Physics **10**, Springer-Verlag 1971
- [6] J.L. Anderson and H.R. Witting, Physica **74** (1974) 466  
*A Relativistic Relaxation Time Model for the Boltzmann Equation*  
J.L. Anderson and H.R. Witting, Physica **74** (1974) 489  
*Relativistic Quantum Transport Coefficients*
- [7] S. Gavin, Nucl.Phys. **A435** (1985) 826  
*Transport Coefficients in Ultra-Relativistic Heavy Ion Collisions*
- [8] A. Hosoya and K. Kajantie, Nucl.Phys. **B250** (1985) 666  
*Transport Coefficients of QCD Matter*
- [9] P. Danielewicz and M. Gyulassy, Phys.Rev. **D31** (1985) 53,  
*Dissipative Phenomena in Quark-Gluon Plasmas*
- [10] G. Baym, Phys.Lett. **B138** (1984) 18  
*Thermal Equilibration in Ultra-Relativistic Heavy Ion Collisions*
- [11] W. Israel and J.M. Stewart, Ann.Phys. **118** (1979) 341  
*Transient Relativistic Thermodynamics and Kinetic Theory*
- [12] S. Chapman and T.G. Cowling, *“The Mathematical Theory of Non-Uniform  
Gases”*, Cambridge University Press 1953
- [13] P. Carruthers and F. Zachariasen, Rev.Mod.Phys. **55** (1983) 245  
*Quantum Collision Theory with Phase-Space Distributions*

- [14] H.T. Elze and U. Heinz, Phys.Rep. **183** (1989) 81  
*Quark-Gluon Transport Theory*
- [15] C. Eckart, Phys.Rev. **58** (1940) 267  
*The Thermodynamics of Irreversible Processes 1: The Simple Fluid*  
C. Eckart, Phys.Rev. **58** (1940) 269  
*The Thermodynamics of Irreversible Processes 2: Fluid Mixtures*  
C. Eckart, Phys.Rev. **58** (1940) 919  
*The Thermodynamics of Irreversible Processes 3: Relativistic Theory of the Simple Fluid*
- [16] C. Marle, Ann.Inst.H.Poincaré **A10** (1969) 127  
*Sur l'établissement des équations de l'hydrodynamique des fluides relativistes dissipatifs 2: Méthodes de résolution approchée de l'équation de Boltzmann relativiste*
- [17] W. Israel, Jour.Math.Phys. **4** (1963) 1163  
*Relativistic Kinetic Theory of a Simple Gas*  
W. Israel, in "General Relativity", Edt. L. O'Raifeartaigh, Clarendon Press 1972  
*The Relativistic Boltzmann Equation*
- [18] U. Heinz, Phys.Rev.Lett. **51** (1983) 351  
*Kinetic Theory for Plasmas with Non-Abelian Interactions*
- [19] U. Heinz, Nucl.Phys. **A418** (1984) 603c  
*Quark-Gluon Transport Theory*
- [20] U. Heinz, Ann.Phys. **161** (1985) 48  
*Quark-Gluon Transport Theory 1: The Classical Theory*
- [21] U. Heinz, Ann.Phys. **168** (1986) 148  
*Quark-Gluon Transport Theory 2: Color Response and Color Correlations in a Quark-Gluon Plasma*
- [22] S. Mrówczyński, Phys.Rev.Lett. **56** (1986) 93  
Comment on *Kinetic Theory for Plasmas with Non-Abelian Interactions*  
U. Heinz, Phys.Rev.Lett. **56** (1986) 94 (C)  
*Heinz responds*
- [23] R.K. Sachs and J. Ehlers, in "Astrophysics and General Relativity",  
Edt. M. Chrétien et. al., Volume 2, 1968  
*Kinetic Theory and Cosmology*
- [24] S. Weinberg, Astrophys.Jour. **168** (1971) 175  
*Entropy Generation and the Survival of Proto-Galaxies in an Expanding Universe*
- [25] S. Weinberg, "Gravitation and Cosmology", John Wiley & Sons 1972

- [26] L.J. van den Horn and C.G. van Weert, *Astron.Astrophys.* **125** (1983) 93  
*Transport properties of Neutrinos in Stellar Collapse 1*  
 L.J. van den Horn and C.G. van Weert, *Astron.Astrophys.* **136** (1984) 74  
*Transport properties of Neutrinos in Stellar Collapse 2*  
 B.T. Goodwin and C.J. Pethick, *Astrophys.J.* **253** (1982) 816  
*Transport Properties of Degenerate Neutrinos in Dense Matter*  
 R.F. Sawyer, *Astrophys.J.* **237** (1980) 187  
*Damping of Neutron Star Pulsations by Weak Interaction Processes*  
 S.R. de Groot, *Physica* **A147** (1987) 1  
*On the Transport Coefficients of Systems Containing Neutrinos*
- [27] B. Svetitsky, *Phys.Rev.* **D37** (1988) 2484  
*Diffusion of Charmed Quarks in the Quark-Gluon Plasma*
- [28] A. Białas and W. Czyż, *Phys.Rev.* **D30** (1984) 2371  
*Boost-invariant Boltzmann-Vlasov Equations for Relativistic Quark-Antiquark Plasma*
- [29] A. Białas and W. Czyż, *Z.Phys.* **C28** (1985) 255  
*Oscillations of Relativistic, Boost-Invariant Quark-Antiquark Plasma*
- [30] A. Białas, W. Czyż, A. Dyrek and W. Florkowski, *Nucl.Phys.* **B296** (1988) 611  
*Oscillations of Quark-Gluon Plasma Generated in Strong Color Fields*
- [31] S. Mrówczyński, in “*Quark-Gluon Plasma*”  
 in *Directions in High Energy Physics*, World Scientific 1990, Edt. R. Hwa,  
*Applications of Transport Theory to Quark-Gluon Plasma*
- [32] G. Gatoff, A.K. Kerman and T. Matsui, *Phys.Rev.* **D36** (1987) 114  
*Flux-tube Model for Ultra-Relativistic Heavy Ion Collisions: Electrohydrodynamics of a Quark-Gluon Plasma*  
 G. Gatoff, A.K. Kerman and D. Vautherin, *Phys.Rev.* **D38** (1988) 96  
*Nonlinear Effects in the Flux-tube model for Ultra-Relativistic Nucleus-Nucleus Collisions*
- [33] H.T. Elze, M. Gyulassy and D. Vasak, *Phys.Lett.* **B177** (1986) 402  
*Transport Equations for the QCD Gluon Wigner Operator*
- [34] H.T. Elze, M. Gyulassy and D. Vasak, *Nucl.Phys.* **B276** (1986) 706  
*Transport Equations for the QCD Quark Wigner Operator*
- [35] L.H. Ryder, “*Quantum Field Theory*”, Cambridge University Press 1985
- [36] S.K. Wong, *Nuovo Cimento* **A65** (1970) 689  
*Field and Particle Equations for the Classical Yang-Mills Field and Particles with Isotopic Spin*
- [37] U. Heinz, *Phys.Lett.* **B144** (1984) 228  
*A Relativistic Colored Spinning Particle in an External Color Field*

- [38] J.D. Bjorken and S.D. Drell, "*Relativistic Quantum Mechanics*", McGraw-Hill 1964
- [39] L.E. Reichl, "*A Modern Course in Statistical Physics*", E. Arnold Publishers 1980
- [40] L.D. Landau and E.M. Lifshitz, "*Fluid Mechanics*", Pergamon Press 1963
- [41] L.H. Thomas, *Quart.J.Math.* **1** (1930) 239  
*The Radiation Field in a Fluid in Motion*
- [42] G. Baym, H. Monien, C.J. Pethick and D.G. Ravenhall, *Phys.Rev.Lett.* **64** (1990) 1867  
*Transverse Interactions and Transport in Relativistic Quark-Gluon and Electromagnetic Plasmas*
- [43] U. Heinz, *Phys.Lett.* **A109** (1985) 385  
*Landau Damping: New Aspects of an Old Story*
- [44] U. Heinz and P.J. Siemens, *Phys.Lett.* **B158** (1985) 11  
*Colored Plasmons in a Quark-Gluon Plasma near Equilibrium*
- [45] G. Baym and C.J. Pethick, in "*The Physics of Liquid and Solid Helium*", Edts. K.H. Bennemann and J.B. Ketterson, Part 2, 1978  
*Landau Fermi-Liquid Theory and Low Temperature Properties of Normal Liquid He<sup>3</sup>*
- [46] R. Horsley and W. Schoenmaker, *Phys.Rev.Lett.* **57** (1986) 2894  
*Transport Coefficients of Quantum Chromodynamics*  
R. Horsley and W. Schoenmaker, *Nucl.Phys.* **B280** (1987) 716  
*Quantum Field Theories out of Thermal Equilibrium 1*  
R. Horsley and W. Schoenmaker, *Nucl.Phys.* **B280** (1987) 735  
*Quantum Field Theories out of Thermal Equilibrium 2*
- [47] S.V. Ilyin, A.D. Panferov and Y.M. Sinyukov, *Phys.Lett.* **B227** (1989) 455  
*The Viscosity Coefficient in Temperature Gauge Theories. QCD Plasma*
- [48] F. Karsch and H.W. Wyld, *Phys.Rev.* **D35** (1987) 2518  
*Thermal Green's Functions and Transport Coefficients on the Lattice*
- [49] S. Chakrabarty, *Pramāna J.Phys.* **25** (1985) 673  
*Transport Coefficients of Quark-Gluon Plasma*
- [50] W. Czyż and W. Florkowski, *Acta Phys.Pol.* **B17** (1986) 819  
*Kinetic Coefficients for Quark-Antiquark Plasma*
- [51] A. Dyrek and W. Florkowski, *Phys.Rev.* **D36** (1987) 2172  
*Kinetic Coefficients for Quark-Antiquark Plasma with Quantum Treatment of Color*

- [52] S. Mrówczyński, Acta Phys.Pol. **B19** (1988) 91  
*On the Transport Coefficients of a Quark Plasma*
- [53] S.R. de Groot and P. Mazur, “*Non-Equilibrium Thermodynamics*”,  
Dover Publications 1962
- [54] S.R. de Groot, C.G. van Weert, W.T. Hermens and W.A. van Leeuwen, Physica  
**40** (1969) 581  
*On Relativistic Kinetic Gas Theory 2: Reciprocal Relations between Transport Phenomena*
- [55] F. Reif, “*Fundamentals of Statistical and Thermal Physics*”, McGraw-Hill 1965
- [56] D.W. von Oertzen and J. Cleymans, S.Afr.J.Phys. **13** (1990) 91  
*Kinetic Coefficients in Ultra-Relativistic Heavy Ion Collisions*
- [57] D.W. von Oertzen, to be published in Lecture Notes in Physics, “*Phase Structure of Strongly Interacting Matter*”, Edt. J. Cleymans, Springer Verlag 1990  
*QCD Transport Coefficients*
- [58] K. Kajantie and H. Kurki-Suonio, Phys.Rev. **D34** (1986) 1719  
*Bubble Growth and Droplet Decay in the Quark-Hadron Phase Transition in the Early Universe*
- [59] D.W. von Oertzen, S.Afr.J.Phys. **11** (1988) 82  
*On the Duration and Temperature of the Quark-Hadron Transition in the Early Universe*
- [60] N. Caderni and R. Fabbri, Phys.Lett. **B69** (1977) 508.  
*Viscous Phenomena and Entropy Production in the Early Universe*
- [61] N. Caderni and R. Fabbri, Lett. Nuovo Cimento **6** (1977) 185  
*Viscous Dissipation and Entropy Production in Bianchi Type 1 Universes*  
N. Caderni and R. Fabbri, Nuovo Cimento **B44** (1978) 228  
*Production of Entropy and Viscous Damping of Anisotropy in Homogenous Cosmological Models: Bianchi Type 1 Spaces*
- [62] G.L. Murphy, Phys.Rev. **D8** (1973) 4231  
*Big-Bang Model without Singularities*
- [63] F. Hoogeveen, W.A. van Leeuwen, G.A.Q. Salvati and E.E. Schelling, Physica  
**A134** (1986) 458  
*Viscous Phenomena in Cosmology 1*
- [64] W.A. van Leeuwen, G.A.Q. Salvati and E.E. Schelling, Physica **A136** (1986)  
417  
*Viscous Phenomena in Cosmology 2*
- [65] T. Hageman and W.A. van Leeuwen, Physica **A146** (1987) 506  
*Viscous Bianchi Type 2 Universes with Intergalactic Magnetic Field*

- [66] J.D. Bjorken, Phys.Rev **D27** (1983) 140  
*Highly Relativistic Nucleus-Nucleus Collisions: The Central Rapidity Regime*
- [67] G. Baym, Nucl.Phys. **A418** (1984) 525c  
*Entropy Production and the Evolution of Ultra-Relativistic Heavy Ion Collisions*
- [68] J.M. Eisenberg and G. Kälbermann, Phys.Rev. **D37** (1988) 1197  
*Pair Production in Transport Equations*
- [69] H. van Erkelens and W.A. van Leeuwen, Physica **A101** (1980) 205  
*Relativistic Boltzmann-Theory for a Plasma 5: Reduction of the Collision Integrals*
- [70] G. Arfken, "Mathematical Methods for Physicists",  
Academic Press, 3rd ed. 1985
- [71] R. Cutler and D. Sivers, Phys.Rev. **D17** (1978) 196  
*Quantum Chromodynamic Gluon Contribution to large  $p_T$  Reactions*
- [72] E. Leader and E. Predazzi, "An Introduction to Gauge Theories and the "New Physics" ", Cambridge University Press 1982
- [73] E.V. Shuryak, "The QCD Vacuum, Hadrons and the Superdense Matter",  
World Scientific 1988
- [74] B.L. Combridge, J. Kripfganz and J. Ranft, Phys.Lett. **B70** (1977) 234  
*Hadron Production at Large Transverse Momentum and QCD*
- [75] J.F. Owens, E. Reya and M. Glück, Phys.Rev. **D18** (1978) 1501  
*Detailed Quantum-Chromodynamic Predictions for High- $p_T$  Processes*
- [76] F. Halzen and A. Martin, "Quarks and Leptons" John & Wiley Sons 1984
- [77] H. van Erkelens, Physica **A107** (1981) 48  
*Relativistic Boltzmann-Theory for a Plasma 6: The Relativistic Landau Equation*
- [78] H. van Erkelens and W.A. van Leeuwen, Physica **A123** (1984) 72  
*Relativistic Boltzmann-Theory for a Plasma 10: Electrical Conduction of the Cosmological Fluid*
- [79] N. Weiss, Nucl.Phys. **A498** (1989) 429c  
*Multiple Length Scales and Screening Lengths in QCD at High Temperatures*
- [80] S.P. Li and L. McLerran, Nucl.Phys. **B214** (1983) 417  
*Towards a Transport Theory of the Quark-Gluon Plasma: Infrared Divergences and Scalar-Meson Theory*
- [81] H.A. Weldon, Phys.Rev. **D26** (1982) 1394  
*Covariant Calculations at Finite Temperature: The Relativistic Plasma*

- [82] C.J. Pethick, G. Baym and H. Monien, Nucl.Phys. **A498** (1989) 313c  
*Kinetics of Quark-Gluon Plasmas*
- [83] A. Białas, W. Broniowski and W. Czyż, Phys.Rev. **D39** (1989) 329  
*Debye Length in an Expanding Quark-Gluon Plasma*
- [84] T. Matsui and H. Satz, Phys.Lett. **B178** (1986) 416  
*J/Ψ Suppression by Quark-Gluon Plasma Formation*
- [85] H. Satz, Nucl.Phys. **A418** (1984) 447c  
*Colour Screening in SU(N) Gauge Theory at Finite Temperature*
- [86] K. Kanaya and H. Satz, Phys.Rev. **D34** (1986) 3193  
*Correlation and Screening in Finite-Temperature SU(2) Gauge Theory*
- [87] C. Gale and J. Kapusta, Phys.Lett. **B198** (1987) 89  
*Modification of Debye Screening in Gluon Plasma*
- [88] F.F. Chen, "An Introduction to Plasma Physics and Controlled Fusion",  
Plenum Press 1985
- [89] M. Abramowitz and I.A. Stegun, "Handbook of Mathematical Functions",  
Dover 1968